Charles University

1st Faculty of Medicine

Study Programme: Human Physiology and Pathophysiology

MUDr. Diana Maláriková

Studium molekulárních mechanismů a patofyziologických aspektů terapie agresivních lymfomů zaměřené na cílenou indukci apoptózy a/nebo inhibici buněčného cyklu

Study of molecular mechanisms and pathophysiological aspects of aggressive lymphoma therapy focused on targeted apoptosis induction and/or cell cycle inhibition

Ph.D. Thesis

Supervisor: prof. MUDr. Pavel Klener, Ph.D.

Prague, 2024

PROHLÁŠENÍ

Prohlašuji, že jsem disertační práci zpracovala samostatně dle připomínek školitele prof. MUDr. Pavla Klenera, Ph.D., a že jsem řádně uvedla a citovala všechny použité prameny a literaturu. Současně prohlašuji, že tato práce nebyla využita k získání jiného nebo stejného titulu.

Souhlasím s trvalým uložením elektronické verze mé práce v databázi systému meziuniverzitního projektu Theses.cz za účelem soustavné kontroly podobnosti kvalifikačních prací.

V Praze, 23. října 2024

MUDr. Diana Maláriková

Podpis:

IDENTIFICATION RECORD

MALARIKOVA, Diana. *Study of molecular mechanisms and pathophysiological aspects of aggressive lymphoma therapy focused on targeted apoptosis induction and/or cell cycle inhibition [Studium molekulárních mechanismů a patofyziologických aspektů terapie agresivních lymfomů zaměřené na cílenou indukci apoptózy a/nebo inhibici buněčného cyklu].* Prague 2024, Number of Pages: 115, Number of Supplements: 2, Ph.D. Thesis, Charles University, First Faculty of Medicine, Institute of Pathological Physiology. Supervisor: prof. MUDr. Pavel Klener, Ph.D.

ACKNOWLEDGEMENTS

I would like to sincerelly thank my mentor – prof. MUDr. Pavel Klener, Ph.D., for his expert and valuable guidance and patience throughout my post-gradual studies, with my deepest gratitude for exceptionaly friendly relationsship and support. I am also deeply grateful to to my friends and coworkers from the lab for encouragement and stimulating discussions that enriched my studies. Additionally, I wish to acknowledge all collaborators from other facilities and groups that significantly contributed to the development of my work, mainly Mgr. Radek Jorda, Ph.D., doc. Dr. Ing. Eva Kriegova and MUDr. Ales Obr, Ph.D. from Palacky University Olomouc and Olomouc University Hospital, doc. MUDr. Ondrej Havranek Ph.D. (Head of Group Lymphoma Tumor Biology) and RNDr. Ladislav Andera, CSc., Institute of Molecular Genetics, Czech Academy of Sciences.. My appreciation extends specially to David Chiron, CRCI2NA for the possibility and warm welcome during my internship in Nantes, France. Additionally I am grateful to the Chief of the Institute of Pathological Physiology prof.. MUDr. Martin Vokurka, CSc. and the Chief of the First Internal Department, General University Hospital prof. MUDr. Marek Trneny, CSc. for their leadership and the opportunities they provided for my professional growth.

GRANT SUPPORT

GAČR: GA23-05474S

GA20-25308S

GA19-08772S

AZV: NU21-03-00386

17-28980A

Institutional: Charles University Center of Excellence UNCE/MED/016,

PRIMUS 17/MED/09

PRIMUS 19/MED/07

National Institute for Cancer Research (EXCELES)

Content:

Abstract:

Aggressive subtypes of B-cell non-Hodgkin lymphomas are characterized by deregulation of cell-cycle and apoptosis due to recurrent molecular and cytogenetic aberrations, including the overexpression of D-type cyclins, the amplification of cyclin-dependent kinases or transcription factors (*MYC*), mutations or deletions of important cell cycle regulators (*RB1, TP53*, *CDKN2A*) or the aberrant expression of anti-apoptotic proteins (*BCL2).* The combined inhibition of a cyclin-dependent kinase 4/6 by palbociclib and anti-apoptotic BCL2 proteins with respective BH3-mimetics represents reasonable treatment combination in experimental therapy of B-NHL.

A panel of 20 mantle cell lymphoma (MCL) and diffuse large B-cell lymphoma (DLBCL) cell lines and 4 patient-derived xenograft (PDX) models derived from chemotherapy and/or ibrutinib-refractory MCL were used for *in vitro* and *in vivo* experiments, respectively. Protein levels before and after treatment were measured by western blotting. Changes in the mitochondrial membrane potential and activity of the AKT kinase were evaluated by JC-1 staining and a genetically encoded fluorescent AKT reporter (a fluorescence resonance energy transfer, FRET assay), respectively. Metabolic pathways and pro-apoptotic priming before and after exposure to the tested inhibitors were measured using Seahorse XF analyser, and BH3 profiling, respectively. Selected genetic aberrations (i.e., mutations, gene deletions, or gene aberrations) were analysed in the cohort of 126 consecutive newly diagnosed MCL patients by fluorescent in-situ hybridization (FISH) and targeted next-generation sequencing. Correlation of the detected genetic changes with response to immunochemotherapy was implemented. Subsequently, cell clones with knockout or transgenic (over)expression of selected prognostically relevant genes were derived and used for preclinical assessment of impact of the studied aberrations on the sensitivity or resistance to the tested inhibitors, i.e., palbociclib, and venetoclax.

Co-targeting CDK4/6 and anti-apoptotic BCL2 proteins with palbociclib and BH3-mimetics was a very effective treatment strategy with synthetic lethality both *in vitro* and *in vivo*. Palbociclib exposure caused downregulation of cyclins, mild downregulation of anti-apoptotic MCL-1 protein and increased levels of proapoptotic BIM bound on BCL2 and BCL-XL. Other mechanisms behind the observed synergy included an increased pro-apoptotic priming after palbociclib exposure caused by metabolic and mitochondrial stress pathways. Loss of *RB1* caused resistance to palbociclib and represents a negative predictive marker, while overexpression of *MYC* resulted in

increased sensitivity to venetoclax. Other tested aberrations did not change sensitivity either to palbociclib or to venetoclax.

The combination of palbociclib and venetoclax is an innovative chemotherapy-free treatment strategy for aggressive lymphoma patients without *RB1* deletion.

Key words: aggressive lymphoma, palbociclib, venetoclax, cyclin-dependent kinase inhibitors, BH3-mimetics

Abstrakt:

Agresivní podtypy B-non Hodgkinských lymfomů jsou charakterizovány deregulací buněčného cyklu a apoptózy z důvodu rekurentně se vyskytujících molekulárních a cytogenetických aberací, včetně zvýšené exprese D-cyklinů, amplifikace genů kódujících cyklin-dependentní kinázy a transkripční faktory (*MYC*), mutací a delecí důležitých regulátorů buněčného cyklu (*RB1, TP53*, *CDKN2A*) a aberantní exprese anti-apoptotických proteinů (*BCL2).* Společná inhibice cyklin-dependentní kinázy 4/6 palbociklibem spolu s inhibicí anti-apoptotických BCL2 proteinů pomocí BH3-mimetik (BCL2 inhibitor venetoklax, MCL1 inhibitor S63845 a BCL-XL inhibitor A11556463) představuje smysluplnou kombinaci pro léčbu B-NHL.

Na experimenty bylo využito 20 buněčných linií lymfomu z buněk pláště a difúzního velkobuněčného lymfomu a 4 xenografty odvozené od pacientů s lymfomem buněk pláště po selhání chemoterapie či ibrutinibu, inhibitoru Brutonovy kinázy. Hladiny proteinů před a po léčbě byly stanoveny pomocí western blotu. Změny potenciálů na mitochondriální membráně a aktivita AKT byly změřeny JC-1 barvením a geneticky kódovaným fluorescentním AKT reportérem. Metabolické změny a náchylnost buněk k apoptóze před a po léčbě byli změřeny pomocí Seahorse XF analyzéru a BH3 profilování. Vybrané genetické aberace (mutace, genové delece či jiné aberace) byly analyzovány na kohortě 126 pacientů s nově diagnostikovaným lymfomem z buněk pláště pomocí fluorescenční in situ hybridizace a cíleného sekvenování nové generace pro možnost hodnocení vlivů rekurentních genetických aberací na rezistenci vůči standardní imunochemoterapii. Následně byli odvozeny buněčné klony s knockoutem nebo zvýšenou expresí vybraných prognosticky relevantních genů s cílem preklinického testování vlivu těchto aberací na citlivost či rezistenci k palbociklibu a venetoklaxu.

Cílená inhibice buněčného cyklu pomocí palbociklibu a indukce apoptózy BH-3 mimetiky byla efektivní léčebnou strategií *in vitro* i *in vivo*. Expozice palbociklibu vedla ke snížení koncentrace cyklinů a mírně i anti-apoptotického MCL-1 proteinu a zvýšení množství proapoptotického proteinu BIM vázaného na BCL2 a BCL-XL. Další mechanismy zodpovědné za synergizmus zahrnovaly zvýšenou náchylnost buněk k apoptóze aktivací mitochondriálních a metabolických stresových reakcí účinkem palbociclibu. Ztráta genu *RB1* byla negativním prediktivním znakem zodpovědným za rezistenci na palbociklib, zatímco zvýšená exprese genu *MYC* vedla k vyšší

citlivosti buněk na venetoklax. Jiné detekované genetické aberace neovlivňovaly citlivost k testovaným inhibitorům.

Kombinace palbociklibu a venetoklaxu je inovativní léčebnou metodou u pacientů s agresivním lymfomem bez delece genu *RB1*.

Klíčová slova: agresivní lymfom, palbociklib, venetoklax, inhibitory cyklin-dependentních kináz, BH3-mimetika

List of abbreviation

ABC	activated B-cell
AML	acute myeloid leukaemia
ASCT	autologous stem cell transplant
ATM	ataxia-telangiectasia mutated
BCL-XL	B-cell lymphoma-extra large
BCL2	B-cell leukaemia/lymphoma-2
BCR	B-cell receptor
BH3	B-cell lymphoma-2 homology domain 3
BL	Burkitt lymphoma
BM	bone marrow
BTKi	Bruton tyrosine kinase inhibitor
CAR-T	chimeric antigen receptor T-cell
CDK	cyclin-dependent kinase
CDKi	cyclin-dependent kinase inhibitor
CDKN2A	cyclin-dependent kinase inhibitor 2A
CLL	chronic lymphocytic leukaemia
CLL/SLL	chronic lymphocytic leukaemia/small lymphocytic lymphoma
CNS	central nervous system
CR	complete remission
DLBCL	diffuse large B-cell lymphoma

EBV	Epstein-Barr virus
ECAR	extracellular acidification rate
EFS	event-free survival
ECAR	extracellular acidification rate
F	female
FBS	fetal bovine serum
FISH	fluorescence in-situ hybridization
FL	follicular lymphoma
FRET	Förster resonance energy transfer
GCB	germinal centre B-cell
HGBL	high-grade B-non Hodgkin lymphoma
IC50	half-maximal inhibitory concentration
IMDM	Iscove's modified Dulbecco's medium
LD50	median lethal dose
M	male
MCL	mantle cell lymphoma
MCL1	myeloid cell leukaemia-1
MIPI	Mantle-cell lymphoma International Prognostic Index
NGS	next-generation sequencing
NHL	non-Hodgkin lymphoma
NK	natural killer

OCR	oxygen consumption rate
ORR	overall response rate
OS	overall survival
PCNSL	primary central nervous system lymphoma
PD	progressive disease
PDX	patient-derived lymphoma xenograft
PFS	progression-free survival
PI3K	phosphatidylinositol-3 kinase
PMBL	primary mediastinal large B-cell lymphoma
PR	partial remission
R/R	relapsed and/or refraktory
RB1	retinoblastoma
ROS	reactive oxygen species
SD	stable disease
TNF	tumour necrosis factor
TP53	tumour protein 53
VAF	variant allele frequency
VTX	venetoclax
WHO	World Health Organization

6. Introduction

Non-Hodgkin lymphomas (NHLs) represent the most frequent hematologic malignancies. According to the clinical behaviour NHLs can be divided into two subgroups: aggressive, and indolent lymphomas. Aggressive lymphomas comprise mantle cell lymphoma (MCL), diffuse large B-cell lymphoma (DLBCL), and Burkitt lymphoma (BL). Clinically, aggressive lymphomas are characterized by rapid growth promptly deteriorating clinical course and imminent need for therapy initiation. At the molecular level, aggressive lymphomas are characterized by the deregulation of cell cycle progression at the G1-S phase transition, and diverse blocks in the apoptotic machinery that result in insensitivity to various proapoptotic triggers. The disruption of cell cycle is usually a consequence of overexpression of D-type cyclins (i.e., cyclin D1, D2 or D3) and recurrent aberrations of important cell cycle regulators like tumour-suppressors retinoblastoma (*RB1*), tumour protein 53 (*TP53)* and cyclin-dependent kinase inhibitor 2A (*CDKN2A*), cyclin-dependent kinase 4 *(CDK4)*, or transcription factors (e.g., *MYC*). Deregulation of apoptosis in lymphoma cells is usually caused by the overexpression of anti-apoptotic B-cell leukaemia/lymphoma-2 (BCL2) protein family (e.g., BCL2 protein, myeloid cell leukaemia-1 (MCL1) protein and B-cell lymphoma-extra large (BCL-XL) protein), and loss of function of important sensors of genotoxic stress (e.g., TP53 or MDM2). Despite several novel anti-cancer agents having been introduced into the clinical practice in the last two decades, the prognosis of patients with relapsed and/or chemotherapy refractory lymphomas remains poor and calls for more effective anti-lymphoma molecules or treatment strategies.[1-12]

Induction of apoptosis through blocking the activity of overexpressed anti-apoptotic proteins by BCL2 homology domain 3 (BH3)-mimetics represents a novel treatment strategy for various hematologic malignancies. Similarly, targeting the deregulated cell cycle by cyclin-dependent kinase inhibitors (CDKi) has shown promising results in preclinical models of many cancer types, including aggressive lymphomas, and encouraging outcomes in clinical trials. [13-17]

6.1 Aggressive lymphomas

Malignant lymphomas can originate at multiple stages of normal lymphocyte development. Traditionally, they are divided into Hodgkin's (10%) and non-Hodgkin's lymphomas (90%). NHL

represent a broad spectrum of diseases which vary from indolent to aggressive subtypes and can also be divided by the cell of origin into B-cell lymphomas (85 - 90% of NHL) and T-cell and natural killer (NK) cell lymphomas. The particular lymphomas subtypes depend on the developmental stage of cells from which they arise. The key processes responsible for B-cell lymphomagenesis are errors occurring during immunoglobulin gene rearrangement, somatic hypermutation and heavy-chain class switching of immunoglobulin genes during the stimulation of a naive mature B-cells with antigens. Hallmarks of many B-NHLs are specific translocations of proto-oncogenes into the immunoglobulin loci for heavy or light chain. Additional events contributing to lymphomagenesis include inactivating mutations or deletions of various tumour-suppressor genes or chronic viral infection of B lymphocytes (e.g., Epstein-Barr virus).[1, 18-20]

DLBCL is the most common aggressive lymphoma subtype. Other aggressive B-NHL include Burkitt lymphoma and MCL. Current standard-of-care first-line treatment of aggressive B-NHLs include the combination of anti-CD20 monoclonal antibody rituximab with conventional chemotherapy regimens. Although approximately 60% of patients with DLBCL and MCL and 80-90% of patients with Burkitt lymphoma can achieve complete remission with intensive treatment, relapsed and/or refractory (R/R) patients have poor prognosis. [12, 21, 22] Patients with R/R lymphoma usually receive salvage chemotherapeutical regimens followed by autologous stem cell transplantation (ASCT). Other options include the recently approved chimeric antigen receptor T-cell (CAR-T) therapy or innovative targeted small molecules, such as Bruton tyrosine kinase inhibitor ibrutinib in the case of MCL or immunomodulatory agent lenalidomide in the case of DLBCL or MCL.[23, 24] However, prognosis of patients with R/R aggressive lymphomas is still not satisfactory, as remissions are usually short-lasting and relapses often occur. Novel treatment options are needed to improve the outcome of both, frontline and salvage therapies.

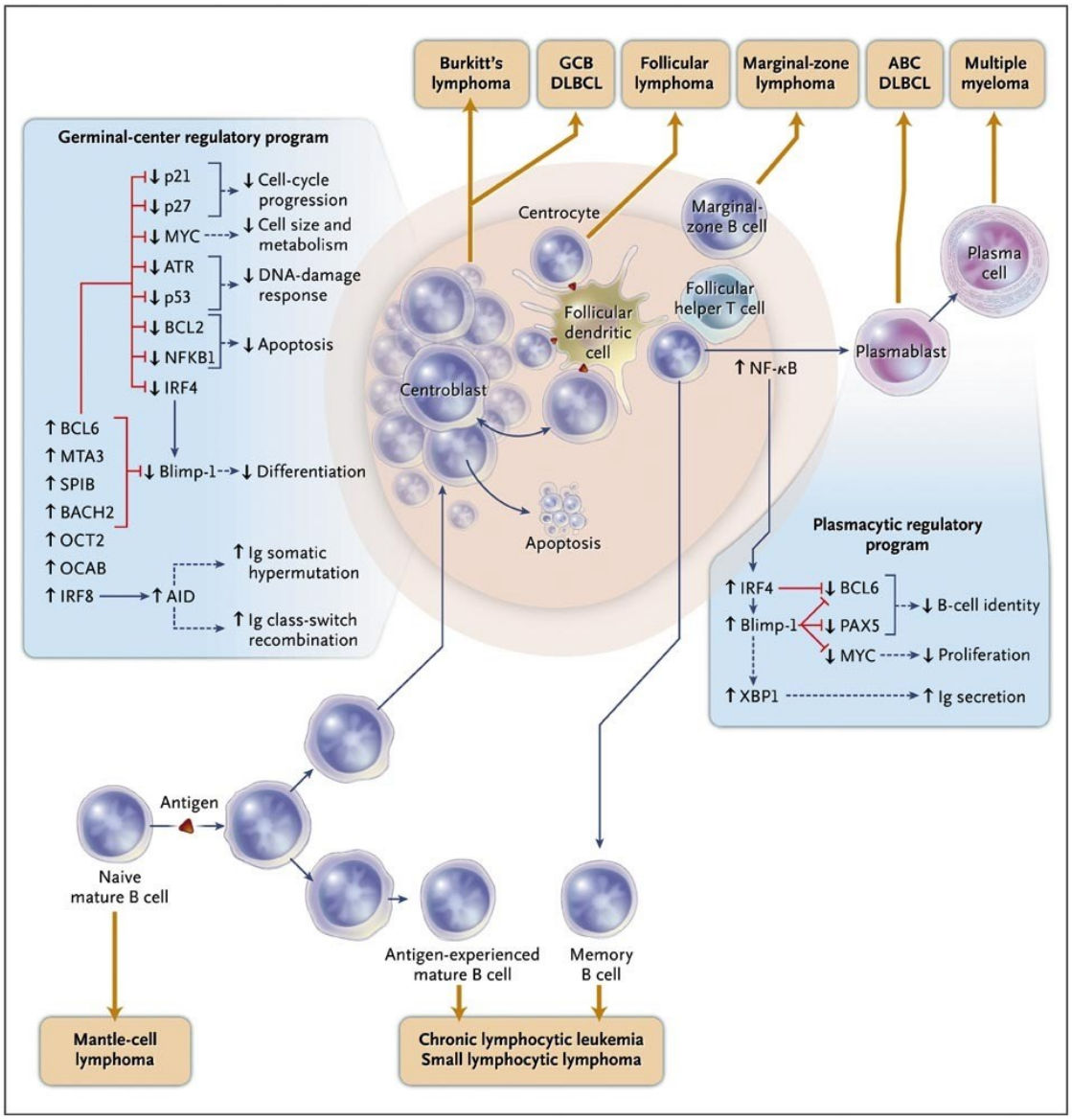

Figure 1. B-cell Differentiation and Lymphomagenesis. The figure shows how various B-NHL subtypes arise according to stages of B-cell development and their regulatory factors. *Lenz et al. Aggressive Lymphomas, NEJM 2010*

6.1.1 Mantle cell lymphoma

MCL represents approximately 7% of all lymphomas. The median age at diagnosis is approximately 65 years, and the disease affects twice as many males than females. Besides the occasional indolent forms mimicking chronic lymphocytic leukaemia (CLL), MCL is considered

to be an aggressive subtype of B-NHL and the treatment is often challenging, since MCL displays a continuous relapse pattern. Patients typically present with lymphadenopathy but extranodal and extrahaematological manifestations occur in almost 90% of cases, mostly including bone marrow infiltration, leukemisation and spleen, liver, or gastro-intestinal tract involvement. According to the World Health Organization (WHO) classification of malignant lymphomas, three categories of MCL can be distinguished – in situ MCL, non-nodal and classic MCL. Patients with the in situ MCL present with localized and indolent form of disease. The non-nodal MCL patients usually lack lymphadenopathy and have bone marrow infiltrated with MCL cells, leukemisation and splenic involvement. The clinical behaviour of non-nodal MCL is usually more indolent than of classic MCL, represented by 80-90% of MCL cases. The nodal (or classic) subtype can be according to morphology subsequently divided into classic, pleomorphic and blastoid variant. Pleomorphic and blastoid variants are associated with worse prognosis. [11, 12, 25-28]

On the molecular level, the hallmark of MCL is the overexpression of cyclin D1 due to chromosomal translocation t(11;14) (q13;q32). Aberrant overexpression of cyclin D1 leads to accelerated transition from G0/G1 phase to S phase of the cell cycle by forming a complex with cyclin-dependent kinase 4 or 6 (CDK 4/6). Cyclin D1 – CDK 4/6 complex phosphorylates RB1 and subsequently E2F transcription factors (responsible for regulation of cell cycle progression through other phases of cell cycle) are released. Besides the cyclin D1 overexpression, several other recurrent molecular-cytogenetic aberrations that affect the cell cycle and the regulation of apoptosis have been described in patients with MCL, such as the mutation or deletion of *TP53* and ataxia-teleangiectasia mutated (*ATM)*, deletion of *CDKN2A*, deletion of *RB1*, *C-MYC* gain or breakage, and amplification of *CDK4* and *BCL2*. [11, 29-35]

Cyclin D1 overexpression together with additional frequently aberrant genes translates into the high proliferation of MCL cells and shorter survival of MCL patients. The level of increase in the proliferation rate is evaluated in MCL by adding the tumour cell proliferation marker MIB-1 (Ki-67 index) to MCL International Prognostic Index (MIPI).[36, 37]

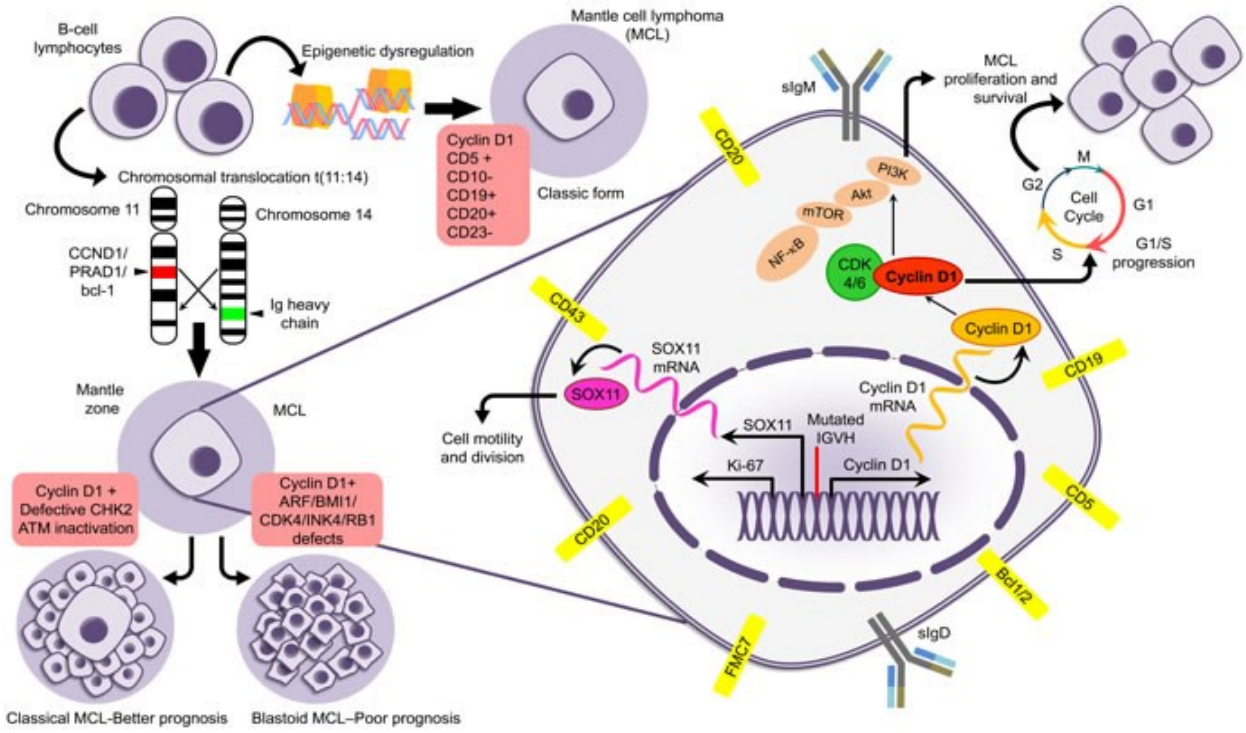

Figure 2. Mantle cell lymphoma pathogenesis. The figure shows the genetic mechanisms and their consequences in MCL cells. *Inamdar et al. Mantle cell lymphoma in the era of precision medicine-diagnosis, biomarkers, and therapeutic agents. Oncotarget 2016*

Due to the aggressiveness of the disease, high proliferation rate and relapsing pattern, MCL is associated with poor prognosis with median overall survival (OS) of 3-5 years. Recent advances in therapy, however, might improve this metric. The current standard front-line treatment consists of alternating the R-CHOP regimen with high-dose cytarabine and/or platinum-based chemotherapy regimens followed by rituximab maintenance. Young and fit patients with aggressive disease after 6 cycles of induction chemotherapy are indicated for consolidation with high-dose therapy and ASCT. The standard treatment for R/R patients is Bruton tyrosine kinase inhibitor (BTKi) ibrutinib. Allogeneic stem cell transplantation should still be considered in eligible individuals with extremely aggressive disease. Other treatment options for R/R MCL include chemotherapy regimens based on other agents that were not used in front-line treatment (rituximab-bendamustine +/- cyrarabine), or immunotherapy approaches with immunomodulatory agent lenalidomide, bispecific CD20xCD3 antibodies (glofitamab) or autologous CD19 CAR-T cells. Alternatively, targeted treatment with proteasome inhibitor bortezomib or mTOR inihitor temsirolimus can be used. Despite many new and promising treatment options the prognosis of patients with multiple relapses, especially after ibrutinib failure is extremely poor due to an

increasing number of genetic aberrations. These highly proliferative and aggressive disease subtypes require novel treatment strategies. [28, 35, 38-42]

6.1.2 Diffuse large B-cell lymphoma

DLBCL is the most common lymphoma in the Western hemisphere, comprising around 40% of all lymphoproliferations. Median age of diagnosis is between the sixth and seventh decades. DLBCL is a clinically and genetically heterogeneous disorder. Determined by immunohistochemistry or gene expression profiling, two subtypes of DLBCL have been defined with regards to their origin – germinal centre B-cell (GCB) and activated B-cell (ABC). The cell-of-origin-based classification is associated with distinct biological features including different distributions of genetic aberrations and clinical course, where ABC DLBCL is associated with worse prognosis. Of the formerly classified DLBCLs, approximately 8% are now re-classified as high-grade B-NHL (HGBL) with *MYC* and *BCL2* and/or *BCL6* rearrangement due to their genetic background. These highly aggressive lymphomas with apoptotic dysregulation are associated with shorter survival and chemoresistance. [2, 26, 43-46]. Another possible classification approach distinguishes primary (cases arising de novo) and secondary DLBCLs - which represent a transformation from less aggressive lymphoproliferative disorders – most commonly from chronic lymphocytic leukaeamia/small lymphocytic lymphoma (CLL/SLL), follicular lymphoma (FL) or Hodgkin lymphoma. DLBCL is also associated with genetic or acquired immunologic deficiency diseases and chronic inflammation. [47-49] There are also several DLBCL subtypes characterized by specific predominant extra-nodal presentation, such as primary central nervous system lymphoma (PCNSL), primary mediastinal (thymic) large B-cell lymphoma (PMBL) and rare intravascular large B-cell lymphoma, primary cutaneous DLBCL, leg type (arises in the skin of lower extremities).[3]

Unlike in MCL, the cell cycle deregulation in DLBCL is not specified to a single mechanism, instead there are several mechanisms leading to its acceleration, including the overexpression of cyclin D2 in 40% of patients with ABC subtype and overexpression of cyclin D3 in most patients with GCB subtype leading to the accelerated transition from G0/G1 phase to S phase of the cell cycle. The inactivation of *CDKN2A* and aberrations of *TP53* have also been observed. Rearrangements of *BCL6* (which are functionally inactivating p53) occur in 30-40% of

cases. *BCL2* translocations are detected in DLBCLs transformed from follicular lymphoma and in approximately 20% of de novo DLBCLs and amplifications of the 18q21 locus resulting in *BCL2* overexpression were described in approximately 20% of ABC DLBCLs. As mentioned before, *MYC* rearrangement is associated with complex genetic alterations (including *BCL2* and/or *BCL6*) leading to the highly aggressive subtype of B-NHL.[4, 50-52]

The first-line treatment for majority of DLBCL patients consists of the combination of anti-CD20 monoclonal antibody rituximab with the CHOP chemotherapy regimen (cyclophosphamide, doxorubicin, vincristine, prednisone), while in genetically high-risk fit patients, escalation to more intense protocols is recommended. For some special subtypes (PCNSL or HGBL) upfront consolidation with high dose therapy and ASCT should be considered, otherwise it is used in patients who did not achieve complete remission (CR) or for relapsed cases after salvage chemotherapy, which usually consist of platinum-based regimens. Novel treatment strategies for R/R DLBCL include mostly immunotherapeutic options like CAR-T cell therapy, several bispecific T-cell engagers (blinatumomab, odronextamab, epcoritamab, glofitamab), polatuzumab vedotin (antibody-drug conjugate, in which monoclonal anti-CD79b antibody is bounded to monomethyl auristatin E, that works as microtubule toxin), the immune modulator lenalidomide or novel antibodies, like the anti-CD19 monoclonal antibody tafasitamab.[3, 53-60]

6.1.3 Burkitt lymphoma

Burkitt lymphoma is a highly aggressive B-NHL with three different subtypes – sporadic, endemic, and immunodeficiency-associated. The sporadic subtype is more common in children, and it accounts for less than 1% of NHL in adults. It occurs more than twice as often in males than in females. The sporadic BL subtype is often related to an Epstein-Barr virus (EBV) infection. The endemic subtype was described and is found mostly in equatorial Africa and New Guinea and presents as a facial tumour. Almost all cases are associated with EBV. Immunodeficiency-associated BL is mostly found in patients with inherited or acquired immunodeficiency, most commonly HIV-positive patients, and to a lesser extent in patients after organ transplantations. Similarly, to the other Burkitt lymphoma subtypes, EBV positivity is also common. [5, 61-64]

The genetic hallmark of BL is the overexpression of the *MYC* proto-oncogene, mostly due to translocation t(8;14), which places the *MYC* gene into the immunoglobulin heavy chain locus which in turn results in an enhanced proliferation rate of BL cells. Acquisition of other genetic aberrations - such as mutations of transcription factor 3 (*TCF3)* or its negative regulator *ID3*, were detected in approximately 70% cases of sporadic BL. Mutations of *TCF3* leads to the dysregulation of the B-cell receptor (BCR)/phosphatidylinositol-3 kinase (PI3K) signalling pathway and cyclin D3 overexpression (found in approximately 30% of BL), which result in global cell-cycle dysregulation and extremely enhanced proliferation. Mutations of *TP53* (detected in 35% of patients with BL), on the other hand, further impair apoptosis. [6, 7, 65, 66]

Because of the rapid tumour growth patients usually present with acute symptoms due to large masses, typically located in the pelvis and abdomen with high rates of extra-nodal infiltration, especially intestinal involvement. However, the involvement of other intra-abdominal organs or masses in the thorax are also common and the central nervous system (CNS) is affected in approximately 15% of newly diagnosed BL patients. [6, 67-69]

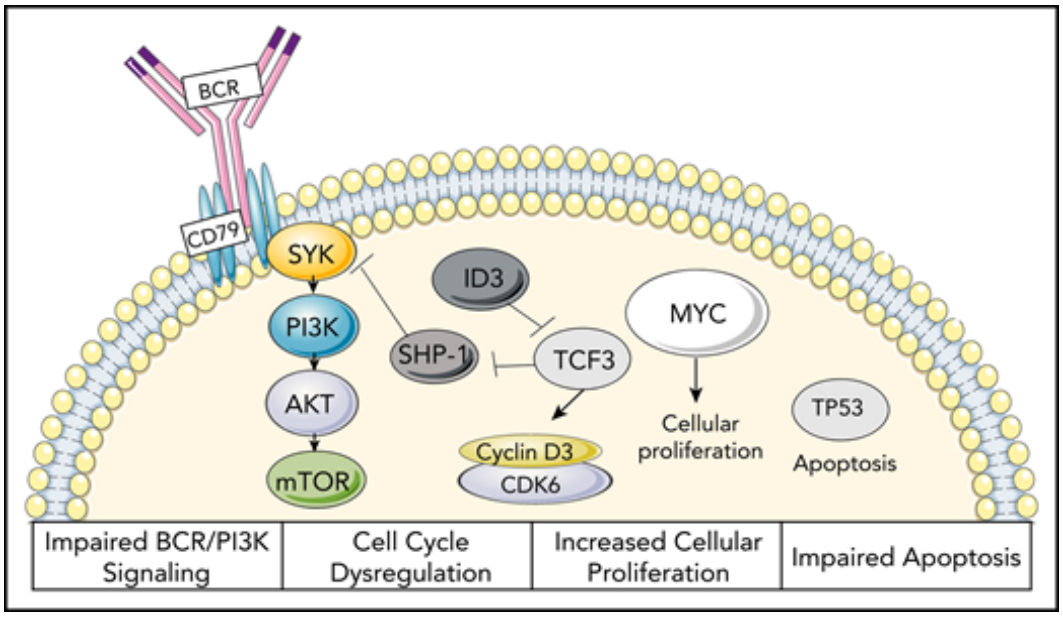

Figure 3. Burkitt lymphoma pathogenesis. The figure shows genetic mechanisms leading to the dysregulation of BCR/PI3K signaling, impaired cell-cycle regulating leading to an increased cellular proliferation, and impaired apoptosis in BL. *Schmitz et al. Oncogenic mechanisms in Burkitt lymphoma, Cold Spring Harbor Perspectives in Medicine 2014*

Owing to the rapid cell proliferation rate, BL is highly chemo-sensitive disease with almost 90% complete remissions after the administration of standard, intensified chemotherapeutical regimens (e.g., R-hyperCVAD/R-HDMTX/AraC, R-CODOX-M/R-IVAC or R-EPOCH), followed by ASCT to lower the risk of further relapse. However, relapsed patients are unfortunately usually chemo-refractory, with median OS of only 2.8 months with allogenic bone marrow transplant as the only potentially curative option. Thus, novel therapeutic strategies are strongly needed for R/R BL patients, or those who are not eligible for intensified front-line treatment due to age or comorbidities. [70-74]

6.2 Apoptotsis

Apoptosis is a highly regulated type of programmed cell death and a crucial process resulting in the removal of damaged, aged, or obsolete cells. Two major apoptosis induction pathways have been described – the extrinsic and the intrinsic. The extrinsic pathway is triggered by the activation of death receptors of the tumour necrosis factor (TNF) superfamily with specific death ligands on the cell surface. The intrinsic, or mitochondrial pathway, is initiated by cellular stress such as DNA damage, uncontrolled proliferation, hypoxia, oxidative stress, or loss of survival signals, which leads to increased outer mitochondrial membrane permeabilisation followed by mitochondrial depolarization and cytochrome c release. The cellular destruction is then driven by the activation of caspases in both pathways. Activated caspases with their proteolytic activity cleave cytoskeletal and nuclear proteins, which leads to controlled disintegration of the cell. Besides the major extrinsic and intrinsic pathways, other apoptotic pathways have been described. Cytotoxic NK and T cells, that kill infected or transformed cells use a third, perforin-granzyme, apoptotic pathway. Perforin creates pores in the cell membrane or can enter the target cell via endocytosis. Granzymes then enter the cells through created pores (or specific receptors) and directly activate caspases. Granzyme B can also trigger apoptosis indirectly by the activation of pro-apoptotic regulators on the mitochondrial membrane, leading to the activation of the mitochondrial pathway. [8, 9, 75-80]

In most cancers, including NHLs, the apoptotic machinery is blocked through dysregulation of the mitochondrial pathway. This pathway is regulated by members of the BCL2 protein family. The key anti-apoptotic proteins from the BCL2 family are BCL2, MCL1 and BCL-XL. The pro-

survival function is exerted by binding and sequestering key pro-apoptotic effectors BAX and/or BAK and thus preventing the downstream induction of intrinsic apoptotic pathways. Pro-apoptotic proteins, represented by BIM, BID and NOXA antagonize the function of anti-apoptotic proteins. In healthy cells, pro-apoptotic effectors BAX and/or BAK are repressed by the anti-apoptotic proteins, which under specific conditions - cellular stress signals, are "neutralized" by pro-apoptotic proteins and BAX and/or BAK are released, and thereby initiate apoptosis.[8, 9, 81]

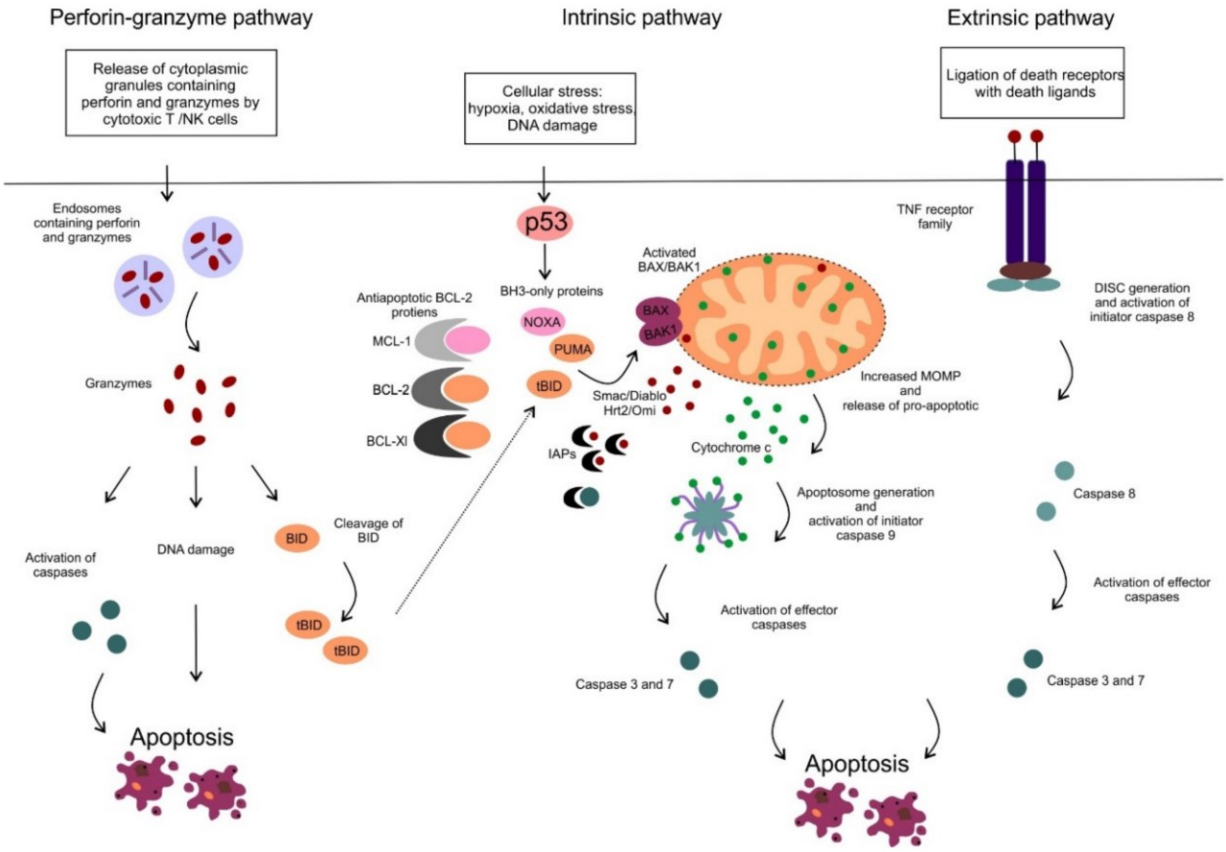

Figure 4. Apoptotic pathways. The figure shows perforine-granzyme, mitochondrial and extrinsic apoptotic pathways. *Klanova et al. BCL2 Proteins in Pathogenesis and Therapy of B-Cell Non-Hodgkin Lymphomas, Cancers 2020*

6.2.1. Deregulation of apoptosis in aggressive lymphomas

The ability to override cell death signaling pathways is a hallmark of many haematological malignancies. High BCL2 expression due to the translocation t(14;18)(q32;q21) is a hallmark of follicular lymphoma, but it is also observed in chronic lymphocytic leukaemia and MCL. Its levels vary in DLBCL and MCL (as was described previously) and acute lymphoblastic leukaemia and

are generally low in BL. Since only subset of DLBCL and MCL patients have deregulated BCL2 and the expression of BCL2 is generally low or undetectable in Burkitt lymphoma, many aggressive lymphomas depend on other anti-apoptotic proteins. [8, 82-84] The MCL1 protein is highly expressed in aggressive B-NHLs (84% of DLBCL and 89% of Burkitt lymphoma) and its potential role in lymphoma pathogenesis was evaluated in transgenic mouse models, where MCL1 knock-in mice developed lymphoma with a higher frequency.[8, 85]

Other mechanism leading to the dysregulation of apoptosis in aggressive lymphomas include lack of pro-apoptotic BCL2 proteins or *TP53* alterations. Although the deletion of *BIM* was found in approximately one-third of MCL cell lines, this alteration in patients with newly diagnosed MCL is rare. However, levels of BIM vary among patients and it was shown, that lower levels negatively correlate with a patient's prognosis. [86, 87] Mutations and/or deletions of *TP53* are commonly detected in aggressive lymphomas and correlate with adverse prognosis and chemoresistance in many cancers, lymphoprolilferative diseases included. One of the many TP53 functions is the activation of pro-apoptotic proteins PUMA and NOXA when critical DNA damage is reported. *TP53* aberrations thus lead to an increased survival of affected cells and genomic instability. [10, 88, 89]

6.2.2 BH3-mimetics

The evidence that cancers, aggressive lymphomas included, highly depend on BCL2 proteins to avoid apoptosis, has led to the development of BH3-mimetics. BH3-mimetics overcome resistance of cancer cells to apoptosis by blocking the activity of pro-survival BCL2 proteins, resulting in the release of pro-apoptotic effectors and eventually to apoptosis. Moreover, targeting BCL2 proteins is independent from the effects of frequently aberrated *TP53*, so it can overcome its negative prognostic impact.[13, 90, 91]

Venetoclax, the orally available selective inhibitor of BCL2 protein and the only BH3-mimetic currently approved by the authorities, is to date used for the treatment of patients with CLL/SLL and acute myeloid leukaemia (AML). However, venetoclax recently underwent several clinical trials and showed clinical activity in MCL, and BCL2-dysregulated DLBCL. Despite high number of patients initially responding to the therapy, remissions were usually short-lived and patients eventually developed resistance to venetoclax monotherapy, that a rational drug combination is needed. The combination of venetoclax and BTKi ibrutinib, with or without anti-

CD20 (rituximab/obinutuzumab) antibodies was tested by Le Gouill et al. and represents a highly effective chemotherapy-free regimen for patients with MCL.[92-99]

Besides BCL2, various MCL1 inhibitors have been recently developed (including S63845, S64315 and AZD5991) which demonstrated great anti-tumour efficacy both *in vitro* and *in vivo*. Interestingly, combined inhibition of MCL1 and BCL2 was shown to be highly effective in preclinical models of aggressive B-NHLs and could even overcome the acquired resistance to BCL2 inhibitors. However, MCL1 inhibitors that have been already tested in clinical trials showed high levels of intolerability and many studies were suspended due to safety reasons. [98, 100-102] BCL-XL, another key anti-apoptotic protein, represents a reasonable therapeutic target and many more or less selective inhibitors of BH3 family proteins have been developed. However, clinical use of BCL-XL inhibitors is limited due to high BCL-XL dependency observed in platelets, leading to rapid destruction of platelets and thrombocytopenias following administration of these agents. [103, 104]

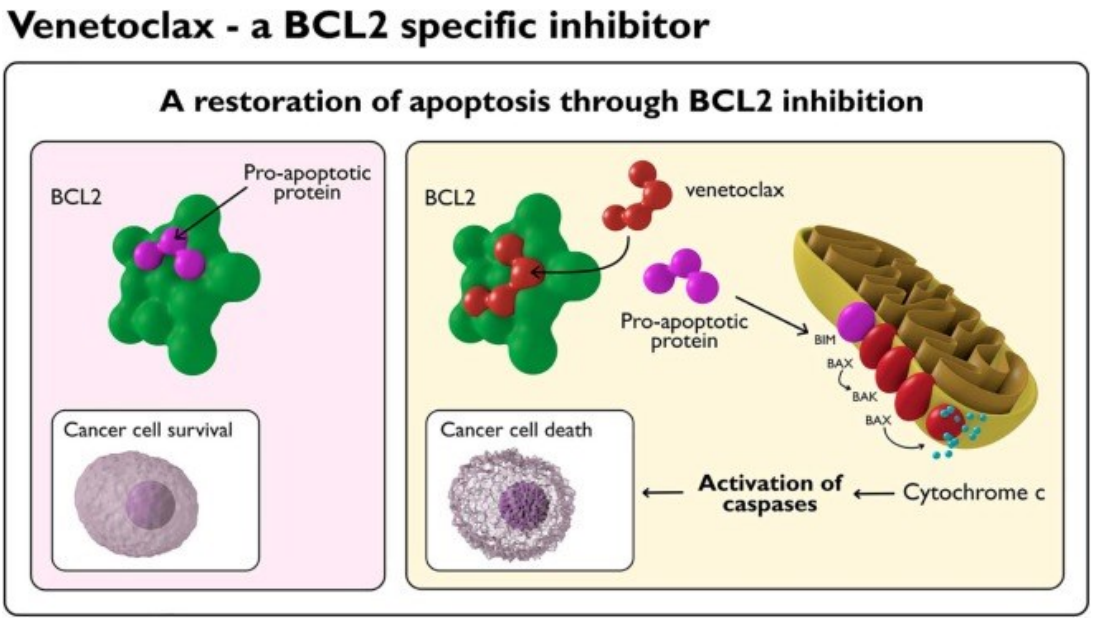

Figure 5. The mechanism of action of venetoclax. The figure shows the release of pro-apoptotic proteins from anti-apoptotic BCL2 and the subsequent activation of pro-apoptotic effectors leading to cytochrome c release and caspase activation after administration of Venetoclax. *Mihalyova et al. Venetoclax: A new wave in hematooncology, Experimental Heatology 2018*

6.3 Cell cycle

The cell cycle is a complex of processes that direct the cell through a specific sequence of events resulting in mitosis. The progression through its phases is regulated by numerous proteins, with cyclin-dependent kinases (CDKs) and cyclins playing a key role. The various CDK-cyclin complexes regulate the passage from one phase of the cell cycle to another. CDKs are serine/threonine protein kinases with relatively constant and stable concentration during all phases of the cell cycle. CDKs need to be activated and driven to the nucleus by noncovalent binding to their respective cyclins, which exhibit cyclic expression during the cycle. Each CDK can interact only with its specific cyclins and thus particular CDKs are activated only at specific times. The CDK-cyclin complexes then phosphorylate a variety of substrates crucial for cell cycle progression and modulate transcription of important genes.[14, 105-108]

6.3.1 Cell cycle deregulation in aggressive lymphomas

Overexpression of cyclin D1 due to the t(11;14)(q13;q32) translocation in MCL patients directly dysregulates and accelerates cell cycle progression and proliferation and leads to an accelerated transition from the G0/G1 phase to the S phase of the cell cycle. In MCL, as well as in other subtypes of aggressive B-NHLs, the cell cycle, and particularly the transition to the S phase, is dysregulated by several other mechanisms. Direct loss of function of the RB1 protein by deletion of *RB1* gene is prevalent in approximately 30% of patients with MCL and functional inactivation of the RB protein by viral oncoprotein has been described in HIV-associated Burkitt lymphoma. [11, 109, 110] Overexpression of cyclin D2 was found in 40% of patients with ABC-DLBCL and was associated with a worse prognosis. On the other hand, in most GCB-DLBCL and in 35% of Burkitt lymphomas, overexpression of cyclin D3 is present. Cyclins D2 and D3, similarly to cyclin D1, bind to CDK4/6 and promote the progression from the G0/G1 phase to the S phase. The inactivation by deletion, mutation, or methylation of the tumour-suppressor gene *CDKN2A* was described in one quarter of MCLs and DLBCLs and is associated with both a worse prognosis and chemoresistance. *CDKN2A* codes for p14ARF, which activates p53 leading to G1-S phase arrest, and p16INK4A that inhibits RB phosphorylation and similarly arrests the cell cycle in the G0/G1

phase. Upregulation of the *MYC* oncogene - the hallmark of Burkitt lymphoma, which is also found in aggressive subtypes of DLBCL and in approximately 20% of MCL, leads to the activation and induction of cyclins and CDKs and the functional inactivation of cell cycle inhibitors. Lastly, *TP53* aberrations and dysregulations of the P53-pathway play an important role in pathogenesis of many malignant diseases since they regulate many target molecules, mainly to promote cell cycle arrest in order to process DNA repairs or the induction of apoptosis. [6, 7, 15, 32, 50-52, 66, 107, 111-114]

In conclusion, the dysregulated progression from the G0/G1 to the S phase of the cell cycle described in aggressive B-NHLs, either direct via the overexpression of D-types cyclins and/or *CDK4*, or indirect via loss of function of *CDKN2A, TP53* or the upregulation of *MYC*, the inhibition of cell cycle progression presents a rational treatment strategy for aggressive lymphomas.

6.3.2 Cyclin-dependent kinase inhibitors

The leading role of CDKs in cell cycle regulation, and their dysregulation in many cancers has lead to a great interest in the development of cyclin-dependent kinase inhibitors (CDKi) since the early 1990s. The mechanism of action of CDKi is induction of cell cycle arrest and subsequent cessation of proliferation. [15, 16, 115, 116]

The first two generations of CDKi included pan-CDK inhibitors (CDKi inhibiting more than 4 CDKs or other kinases) or multi-CDK inhibitors (CDKi inhibiting more than 2 CDKs) which had its challenges. For example, roscovitine and dinaciclib were effective but highly toxic. The third generation is consituted by highly selective CDK4/6 inhibitors palbociclib, abemaciclib, ribociclib and trilaciclib. In 2015 palbociclib was the first CDKi approved by the FDA for the treatment of HR-positive and HER2-negative advanced or metastatic breast cancer in women with disease progression following endocrine therapy. Since then, palbociclib has undergone several clinical trials as a single agent or in combination with other treatment strategies for treatment of various breast cancer subtypes, pancreatic neuroendocrine tumours and pancreatic adenocarcinomas, ovarian cancer, urothelial carcinoma, colorectal carcinoma, melanoma, glioma, sarcomas, and hematologic malignancies. Ribociclib and abemaciclib have also been approved by the authorities for HR+ metastatic breast cancer and are currently being tested in numerous clinical

trials. Meanwhile and interestingly, trilaciclib is being used to reduce chemotherapy-induced bone marrow suppression.[15-17, 109, 115-121]

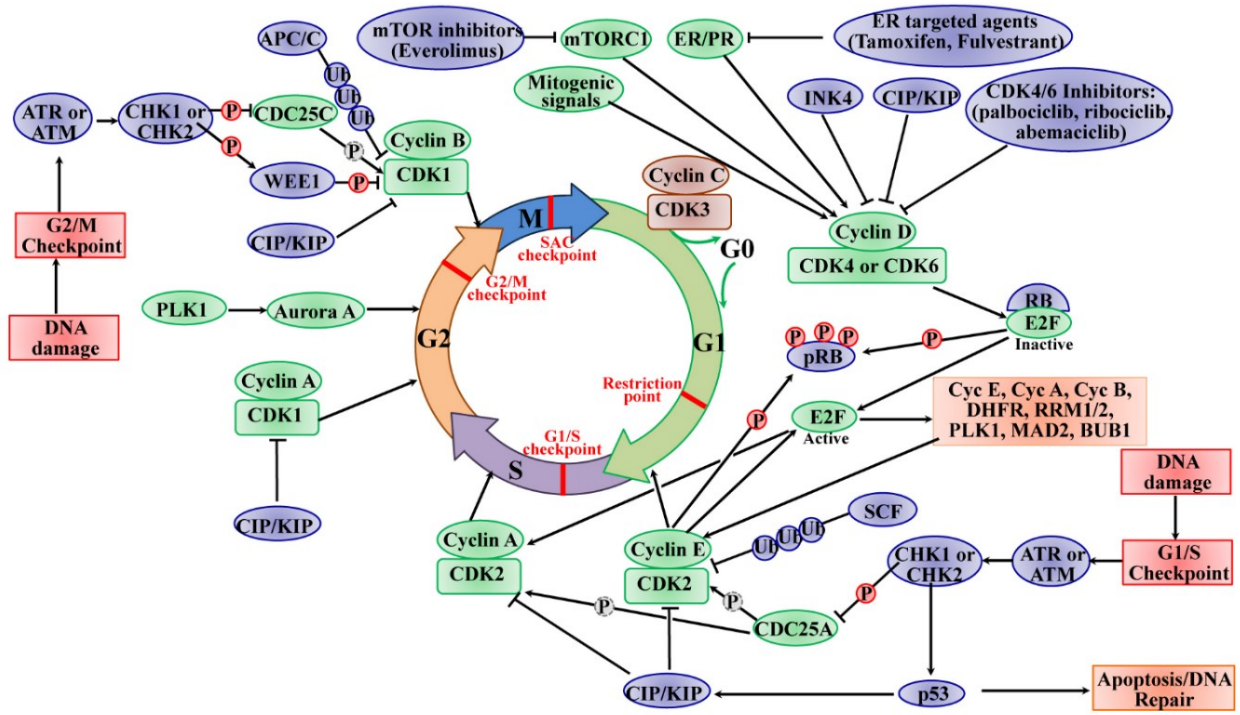

Figure 6. Cell cycle and its regulatory pathways with possible therapeutic targets in case of deregulation. Cell cycle phases and complex regulatory mechanisms leading to the cell cycle progression or arrest with possible therapeutic targets. *Ding et al. The Roles of Cyclin-Dependent Kinases in Cell-Cycle Progression and Therapeutic Strategies in Human Breast Cancer, Cancers 2020*

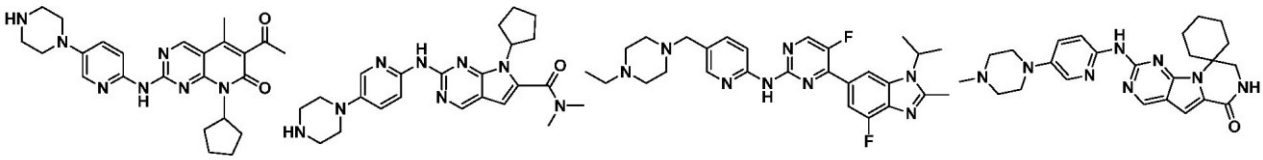

Figure 7. Chemical structure of palbociclib, ribociclib, abemaciclib and trilaciclib

Since CDKis have shown promising activity in numerous preclinical models of aggressive lymphomas, several clinical trials have been conducted. In 2010, 17 patients with relapsed MCL were treated with single agent palbociclib in a phase I study (NCT00420056). The treatment was well tolerated, no patient discontinued the treatment due to adverse events, and the most common toxicities included gr. 3-4 neutropenia and thrombocytopenia leading to dose reduction. One patient (6%) achieved CR, 2 patients (12%) partial response and 7 patients (41%) had stable disease. Both median time to progression and progression-free survival were 4 months, however responders have been on treatment for more than 2 years. Despite manageable safety profile and promising activity of single-agent palbociclib, combinations with other agents were tested to further improve treatment efficacy. In other clinical studies palbociclib was administered in combination with either ibrutinib (BTKi) or bortezomib (proteasome inhibitor). In the study with bortezomib (NCT01111188) overall response rate (ORR) was only 21%, however the combination of palbociclib with ibrutinib was very effective, with 68% responders and 37% CR. [122-124]

7. Hypotheses

1. Aberrant (over)activation of cyclin-dependent kinases, and oncogenic (over)expression of anti-apoptotic BCL2 proteins both represent rational and actionable targets in aggressive lymphomas that can be effectively inhibited by specific small molecule inhibitors with a promising potential for a synthetic lethality.

2. *TP53* and *CDKN2A* aberrations belong to the most frequent recurrent genetic lesions in mantle cell lymphoma patients causing deregulation of the cell cycle and apoptosis. We hypothesise that concurrent aberration of *TP53* and *CDKN2A* will be associated with resistance to chemotherapy and calls for innovative treatments.

8. Aims

1. To study the efficacy, molecular mode of action, and predictive markers of susceptibility to cyclin-dependent kinase inhibitor palbociclib, single-agent or in combination with selected BH3-mimetics (namely – the BCL2 inhibitor venetoclax, MCL1 inhibitor S63845 and BCL-XL inhibitor A1155463) using *in vitro* and *in vivo* models of chemotherapy refractory aggressive lymphomas. Additionally, upon understanding pathophysiological and genetic mechanisms of susceptibility, to evaluate which patients would benefit most from the novel treatment combination.

2. To analyse *TP53* and *CDKN2A* by FISH and targeted NGS in consecutive MCL patients treated at the General University Hospital.

9. Materials and methods

9.1 Cell lines and patient-derived xenografts

UPF1H, UPF7U, and UPF4D cell lines were derived in our laboratory from patients with treatment-refractory MCL (UPF7U, UPF1H) and DLBCL (UPF4D). HBL2 cell line was a gift of prof. Martin Dreyling. Remaining cell lines were purchased from DSMZ or ATCC cell banks. Cell lines were cultured in Iscove's modified Dulbecco's medium (IMDM) supplemented with 15% fetal bovine serum (FBS) and 1% penicillin/streptomycin. All patient-derived xenografts (PDX) models were established using immunodeficient NOD.Cg-*Prkdc*^{scid} *Il2rg*^{tm1Wjl}/SzJ mice (commonly referred to as NSG mice), approved by the Animal Care and Use Committee (MSMT-21527/2017-8). The primary lymphoma specimens were either homogenized through 45-microM nylon mesh and subcutaneously injected (10–30 × 10^6 cells/ mouse) into the adult NSG mice, or re-suspended in BD Matrigel Matrix (BD Biosciences) and surgically inserted into sub-renal capsules. After the subcutaneous tumors reached 2 cm in the largest dimension or when tumor-engraftment in the sub-renal region became visible by ultrasound examination (Vevo 3100/LAZR-X), the animals were euthanized, tumors excised and used for further analyses. Clinical parameters of derived PDX models are shown in Table 1.

PDX model	Lymphoma Subtype	Disease Course	Previous Treatment	
VFN-M1	MCL	1. relapse	Nordic protocol (R-maxiCHOP / HD-AraC) + ASCT	
VFN-M2	MCL	1. relapse	R-CHOP / HD-AraC + Rituximab maintenance	
VFN-M3	MCL	2. relapse	Nordic protocol (R-maxiCHOP / HD-AraC) + ASCT	ibrutinib
VFN-M8	MCL	1. relapse	R-CHOP / HD-AraC + rituximab maintenance	

Table 1. Clinical parameters of derived PDX models

9.2 Reagents, apoptosiss and proliferation assays

Palbociclib, venetoclax, S63845, and A1155463 were purchased from MedChemExpress. Annexin-V-FITC was from Apronex, Propidium Iodide from Sigma Aldrich and WST8 Quick Cell Proliferation Assay from BioVision.

The number of apoptotic cells was measured by flow cytometry (BD Canto II) after Annexin-V-FITC staining according to manufacturer's protocol. The anti-proliferative effect of drugs was determined using WST8 Quick Cell Proliferation Assay according to protocols after 72 hours preincubation of cells with several different concentrations and then measured on ELISA reader. Drug concentrations that induced apoptosis in 50% cells (LD50) or reduced proliferation to 50% cells (IC50) were determined using GraphPad Prism software by nonlinear regression. CompuSyn version 1.0 software (ComboSyn) was used to assess drug synergism between CDKi and selected BH3-mimetic. Combination indexes (CI) were calculated for different concentration of drugs depending on sensitivity.

9.3 Cell cycle analysis

Analysis of the cell cycle was performed after 24 hours of palbociclib pretreatment. The treated and untreated cells were firstly trypsinized, then washed with PBS and fixed with 70% ethanol and incubated on ice overnight. Then the cells were stained with propidium iodide for 1 hour (room temperature in the dark) and analyzed by flow cytometry.

9.4 Western blotting

After 24 hours pre-treatment with 1μM and 10 μM palbociclib of selected cell lines treated and untreated cells were harvested and lysed in RIPA buffer. Proteins were separated on SDS-polyacrylamide gels and electroblotted into nitrocellulose membranes. The membranes were overnight incubated with primary antibodies, washed and then incubated with specific peroxidase-conjugated secondary antibodies. Peroxidase activity was detected using Pierce™ ECL Western blotting substrates and a CCD camera LAS-4000 (Fujifilm). The specific used antibodies are listed in Table 2.

Target	Manufacturer	Cat. N.	Dilution
INK4a	Abcam	ab108349	1:2000
ARF	Thermo Fisher	MA5-14260	1:1000
Rb1	Santa Cruz Biotechnology	sc-50	1:1000
Rabbit IgG	Jackson ImmunoRes	711-036-152	1:10000
Mouse IgG	Jackson ImmunoRes	715-036-150	1:10000
PARP-1	Cell Signaling Technology	9532	1:500
Cleaved Caspase-9 (Asp330)	Cell Signaling Technology	52873	1:500
Caspase-7	Cell Signaling Technology	9492	1:500
Mcl-1	Cell Signaling Technology	5453	1:500
Bcl-2	Merck	B3170	1:500
Bcl-xl	Cell Signaling Technology	2764	1:1000
Bim	Cell Signaling Technology	2933	1:1000
Bak	Cell Signaling Technology	6947	1:1000
pRB S780	Cell Signaling Technology	8180	1:1000
Rb	Cell Signaling Technology	9309	1:1000
cyclin A	Cell Signaling Technology	4656	1:500
cyclin B	Cell Signaling Technology	4135	1:500
cyclin D1	Cell Signaling Technology	2978	1:250
cyclin D3	Invitrogen	AHF0132	1:250
CDK4	Cell Signaling Technology	2906	1:500
c-myc	Cell Signaling Technology	13987	1:1000
Hsp70	Cell Signaling Technology	9965	1:1000
α-tubulin	Merck	T6199	1:1000
Akt	Cell Signaling Technology	4691	1:1000
pAkt (S473)	Cell Signaling Technology	2965	1:1000
Bax	Cell Signaling Technology	5023	1:1000
Bid	Cell Signaling Technology	2002	1:1000
mTOR	Cell Signaling Technology	9964	1:1000
cyclin E	Cell Signaling Technology	4129	1:500
CDK1	Cell Signaling Technology	9116	1:500
CDK2	Cell Signaling Technology	2546	1:500
CDK7	Merck	C7089	1:5000

Table 2: List of primary and secondary antibodies

9.5 Experimental therapy of lymphoma-bearing mice

The experimental design was approved by the Institutional Animal Care and Use Committee (MSMT-11255/2015-4 and MSMT-37330/2020-2). Immunodeficient adult female NOD.Cg-PrkdcscidIl2rgtm1Wjl/SzJ mice (NSG mice) were used. Venetoclax was administered by oral

gavage (50 mg/kg) on days 1 - 5., palbociclib was given 5 hours after venetoclax administration by oral gavage at 150 mg/kg on days 1-5.

9.6 Co-immunoprecipitation

Cells harvested from subcutaneously grown tumours 24 and 48-hours after palbociclib treatment were lysed at 4°C for 25 min in a non-denaturing lysis buffer [1% (w/v) Triton X-100, 50 mmol/L Tris-HCl (pH 7.4), 300 mmol/L NaCl, 5 mmol/L EDTA, 0.02% (w/v) sodium azide supplemented with protease inhibitor (Sigma-Aldrich)] and centrifuged (16,000 × g, 4°C, 15 min). Protein concentration was measured with the BCA (bicinchoninic acid) Protein Assay Kit (Pierce). Protein samples were firstly three-times precleared with Protein A/G Agarose bead slurry (Pierce) which was incubated with anti-IgG antibody for 30 minutes at 4°C, followed by centrifugation (16,000 × g, 4°C, 2 sec). Cell lysates were split and incubated for 1 hour at 4°C with 10% BSA and Protein A/G Agarose beads with either a specific antibody or a corresponding isotype control immunoglobulin bound to them. Immunocomplexes were then centrifuged (16,000 × g, 4°C, 2 seconds), three times washed in ice-cold wash buffer [0.1% Triton X-100, 50 mmol/L Tris-HCl (pH 7.4), 300 mmol/L NaCl, 5 mmol/L EDTA, 0.02% sodium azide)] and once more in ice-cold 1% PBS. Then, the samples were fractionated by 12 % SDS-PAGE, followed by western blotting. To detect BCL2 and BCL-XL interaction with BIM, anti-BIM antibody (Cell Signaling) was used for the immunoprecipitation, and the precipitates were subjected to immunoblot analysis using anti-BCL2 (Dako) and anti-BCL-XL antibody (Cell Signaling).

9.7 Mitochondrial membrane potential assessment

Mitochondrial membrane potential was assessed by JC-1 dye (ThermoFisher) used according to the manufacturer´s protocols and measured by flow cytometry (BD FACS Canto II) after 72 hours cultivation with or without 1μM palbociclib. JC-1 exhibits potential-dependent accumulation in mitochondria indicated by a fluorescence emission at ~529nm for the monomeric form (present at low mitochondrial membrane potential) or ~590nm for the J-aggregates (formed at higher potentials). To set gates for red fluorescence, FCCP was added 20minutes before staining.

9.8 Oxygen consumption rate (OCR) and extracellular acidification rate (ECAR) assays

OCR and ECAR experiments were performed using Seahorse XFe96 analyzer (Agilent Technologies). Cells cultured in a 6-well plate (106 cfu per well) were treated with 1μM palbociclib for 24 and 72 hours. On the day of the measurement, cells were seeded onto Corning®Cell-Tak coated XF96 cell culture microplates in Seahorse base media and incubated at 37°C without CO_2 for 1 hour. Seahorse base medium was supplemented with 500mM pyruvate, 2mM L-glutamine, 10mM glucose for OCR measurement, and with 2mM L-glutamine, for ECAR measurement. The mito stress test was performed by series of injections - 1μM oligomycin (inhibits ATP-synthase), 2μM CCCP (mitochondrial uncoupler) and a combination of 0.5μM antimycin and rotenone (inhibitors of RCIII and RCI). The glycolytic stress test was performed by injections starting with 10mM glucose (substrate of glycolysis), followed by 1μM oligomycin (ATP synthase inhibitor) and 50mM 2-deoxy-D-glucose (glycolysis inhibitor). Both OCR and ECAR were measured after each injection. After the assay, the cells were stained with Hoechst and counted. OCR and ECAR values were normalized based on the cell number. The effect of palbociclib treatment on mitochondrial respiration was determined by comparing it with the respiration of non-treated cells.

9.9 Formation of reactive oxygen species

For generation of reactive oxygen species (ROS), cells were seeded into a 6-well plate and 24h and 48 hours prior to the measurement treated with 1 μM palbociclib. For ROS levels assessment, cells were incubated with MitoSox-Mitochondrial Superoxide Indicator (Thermo Fisher Scientific, Waltham, Massachusetts, United States) for 15 min at 37°C. The ROS-linked fluorescence was measured using the PerCP-Cy5-5 (585/42) and the LSR Fortessa SORP flow cytometer (Beckton Dickenson, New York, USA). Data were analysed using the FlowJo software.

9.10 AKT activity measurement

AKT activity measurement was based on the genetically encoded Förster resonance energy transfer (FRET) biosensor and analysed using flow cytometry. Cell lines were cultivated with palbociclib or DMSO 24 hour prior to assessement.

9.11 Intracellular BH3 profiling

Cells were resuspended in DTEB buffer with 0.001% digitonin and plated at a cell density of 100,000 cells/100ul with BH3 mimetics (venetoclax, S635845, A1155463) and peptides (BIM - GeneCust) for 60min at 27°C. Then the cells were fixed with formaldehyde at room temperature for 15 minutes. After the addition of neutralizing buffer for 5 minutes, cells were stained with anti-cytochrome C–Alexa647 (BLE612310, Ozyme) 1:40 in 2%FBS/0.1% Saponin/1%BSA/300uM NaN3/PBS overnight at 4°C. Loss of cytochrome c was analysed by a flow cytometry (BD FACS Canto I).

9.12 Establishment of MCL clones with transgenic overexpression of *MYC*, *CDK4* or *CDKN2A*

Cell lines with stably integrated cDNA carrying either *MYC* or *CDK4* were prepared using Sleeping Beauty transposon system. [125] Gene of interest was cloned into pSB vector using SfiI restriction sites. The payload also contained puromycin resistance gene and doxycycline-inducible promoter. pSB was co-transfected into MCL cells together with transposase vector SB100X (Addgene, plasmid 34879) using Neon transfection system.

Exogenous expression of INK4a was achieved using modified pLX lentiviral system. cDNA was cloned into pLX401-P2A-DsRed2 vector (derived from Addgene plasmid #121919). Resulting vectors together with vectors pMD2.G (Addgene, plasmid 12259), psPAX2 (Addgene, plasmid 12260) were introduced into HEK293T cells using Lipofectamine 3000 reagent (Thermo Fisher). After 36 hours, lentiviral supernatant was harvested and added to media containing MCL cells in 1:1 ratio.

In both cases cells were selected using 2 µg/ml puromycin and transgenic expression was induced by adding 0.1 µg/ml doxycycline. The overexpression was confirmed by western blotting (Figure 8 A, B, C).

9.13 Establishment of MCL clones with *CDKN2A* or *RB1* gene deletion

Cell lines with gene knockouts were generated according to the methodology described by Cong et al [126]. Specific sgRNA targeting particular exon in the gene of interest was cloned into the pX330 recombinant plasmid (Addgene plasmid #42230) carrying Cas9 nuclease. All sgRNA sequences used in this study are listed in Table 3. The plasmids were cloned and delivered into lymphoma cells by electroporation using Neon transfection system. For any given protein-coding exon two sgRNAs were used to create at least 70bp long deletion resulting in the knockout allele. pX330 plasmids were co-transfected with pcDNA-EmGFP plasmid. GFP-positive cells were sorted using BD FACS Aria and seeded into 96-well plate, 1 cell per well. After establishing clonal cultures gDNA and protein lysates were isolated to confirm the deletion by PCR and western blotting (Figure 8 D, E)

A

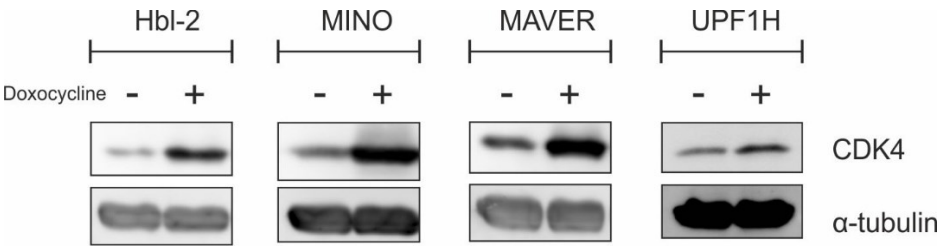

B

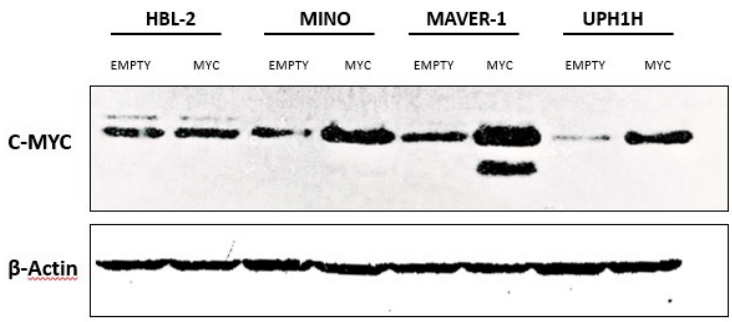

C

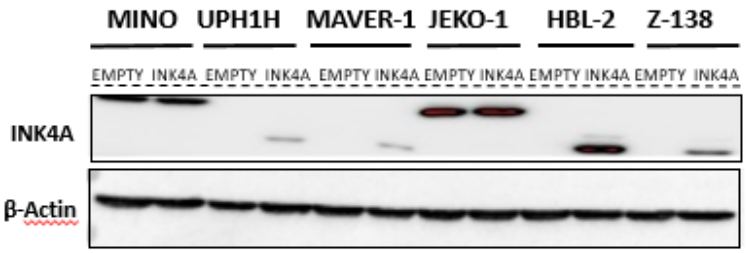

D

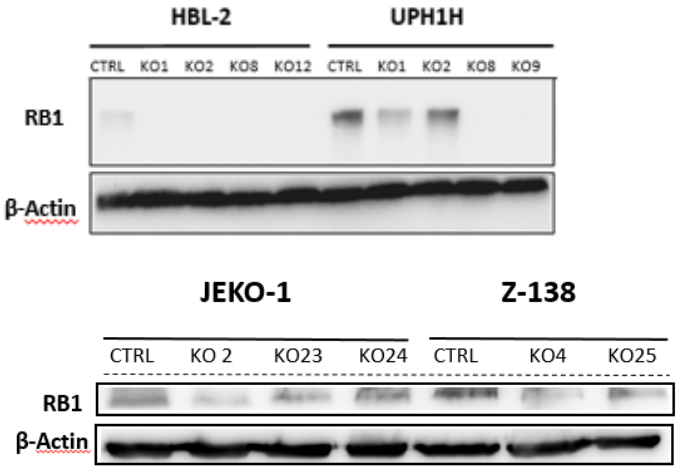

E

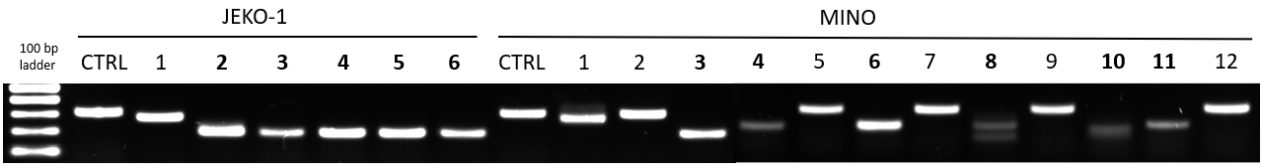

Figure 8. Validation of selected genes editing in tested cell lines. A Overexpression of *CDK4*, B Overexpression of MYC, C Overexpression of INK4A, D RB1 K/O, E CDKN2A K/O. DNA agarose gel electrophoresis showing a region containing exon 2 of Cdkn2a amplified using PCR. Wild-type product is 324 bp and expected K/O product is 208 bp. First lane shows 100-500 bp standard bands.

Gene	Exon	Cut position	FWD oligo	REV oligo
CDKN2A	Exon 2	Chr9:21971014	caccGCACGGGTCGGGTGAGAGTGG	aaacCCACTCTCACCCGACCCGTGC
		Chr9:21971130	caccGAGCTCCTCAGCCAGGTCCAC	aaacGTGGACCTGGCTGAGGAGCTC
RB1	Exon 3	Chr13:48342039	caccGTATACTATATACTACGCCAA	aaacTTGGCGTAGTATATAGTATAC
		Chr13:48342877	caccGCATAAATACACTTTCATAA	aaacTTATGAAAGTGTATTTATGC

Table 3. Sequences of DNA oligos coding for single guide RNA used to produce CRISPR/Cas9 knockouts of CDKN2A and RB1. Forward and reverse oligos are hybridized resulting in a short dsDNA fragment with sticky ends for cloning into pX330 vector. Genomic position of double-stranded cuts is given using GRCh38 human genome assembly as a reference.

9.14 Patient samples, cytogenetics and mutation assessment

To evaluate which lymphoma patients are not responding to standard immunochemotherapy and therefore would benefit most from the studied novel drug combination the cohort of 126 newly diagnosed MCL patients with available diagnostic samples of bone marrow at the First Dept. of Internal Medicine - Hematology, General University Hospital and First Faculty of Medicine, Charles University were subject to analysis. Only patients with bone marrow infiltration ≥ 5% were selected to properly evaluate cytogenetic changes in obtained samples using fluorescence in situ hybridization (FISH). These analyses were performed in the Center of oncocytogenomics, General University Hospital and Charles University. From these 126 patients, 113 patients were also subject to mutational analysis of selected genes (*TP53* and *CDKN2A)* by next generation sequencing (NGS). NGS was implemented at the University Hospital Olomouc. All detected variants were manually inspected using mutation databases and variant population databases and/or functional prediction tools. Polymorphisms were filtered out and only pathogenic or likely pathogenic variants were disclosed. Patient-related studies were approved by University General Hospital Ethics Committee 48/18.

9.15 Statistics

Statistical analyses were conducted in GraphPad Prism, R and Statistica. P value of less than 0.05 was considered as statistically significant. To assess the statistical significance of treatment

effectiveness, differences between mean tumor volumes in compared groups were calculated for particular (available) time points (i.e. days) and statistical hypothesis tests of linear trend slopes equality to zero were carried out. The Bonferroni correction was used to smooth the significance level for multiple simultaneous hypothesis tests. To estimate OS and event-free survival (EFS) the Kaplan-Meier survival analysis was used. Event was defined as either progression or any change of treatment in case patient did not respond sufficiently to first-line therapy (achievement of only stable disease / partial response).

10. Results

10.1 Sensitivity of aggressive lymphoma cell lines to palbociclib

Anti-proliferative and cytotoxic effect of palbociclib was studied using a panel of nine MCL cell lines, six DLBCL cell lines with GCB immunophenotype, and five ABC-DLBCL cell lines (Table 4).

A

MCL	IC50 [nM]	LD50 [µM]
UPF7U	0.4	11
MINO	5.2	17.7
HBL-2	7.8	13.9
UPF1H	9.4	11.4
Z-138	13.6	11.5
GRANTA-519	31.5	15.4
JEKO-1	59.6	12
REC-1	211.3	11
MAVER-1	268.5	11
AVERAGE	**67.5**	**12.8**
MEDIAN	**13.6**	**11.5**

B

GCB-DLBCL	IC50 [nM]	LD50 [µM]
K-422	4.7	12.9
SU-DHL-4	43.1	8.5
HT	52.9	17.3
SU-DHL-5	73.2	8
UPF4D	126.9	5
WSU-DLCL2	289	10
AVERAGE	**98.3**	**10.3**
MEDIAN	**63.1**	**9.3**

C

ABC-DLBCL	IC50 [nM]	LD50 [μM]
NU-DUL-1	192.9	24
TMD8	346.6	15.7
OCI-LY3	416.1	17.7
RIVA	1269	12
U-2932	3236	11.9
AVERAGE	**1092.1**	**16.3**
MEDIAN	**416.1**	**15.7**

Table 4. Sensitivity of aggressive lymphoma cell lines to palbociclib. A Sensitivity of MCL cell lines to palbociclib. B Sensitivity of GCB-DLBCL cell lines to palbociclib. C Sensitivity of ABC-DLBCL cell lines to palbociclib. IC50 = half-maximal inhibitory concentration, LD50 = median lethal dose

The greatest anti-proliferative effect of palbociclib from the analyzed aggressive lymphoma subtypes was visible in MCL cell lines with median IC50 13.6nM, followed by GCB-DLBCL (median IC50 63 nM). The least sensible were ABC-DLBCL cell lines with median IC50 416nM. The cytotoxic effect of palbociclib was detected only after extremely high concentrations with median LD50 around or exceeding 10 μM.

10.2 The effect of palbociclib on cell cycle and protein levels in MCL cell lines

As expected, cell cycle analysis of MCL cells incubated for 24 hours with 1μM palbociclib showed that palbociclib induces cell cycle arrest in G1 phase of the cell cycle (Figure 9). On protein level, exposure to palbociclib led to downregulation of critical cell cycle regulators including cyclins (likely due to higher proportion of cells in G1 phase of the cell cycle), and RB1 protein. Expression of CDKs and levels of BCL2 family proteins regulating apoptosis remained unchanged (Figure 10).

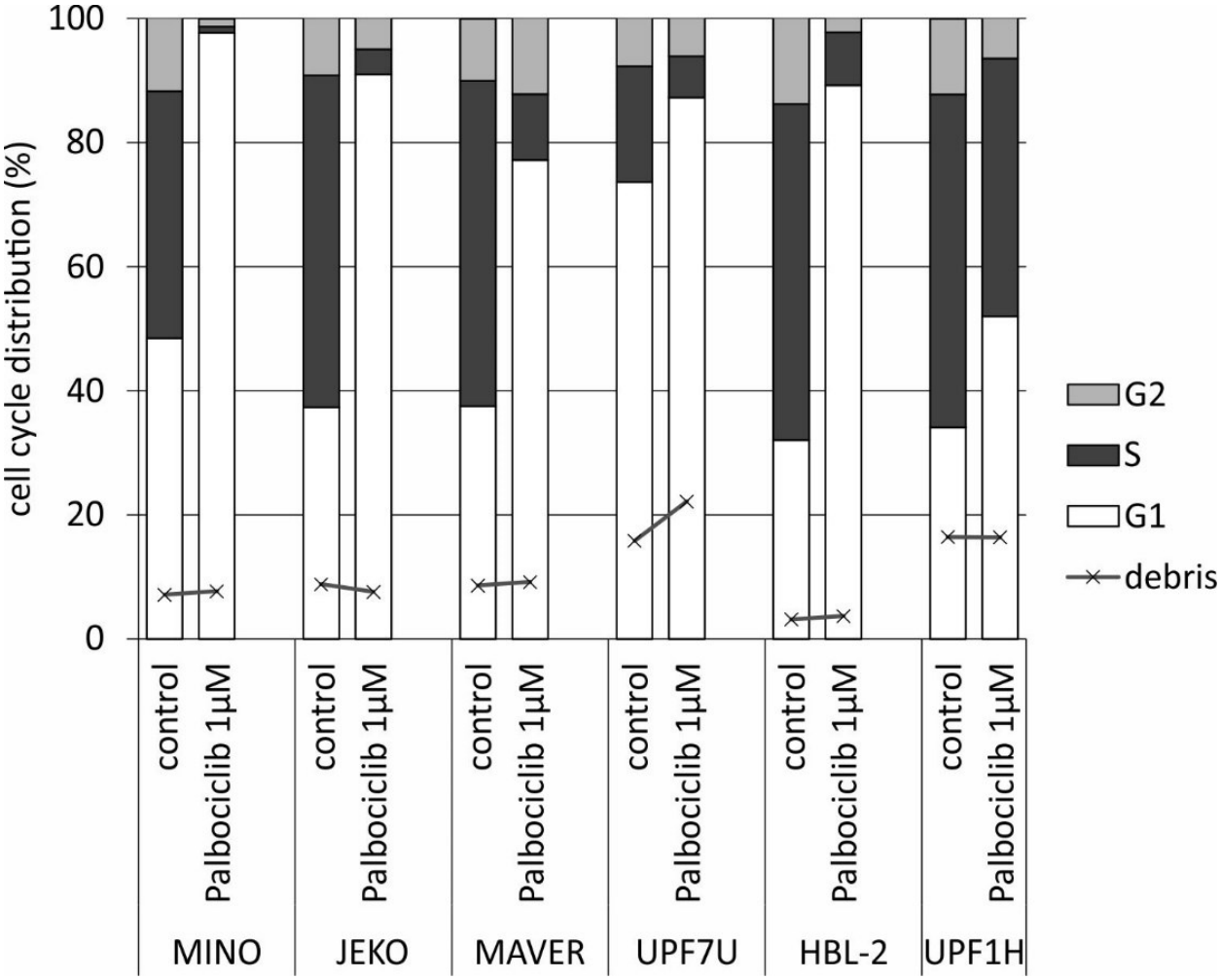

Figure 9. Increased amount of cells arrested in G1-S phase after 24-hour palbociclib exposure. Figure shows the distribution of MCL cells in different stages of cell cycle before and after 24 hour palbociclib exposure.

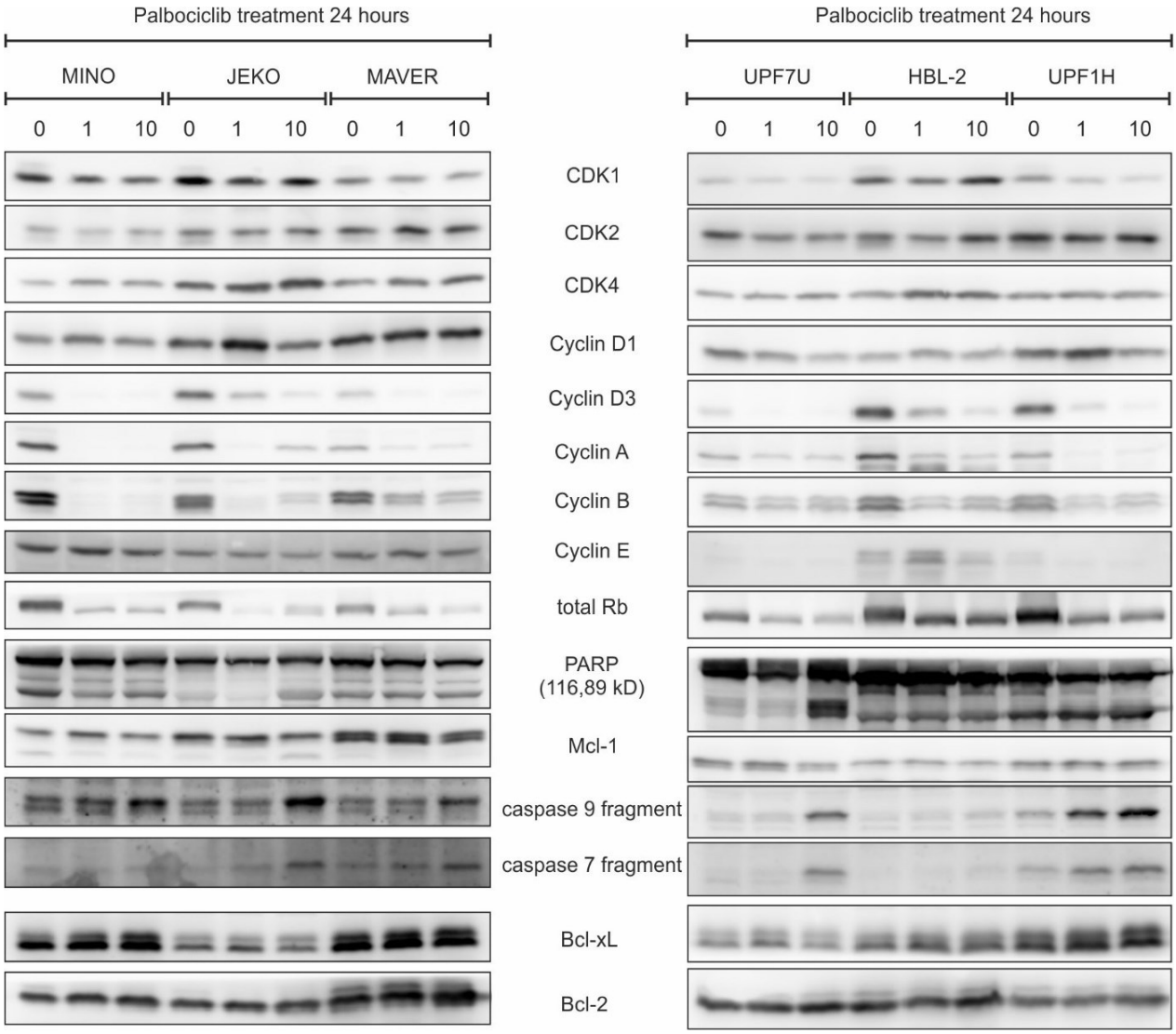

Figure 10. Expression of regulators of cell cycle and apoptosis in MCL cell lines after 24-hour exposure to 1 μM and 10 μM of palbociclib.

10.3 The effect of combination therapy with palbociclib and BH3-mimetics on aggressive lymphoma cell lines

As described, palbociclib proved significant anti-proliferative effect, especially in MCL and GCB-DLBCL cell lines, but lacked the cytotoxic effect in clinically relevant concentrations. Therefore, the combination of anti-proliferative effect of palbociclib with BH3-mimetics, the inductors of

apoptosis, represents a rational therapy strategy. The potential synergy between palbociclib and selected BH3 mimetics, including venetoclax (a BCL2 inhibitor), S63845 (a MCL1 inhibitor) and A1155463 (a BCL-XL inhibitor) was analyzed on a panel of three MCL cell lines at 24 hour time point (Table 5) and proved, that palbociclib exerts cytotoxic synergy with all (BCL2, MCL1 and BCL-XL) inhibitors. The concentrations of BH3-mimetics were used according to the sensitivity of selected cell lines. In the next step, venetoclax, the only clinically approved BH3 mimetic, was used to evaluate potential cytotoxic synergy with palbociclib on a larger panel of aggressive lymphoma cell lines. Additive to synergistic effect of the combination was observed in the majority of MCL and ABC-DLBCL cell lines (Table 6). As expected, synergistic effect between venetoclax and palbociclib was not observed in GCB-DLBCL cell lines that do not express a BCL2 protein (HT, SU-DHL-5, and UPF4D), the molecular target of venetoclax.

		Dose BH3-mimetic [μM]	CI
JEKO-1	**A1155463**	10	**0.54**
		30	**0.83**
	S63845	0.1	**0.47**
		0.5	**0.29**
	venetoclax	5	**0.28**
		10	**0.28**
Z-138	**A1155463**	0.01	**0.26**
		0.025	**0.2**
	S63845	0.05	**0.3**
		0,5	**0.01**
	venetoclax	0,5	**0.02**
		1	**0.01**
Granta-519	**A1155463**	1	**0.14**
		10	**0.37**
	S63845	0.1	**0.01**
		0.5	**0.03**
	venetoclax	0.2	**0.34**
		0.5	**0.31**

Table 5. The effect of combination therapy with palbociclib and BH3-mimetics on MCL cell lines (CI = combination index calculated by Chou-Talalay method after 24 hour exposure to palbociclib and selected BH3-mimetic).

	Dose Palbociclib [uM]	Dose Venetoclax [nM]	CI
UPF7U	1	5	0.13
		10	0.11
	10	5	0.38
		10	0.37
MINO	1	100	0.8
		1000	0.81
	10	100	0.26
		1000	0.15
HBL-2	1	5	0.99
		10	0.85
	10	5	0.52
		10	0.4
UPF1H	1	10	0.7
		100	0.75
	10	10	0.79
		100	0.32
Z-138	1	100	0.3
		1000	0.17
	10	100	0.95
		1000	0.57
GRANTA-519	1	10	0.32
		100	0.39
	10	10	0.48
		100	0.38
JEKO-1	1	10	0.17
		100	0.16
	10	10	0.38
		100	0.34
REC-1	1	100	0.56
		1000	0.76
	10	100	1,15
		1000	0.83
MAVER-1	1	5	0.91
		10	0.93
	10	5	0.48
		10	0.35

	DosePalbociclib [uM]	Dose Venetoclax [nM]	CI
NU-DUL-1	1.0	100.0	0.59
		1000.0	0.67
	10.0	100.0	0.95
		1000.0	0.66
TMD8	1.0	100.0	0.1
		1000.0	0.05
	10.0	100.0	0.09
		1000.0	0.07
OCI-LY3	1.0	100.0	0.16
		1000.0	0.27
	10.0	100.0	0.76
		1000.0	0.5
RIVA	1.0	5.0	0.84
		10.0	0.63
	10.0	5.0	0.23
		10.0	0.2
U-2932	1.0	5.0	0.25
		10.0	0.21
	10.0	5.0	0.19
		10.0	0.18
K-422	1.0	5.0	1,2
		10.0	1,24
	10.0	5.0	0.58
		10.0	0.6
SU-DHL-4	1.0	100.0	0.22
		1000.0	0.18
	10.0	100.0	0.4
		1000.0	0.33
HT	1.0	10.0	0.89
		1000.0	0.63
	10.0	10.0	3,14
		1000.0	3,46
SU-DHL-5	1.0	100.0	2,52
		1000.0	1,89
	10.0	100.0	0.22
		1000.0	0.23
UPF4D	1.0	100.0	1,37
		1000.0	1,12
	10.0	100.0	1,27
		1000.0	1,64
WSU-DLCL2	1.0	100.0	0.32
		1000.0	0.2
	10.0	100.0	0.25
		1000.0	0.25

Table 6. The effect of combination therapy with palbociclib and venetoclax on MCL and DLBCL cell lines (CI = combination index calculated by Chou-Talalay method after 24 hour exposure to palbociclib and venetoclax).

10.4 The effect of combination therapy with palbociclib and venetoclax on PDX models derived from R/R MCL patients

To confirm the promising findings from *in vitro* experiments (especially in MCL with the greatest sensitivity to palbociclib and synergistic effect in all tested cell lines), *in vivo* experiments were conducted using four PDX models derived from patients with relapsed and/or refractory MCL (Figure 11). All four PDX models were sensitive to single agent palbociclib. Three out of four PDX models were sensitive to single agent venetoclax, while one PDX model (VFN-M8) was venetoclax resistant. Synthetic lethality was observed in all four PDX models, including the venetoclax-resistant VFN-M8 PDX model and proved that co-targeting CDK4/6 with palbociclib and BCL2 with venetoclax is synergistic *in vivo.* Of note, synthetic lethality of tested combination was also detected in the VFN-M3 PDX model derived from the patient after ibrutinib failure. Subsequently, the statistical analysis of mean tumour volume differences was conducted (Table 7).

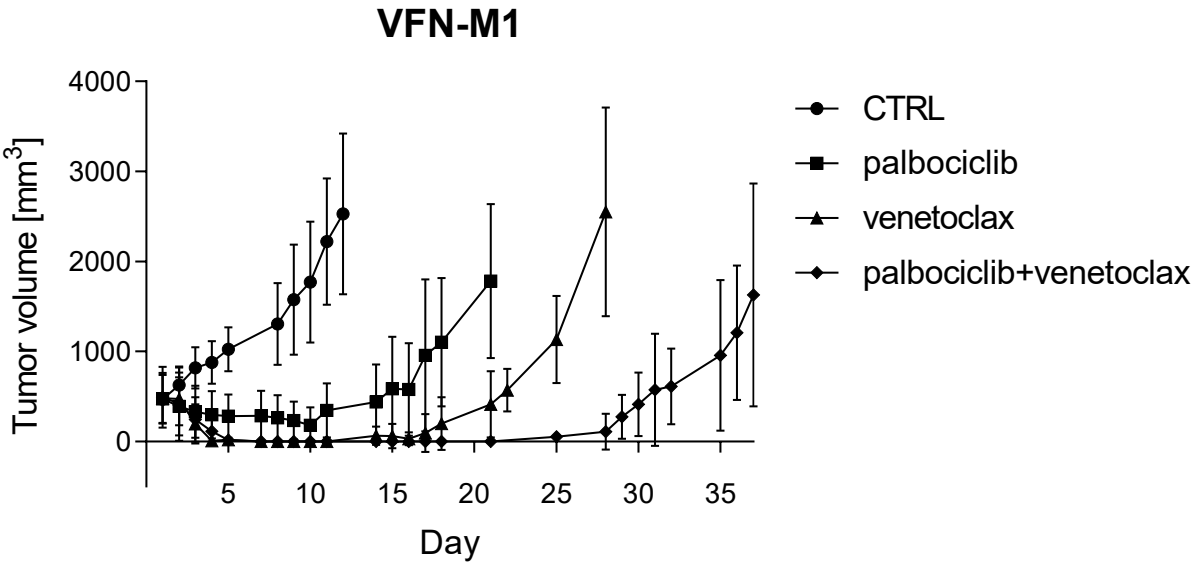

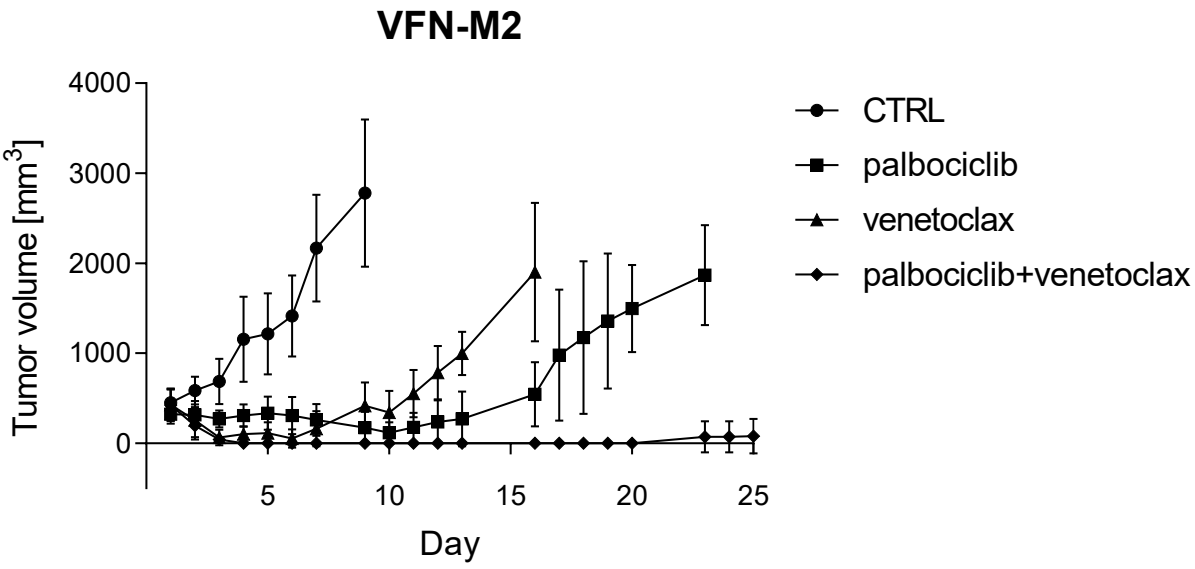
VFN-M2
Tumor volume [mm3]
4000
3000
2000
1000
0
5
10
15
20
25
Day
CTRL
palbociclib
venetoclax
palbociclib+venetoclax

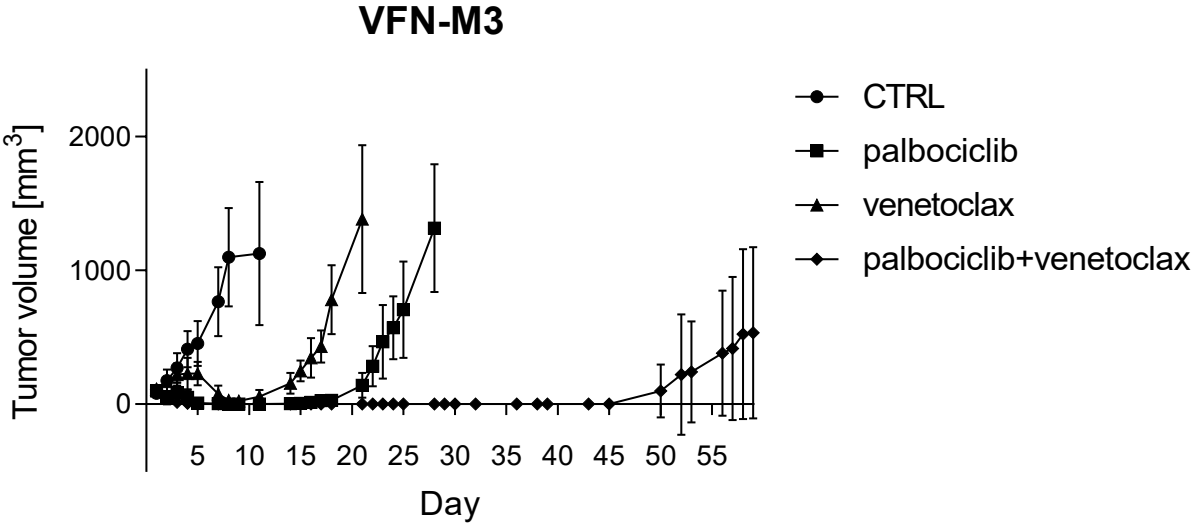
VFN-M3
Tumor volume [mm3]
2000
1000
0
5
10
15
20
25
30
35
40
45
50
55
Day
CTRL
palbociclib
venetoclax
palbociclib+venetoclax

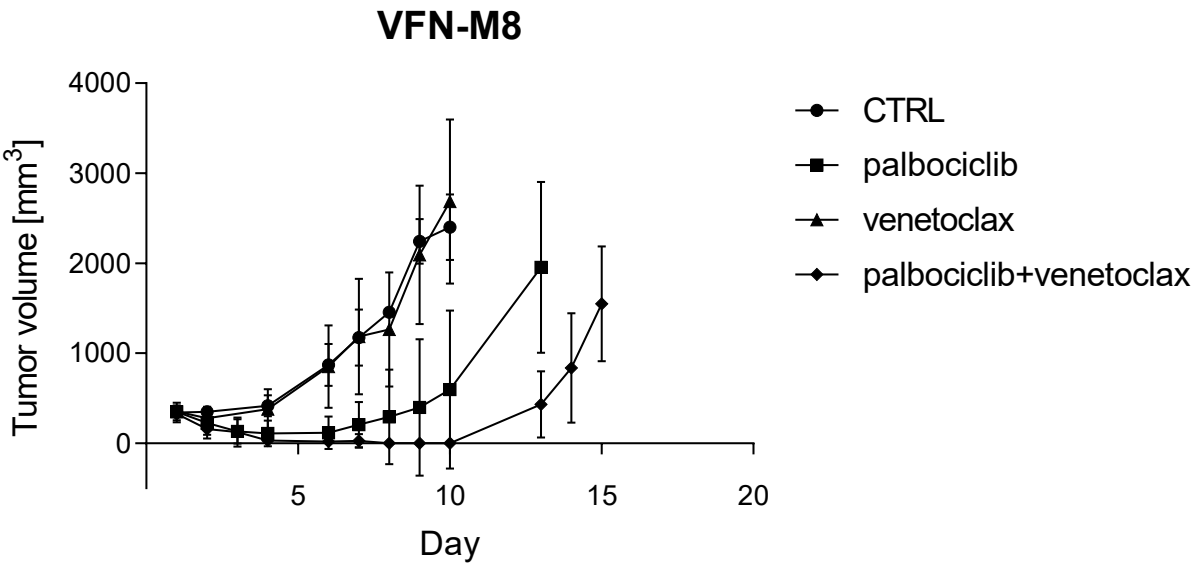

Figure 11. The effect of combination therapy with palbociclib and venetoclax on PDX models derived from R/R MCL patients. X-axis shows days from initiation of therapy. Y-axis shows calculated tumour volume of PDX-bearing mice (Mean ± standart deviation)

Differences	VFN - M1	VFN - M2	VFN – M3	VFN-M8
CTRL vs. palbociclib	0.000001**	0.000082**	0.000049**	0.000079**
CTRL vs. venetoclax	0.000003**	0.000003**	0.000277**	(0.658492)
palbociclib vs. palbociclib + venetoclax	0.000007**	0.000004**	0.000321**	0.001949*
venetoclax vs. palbociclib + venetoclax	0.000551**	0.000059**	0.003418*	0.000406**

Table 7. The p-values of partial t-tests about zero slope of mean tumour volume differences. Statistical significance: * 10% and ** 1% simultaneous significance level, p-value in brackets refer to negative slope

Ex vivo analysis of subcutaneously grown MCL tumours 24 and 48 hours after palbociclib treatment (i.e., after one, and after two doses of palbociclib) confirmed decreased expression of total and phosphorylated RB1 protein, as well as cyclin A and cyclin D3, similarly to the results performed on MCL cell lines. However, moderate downregulation of MCL1 protein was observed

after the exposure to palbociclib *in vivo*, which differ from *in vitro* results (Figure 12). Furthermore, to clarify the effect of palbociclib on BH3-family proteins, co-immunoprecipitation analyses after palbociclib exposure were performed and revealed slightly increased amounts of BCL2 and BCL-XL bound to BIM both *ex vivo* and *in vitro*. However, to observe this effect *in vitro*, cell lines had to be cultivated with palbociclib for a longer period of time (72 hours) and shorter exposure (24hours) did not show significant changes. (Figure 13).

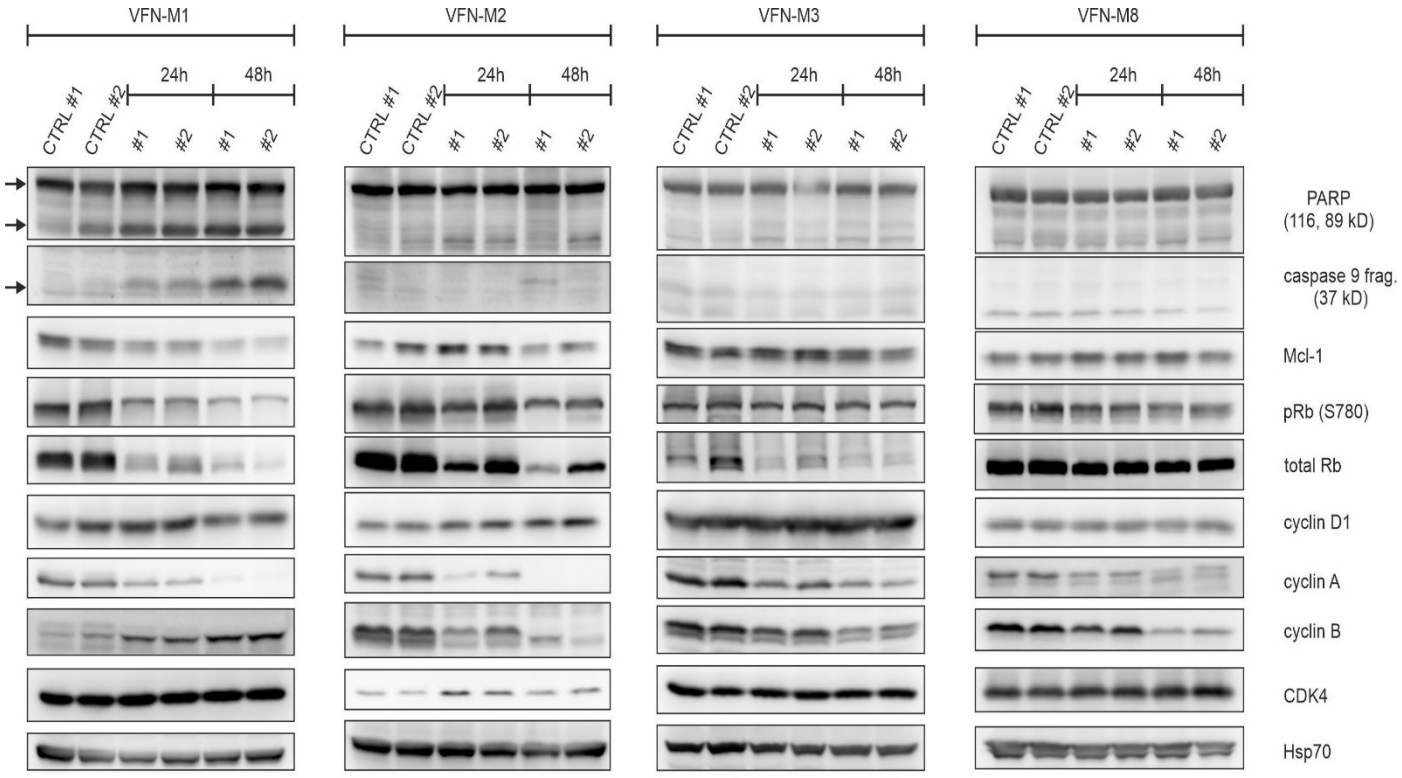

Figure 12. Expression of cell cycle and apoptosis regulators after 24 and 48 hours palbociclib pre-treatment on cells harvested from R/R MCL PDX tumours

A

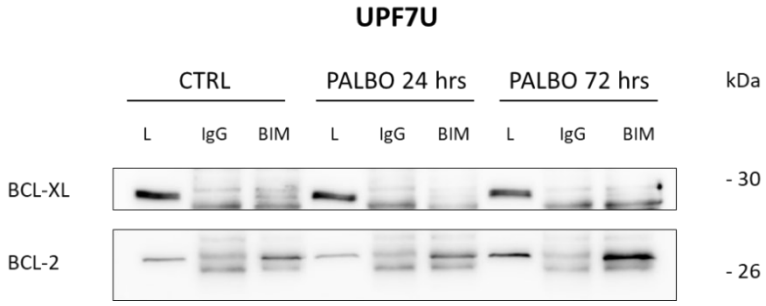

B

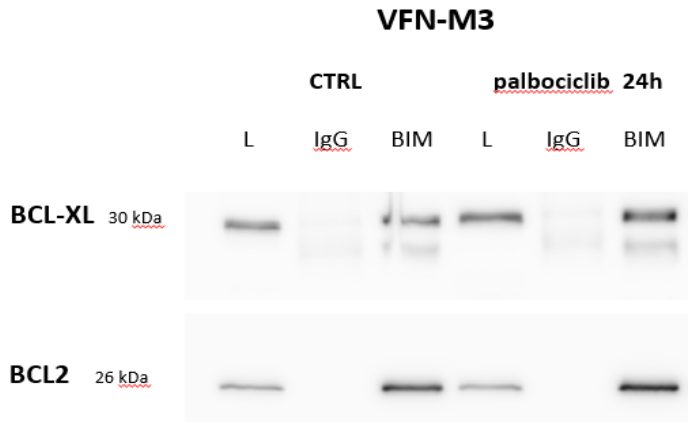

Figure 13 The amount of BCL2 and BCL-XL bound to BIM after exposure to palbociclib. A The amount of BCL2 and BCL-XL bound to BIM after 24 and 72 hours palbociclib pre-treatment on UPF7U cell line. B The amount of BCL2 and BCL-XL bound to BIM after 24 hours palbociclib pre-treatment on VFN-M3 PDX model

10.5 Mitochondrial changes in MCL cell lines after palbociclib exposure

Because the observed synergy between palbociclib and BH3-mimetics could not be fully explained by changes in levels of free or bound BCL2 proteins, and the fact the synergism was observed in all types of BH3-mimetics (BCL2 inhibitor venetoclax, BCL-XL inhibitor A1155463 and MCL1 inhibitor), the experiments focusing on cellular metabolism and potential mitochondrial functional changes due to cell cycle arrest induced by palbociclib were performed.

First, mitochondrial membrane potential assessed by JC-1 dye on MCL cells revealed higher levels of JC-1 monomers in mitochondria, which associates with mitochondrial depolarization after the cultivation with 1μM palbociclib (Figure 14).

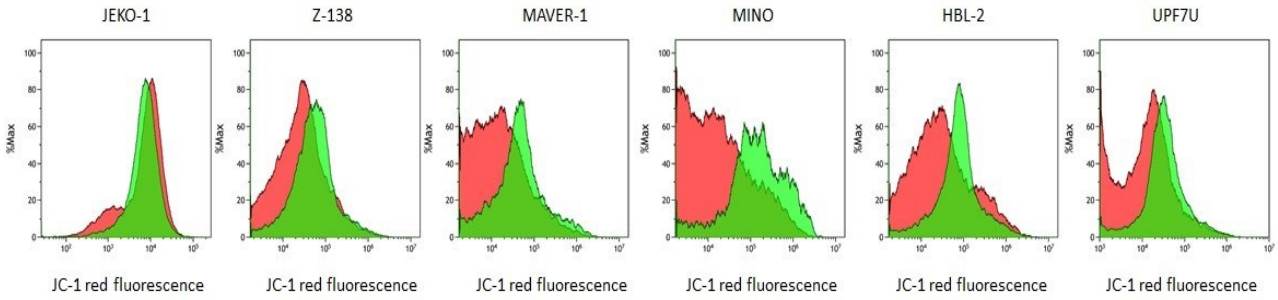

Figure 14. JC-1 staining after 72 hour incubation with palbociclib. Green overlay represents cells cultivated without palbociclib. Red overlay represents cells cultivated with palbociclib. To set intensity for red fluorescence, FCCP (mitochondrial uncoupler) was added 20minutes before staining.

Second, palbociclib-triggered cellular metabolic changes were evaluated by the measurement of the levels of oxidative phosphorylation and glycolysis using SeaHorse analyser (Figure 15 and 16). No specific impact of palbociclib on oxidative phosphorylation was observed, but palbociclib decreased both basal and maximal glycolytic activity in 6 out of 7 analysed MCL cell lines.

A

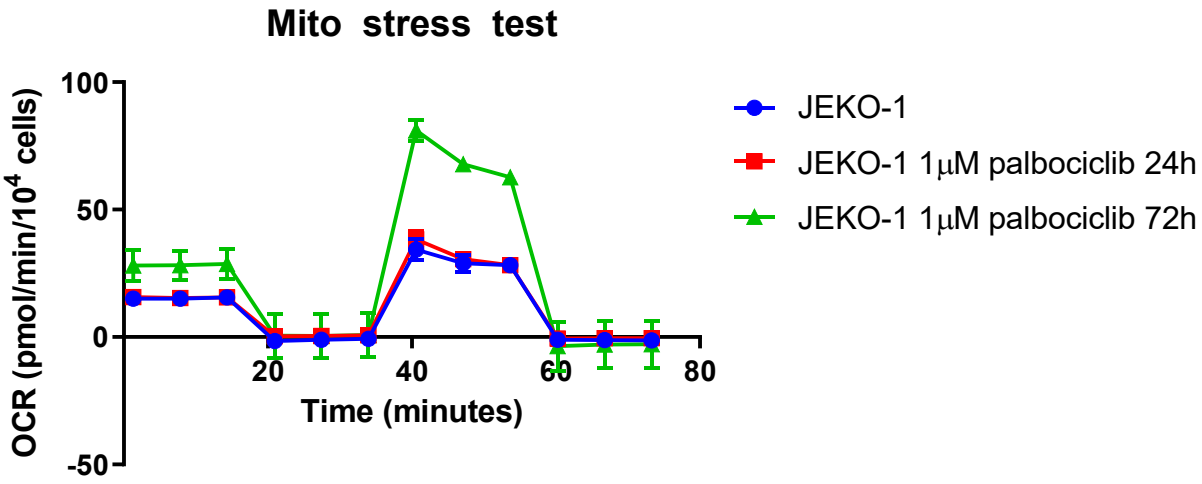
Mito stress test
OCR (pmol/min/10^4 cells)
100
50
0
-50
20
40
60
80
Time (minutes)
JEKO-1
JEKO-1 1μM palbociclib 24h
JEKO-1 1μM palbociclib 72h

B

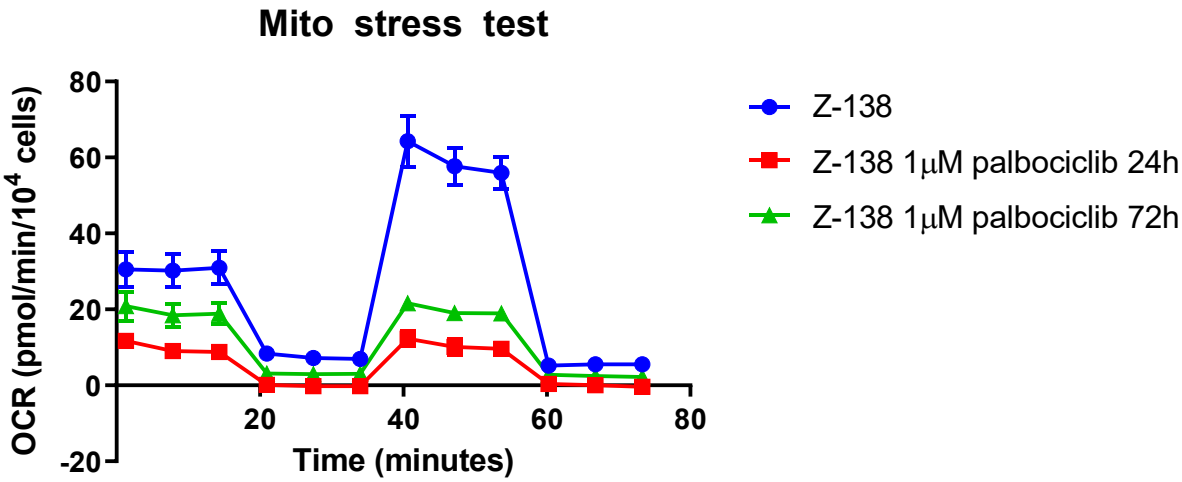
Mito stress test
OCR (pmol/min/10^4 cells)
80
60
40
20
0
-20
20
40
60
80
Time (minutes)
Z-138
Z-138 1μM palbociclib 24h
Z-138 1μM palbociclib 72h

C

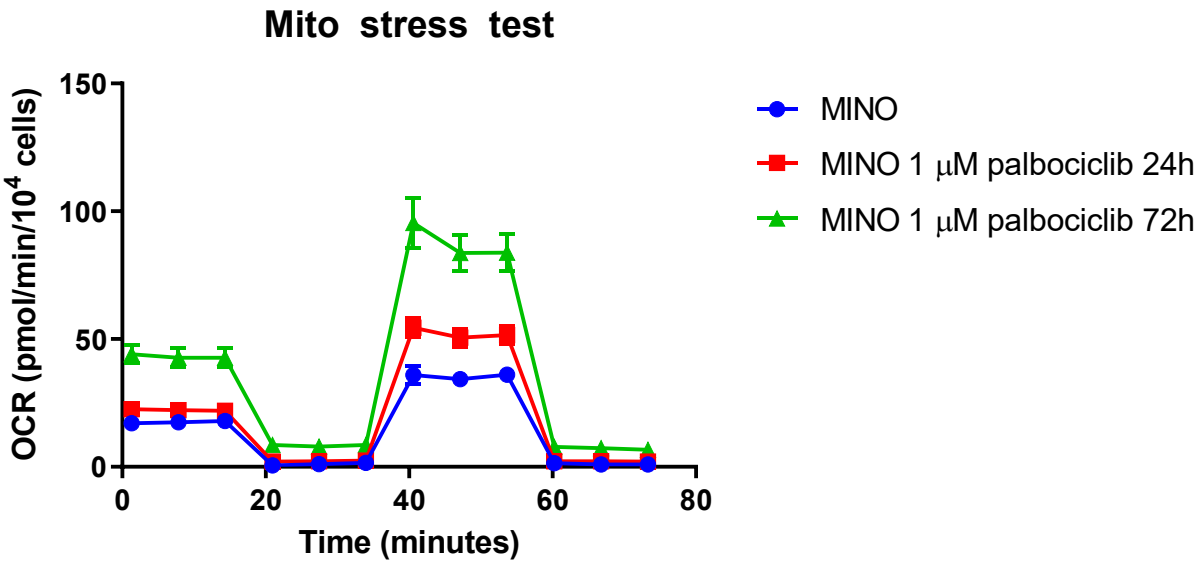
Mito stress test
OCR (pmol/min/10^4 cells)
150
100
50
0
0
20
40
60
80
Time (minutes)
MINO
MINO 1 μM palbociclib 24h
MINO 1 μM palbociclib 72h

D

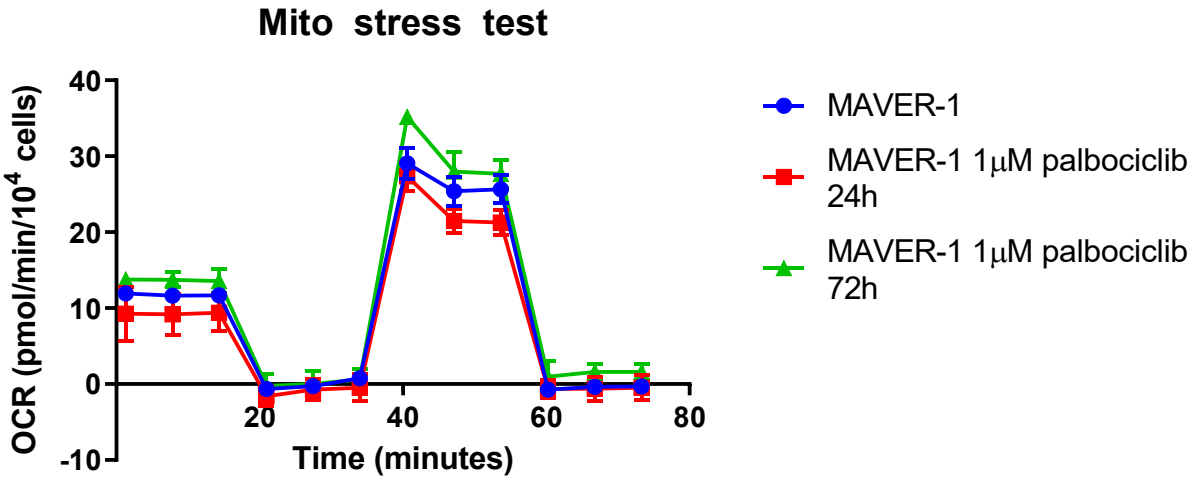
Mito stress test
OCR (pmol/min/10^4 cells)
40
30
20
10
0
-10
20
40
60
80
Time (minutes)
MAVER-1
MAVER-1 1μM palbociclib 24h
MAVER-1 1μM palbociclib 72h

E

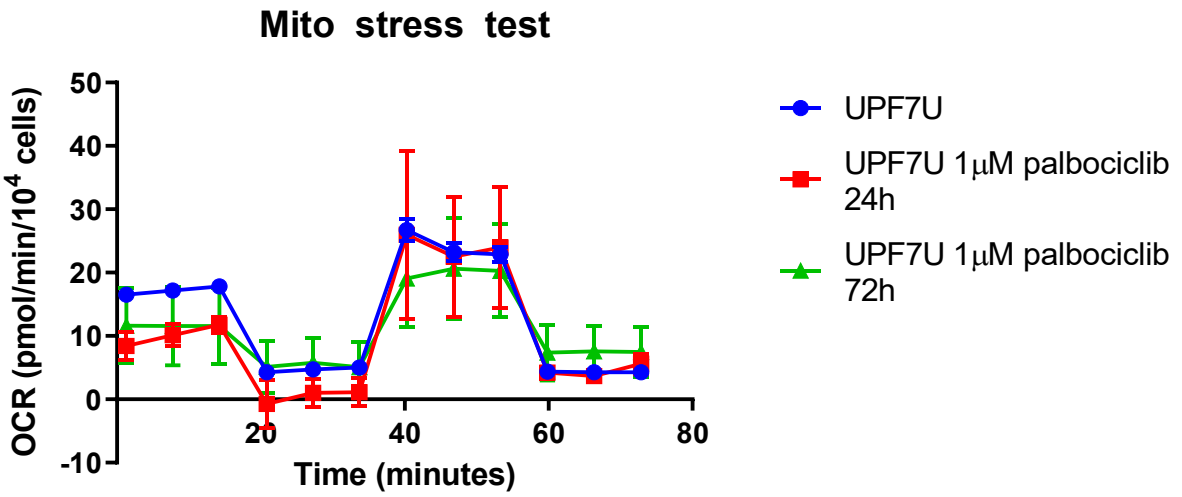
Mito stress test
OCR (pmol/min/10^4 cells)
50
40
30
20
10
0
-10
20
40
60
80
Time (minutes)
UPF7U
UPF7U 1μM palbociclib 24h
UPF7U 1μM palbociclib 72h

F

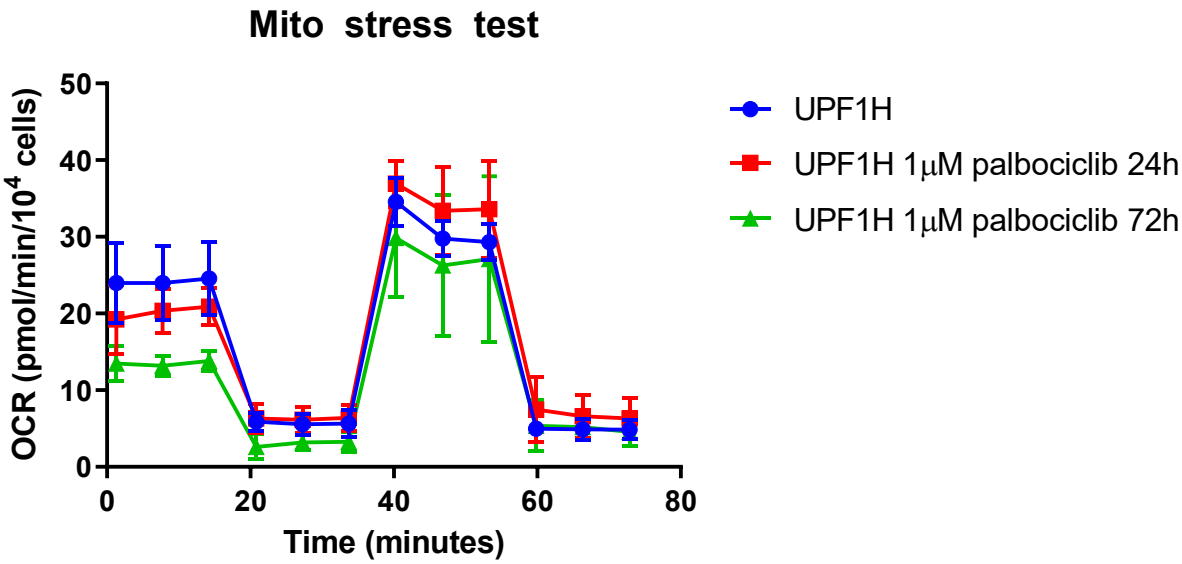
Mito stress test
OCR (pmol/min/10^4 cells)
50
40
30
20
10
0
0
20
40
60
80
Time (minutes)
UPF1H
UPF1H 1μM palbociclib 24h
UPF1H 1μM palbociclib 72h

G

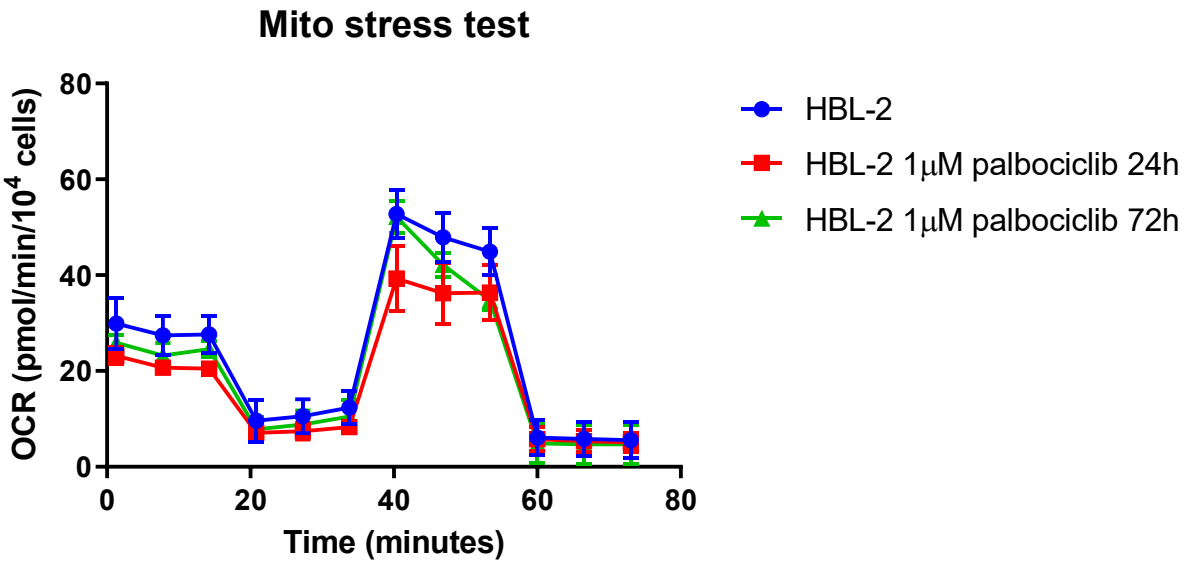

Figure 15. Respiratory changes after 24 and 72 hours palbociclib exposure in MCL cell lines measured by SeaHorse analyser (OCR = oxygen consumption rate)**. A Mito stress test course in time in JEKO-1 cell line. B Mito stress test course in time in Z-138 cell line. C Mito stress test course in time in MINO cell line. D Mito stress test course in time in MAVER-1 cell line. E Mito stress test course in time in UPF7U cell line. F Mito stress test course in time in UPF1H cell line. G Mito stress test course in time in HBL-2 cell line.**

A

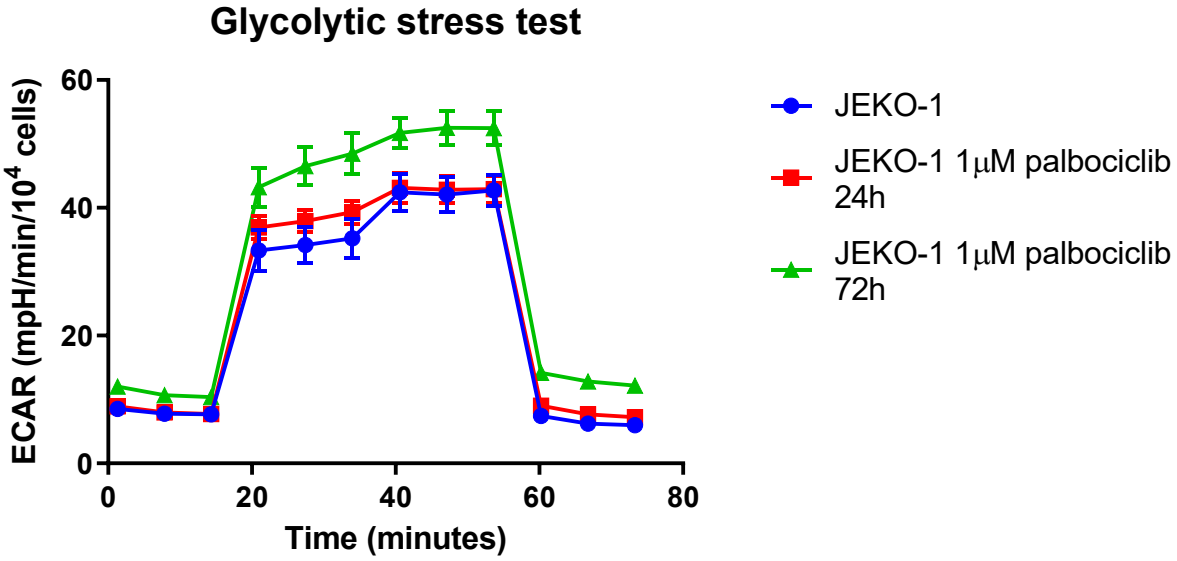

B

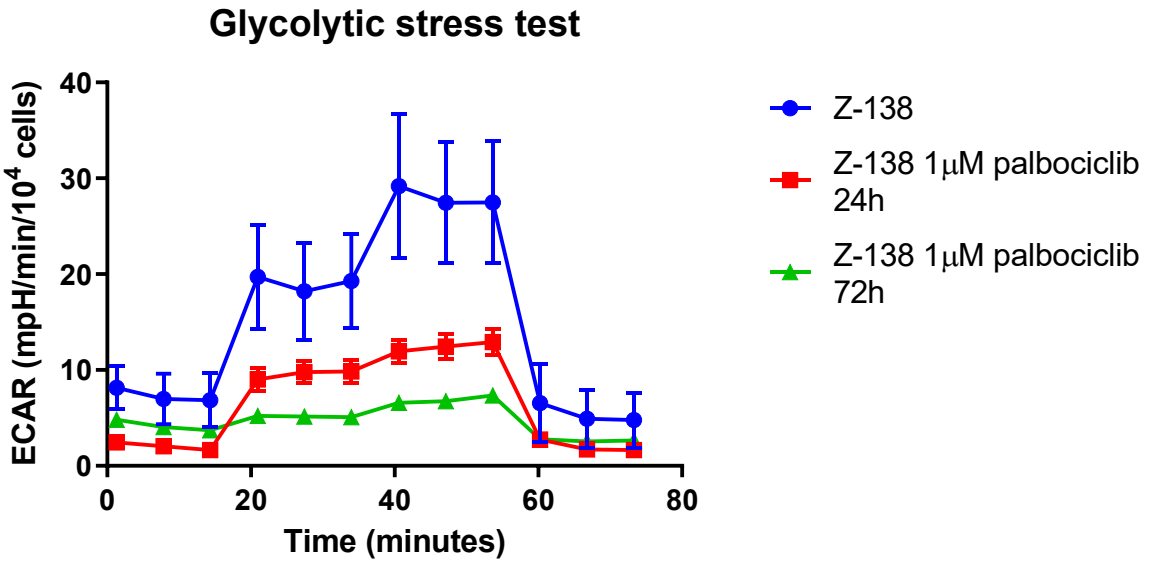
Glycolytic stress test
ECAR (mpH/min/10^4 cells)
Time (minutes)
Z-138
Z-138 1μM palbociclib 24h
Z-138 1μM palbociclib 72h

C

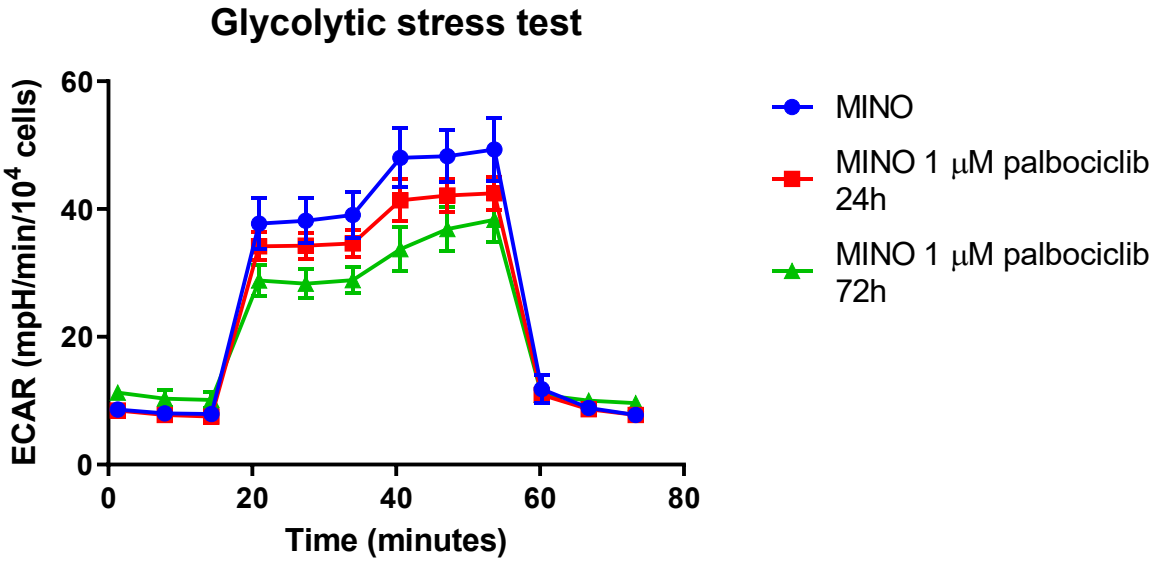
Glycolytic stress test
ECAR (mpH/min/10^4 cells)
Time (minutes)
MINO
MINO 1 μM palbociclib 24h
MINO 1 μM palbociclib 72h

D

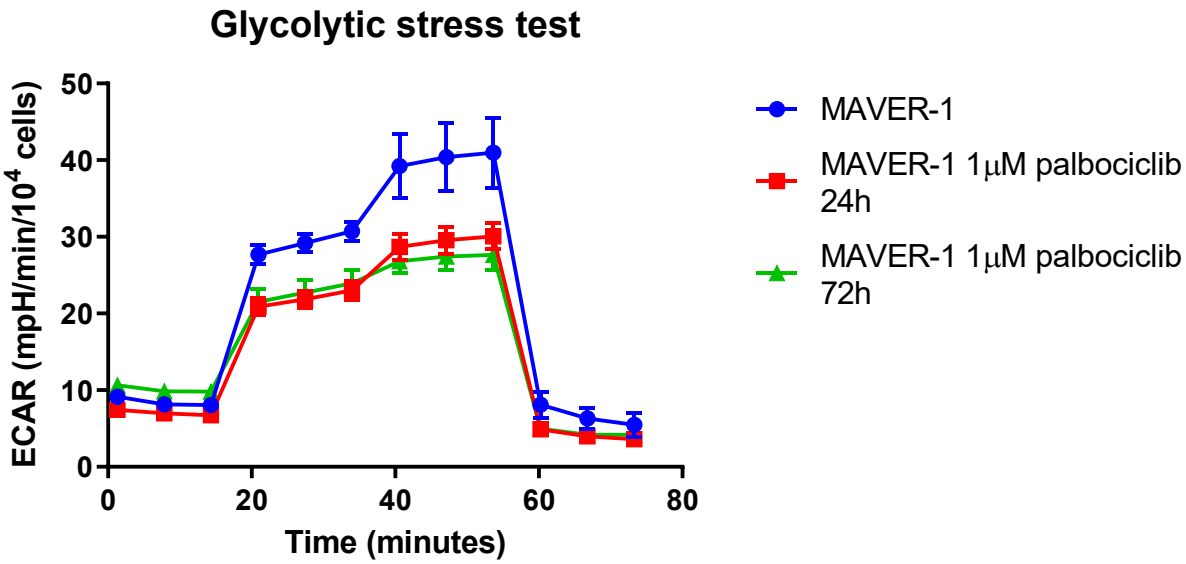
Glycolytic stress test
ECAR (mpH/min/10^4 cells)
Time (minutes)
0
10
20
30
40
50
0
20
40
60
80
MAVER-1
MAVER-1 1μM palbociclib 24h
MAVER-1 1μM palbociclib 72h

E

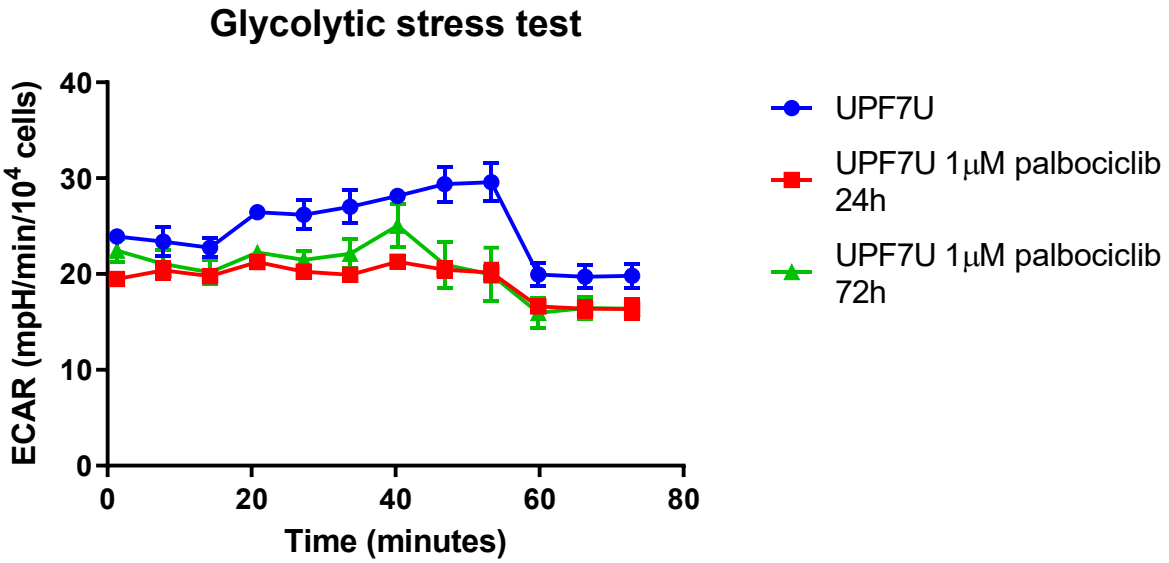
Glycolytic stress test
ECAR (mpH/min/10^4 cells)
Time (minutes)
0
10
20
30
40
0
20
40
60
80
UPF7U
UPF7U 1μM palbociclib 24h
UPF7U 1μM palbociclib 72h

F

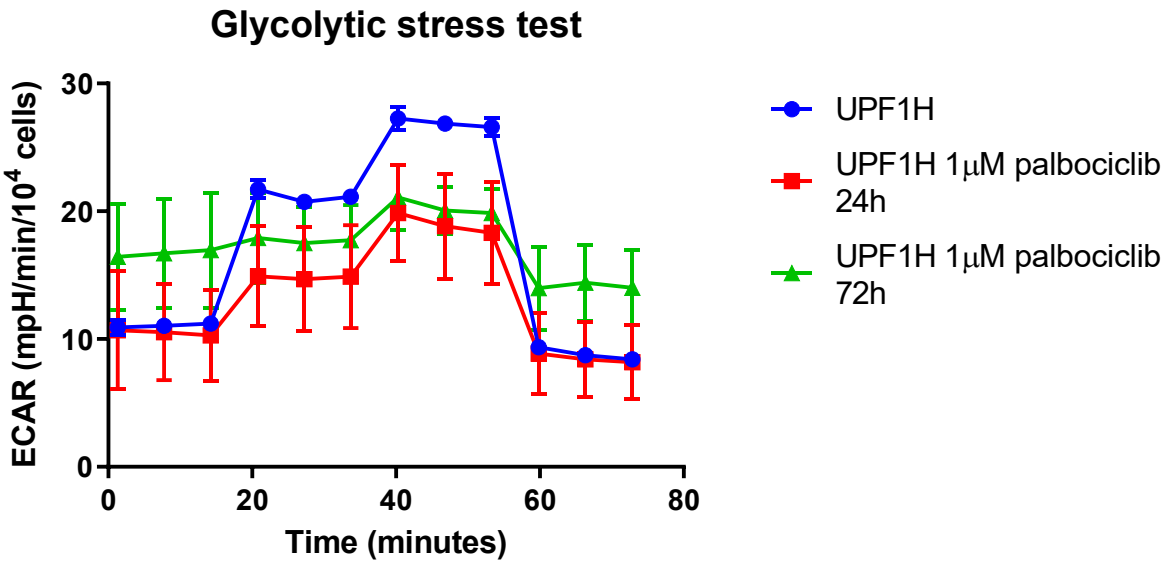

G

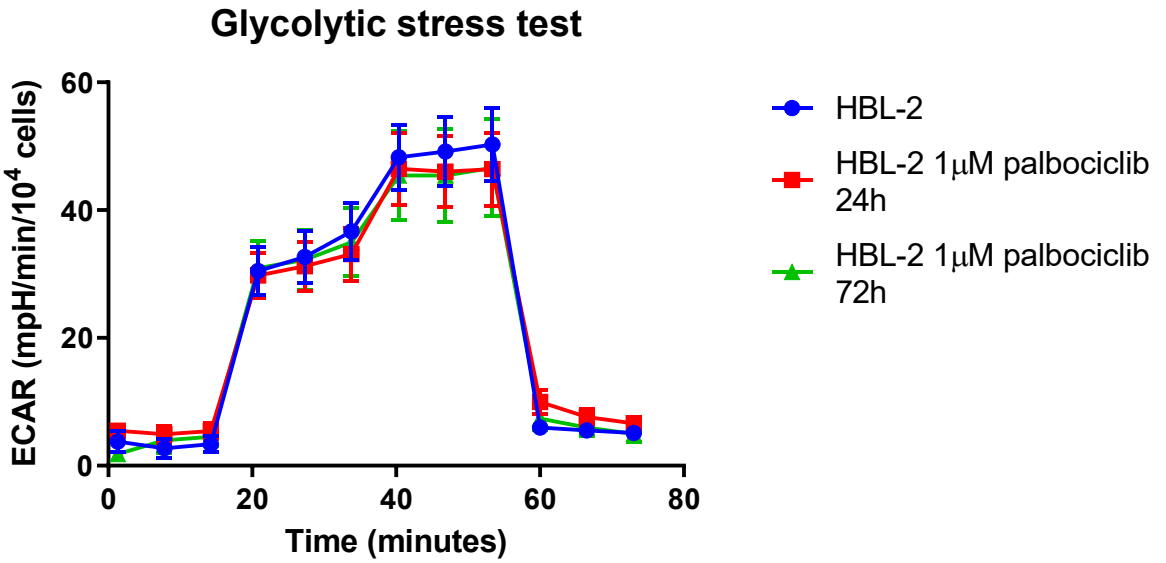

Figure 16. Changes in glycolysis and glycolytic capacity after 24 and 72 hours palbociclib exposure in MCL cell lines (ECAR = extracellular acidification rate). **A Glycolytic stress test course in time in JEKO-1 cell line**. **B Glycolytic stress test course in time in Z-138 cell line. C Glycolytic stress test course in time in MINO cell line. D Glycolytic stress test course in time in MAVER-1 cell line. E Glycolytic stress test course in time in UPF7U cell line. F Glycolytic**

stress test course in time in UPF1H cell line. G Glycolytic stress test course in time in HBL-2 cell line.

To evaluate the effect of mitochondrial depolarization and metabolic changes in cells after cultivation with palbociclib deeper, the levels of reactive oxygen species and AKT activity were measured. The results showed increased production of ROS in mitochondria in cells after 72-hour palbociclib exposure (Figure 17) and interestingly, AKT kinase activity corresponded with glycolytic capacity changes after palbociclib – it decreased in MINO and UPF1H cell lines, and on the other side, was increased in JEKO-1 cells (Figure 18).

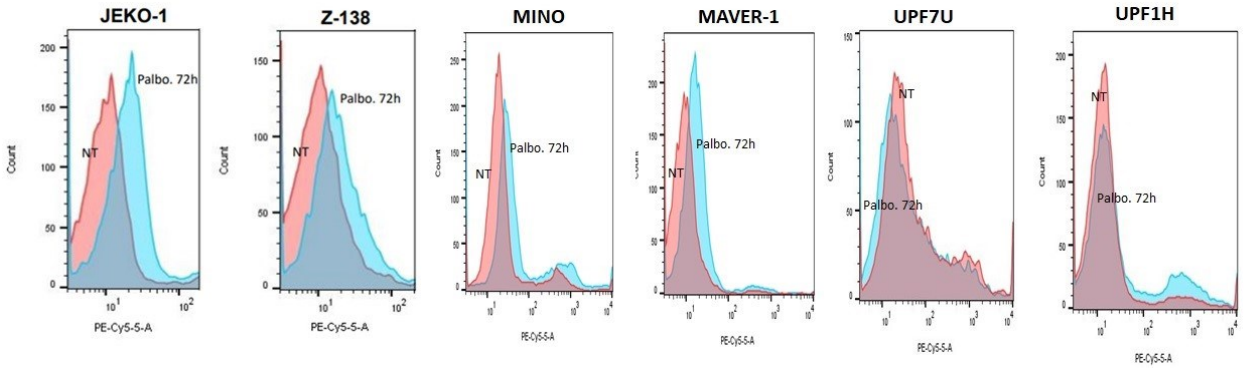

Figure 17. Reactive oxygen species (ROS) levels after 72 hour incubation with palbociclib. Red overlay represents cells cultivated without palbociclib. Blue overlay represents cells cultivated with palbociclib.

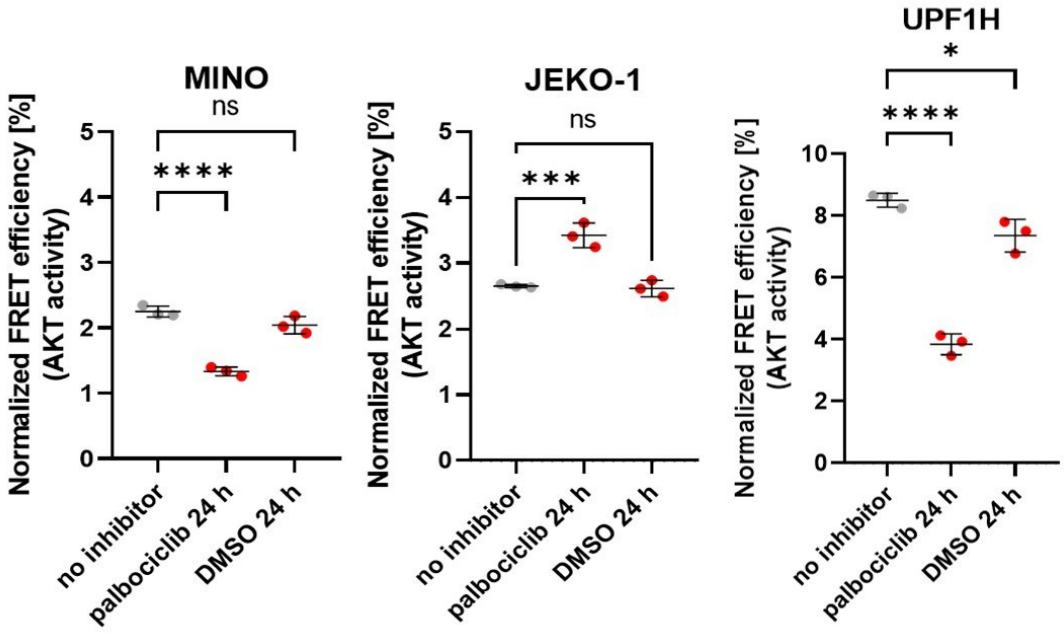

Figure 18. AKT activity after 24 hour incubation with 1μM palbociclib (FRET = Förster resonance energy transfer).

At clinically relevant concentrations, palbociclib does not have a significant proapoptotic effect. However, previous data show that palbociclib-triggered cell cycle arrest leads to complex deregulation of key cellular metabolic and mitochondrial pathways, which might not directly cause cellular death, but might prime cells towards apoptosis and make them an easier target for pro-apoptotic molecules. To prove that intracellular BH3 profiling 24 hours after the exposure to palbociclib was performed and demonstrated that lower concentration of BIM was needed to induce cytochrome c release in palbociclib-exposed cells in comparison to controls. This demonstrates an increased proapoptotic mitochondrial priming of MCL cells after palbociclib exposure (Figure 19).

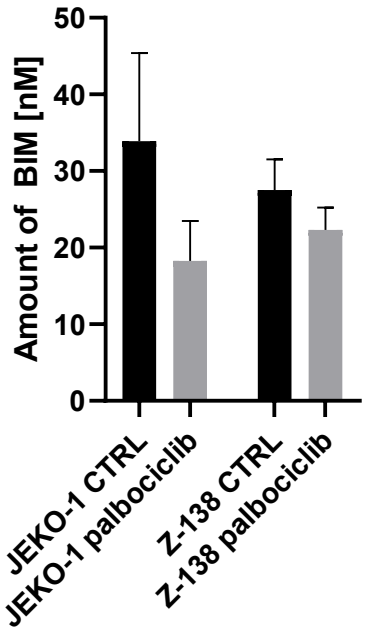

Figure 19. Intracelullar BH3 profiling. The concentration of intracellulary-added BIM leading to cytochrome c release in 50% of cells.

10.6 Clinical impact of novel treatment strategy based on CDK4/6 inhibition and BCL2 inhibition

Previous pre-clinical results on cell lines and PDX models showed that from patients with aggressive B-NHL the subgroup of MCL patients might benefit most from the proposed novel chemotherapy-free treatment combination. MCL is characterised by the translocation t(11;14) leading to the overexpression of cyclin D1, so the treatment based on cell cycle inhibition by cyclin-dependent kinase 4/6 inhibitors has pathophysiologically reasonable core. To evaluate potential clinical impact of this novel treatment strategy 126 newly-diagnosed consecutive patients were subjects to analysis. Baseline characteristics of analysed patients are shown in Table 8.

	N	%
M	88	70
F	38	30
Age (median; years)	68	
Age (range; years)	29 - 82	
< 65 years	47	37
≥ 65 years	79	63
Stage I-II	0	0
Stage III	0	0
Stage IV	126	100
Ki-67 ≥ 30%*	36	47
MIPI 1	19	15
MIPI 2	29	23
MIPI 3	78	62
B-symptoms	52	41
BM infiltration	126	100
BM infiltration ≥ 5%	126	100
Nodal involvement	108	86
Splenomegaly	89	71
Extra-hematological involvement	50	40
Bulky disease (≥ 5 cm)	45	36
CNS involvement**	17	13
Intensified therapy	37	29
R-CHOP-like therapy	71	56
Palliative therapy	8	6
Watch and wait	7	6
Died before initiation of therapy	3	2
Died during induction	9	7
ORR (CR/PR)	90	71
CR	61	48
PR	29	23
SD	4	3
PD	15	12
Event	78	62
Relapse	48	38
Death**	55	44

Table 8. Baseline characteristics of analysed patients. M = male; F = female; MIPI = MCL international prognostic index; BM = bone marrow; CNS = central nervous system; ORR = overall response rate; CR = complete remission; PR = partial remission; SD = stable disease; PD =

progressive disease; response was assessed by international workshop criteria published by Cheson B et al in 1999[127]. * of the analyzed samples, ** anytime from diagnosis until database lock; differences > 20% between cohorts are highlighted in gray.

Besides t(11;14) presented in (almost) all MCL patients, there are other recurrent cytogenetic changes described in MCL. By the cooperation with Center of Oncocytogenomics, General University Hospital in Prague and University Hospital Olomouc we analyzed molecular-cytogenetic aberrations of *TP53, CDKN2A, ATM, BCL2, MYC, RB1* and *CDK4* using FISH in 126 newly diagnosed (between years 2009 and 2018) MCL patients and in 113 patients with available samples also *TP53* and *CDKN2A* by NGS. Because FISH was analysed only for bone marrow with infiltration ≥ 5%, but not for formalin-fixed paraffin-embedded tissue sections, the analysed patients represented approx. 57% of all MCL patients (n=223) diagnosed in General University Hospital during the time period (Figure 20). The rest of patients had undetectable or low infiltration of bone marrow or no available samples for analysis. Thus, the applied methodology inevitably led to over-representation of high-risk patients, with diminished prognostic parameters (median EFS = 27 months, median OS 56 months). 5-year EFS and OS were 33.4 and 44.8%, respectively. Median follow-up of the living patients reached 42 months (Figure 21).

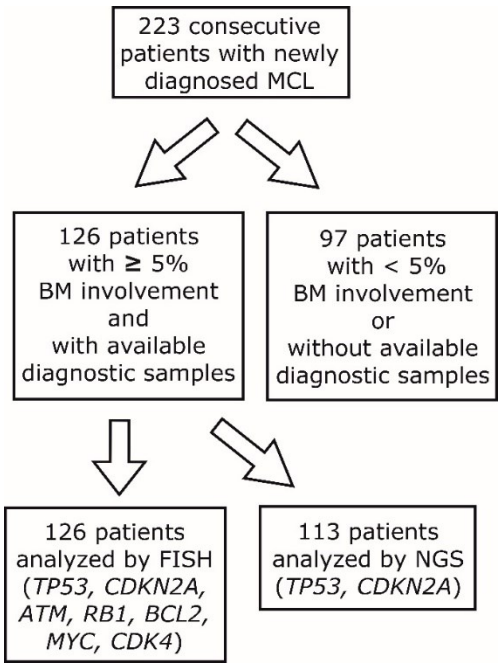

Figure 20. Flow chart of patient analysis

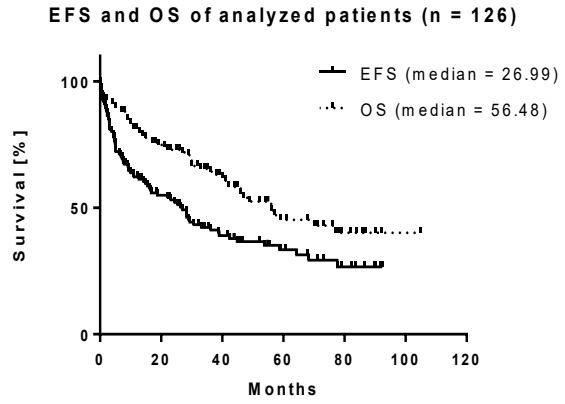

Figure 21. Survival parameters of analysed patients. EFS= event-free survival, OS= overall survival

The distribution and types of analysed aberrations are displayed in Figure 22. Only 25 patients (not shown in Figure/Table) had, apart from the translocation t(11;14), no other detectable gene aberration. Isolated (one) aberration of one analysed gene was observed in 39 patients (31%), two aberrations were found in 22 patients (17.5%), three, four, five, and six aberrations were detected in 16 (12.7%), 16 (12.7%), 5 (4%), and 3 (2.4%) patients, respectively. From patients with an isolated gene aberration, the most common aberration was TP53 mutation and/or deletion (15 patients), 9 patients had deletion of *ATM* (7.1%), and 5 patients had *RB1* deletion (4%). Isolated aberrations of other genes (*BCL2* (n=3, 2.4%), *MYC* (n=3, 2.4%), *CDK4* (n=3, 2.4%) and *CDKN2A* (n=1, 0.8%)) were rare.

The aberration of *TP53* (either mutation or deletion) was detected in 52 (41.3%) out of 126 patients. Most patients (n = 31; 59,6%) with *TP53* aberration were presented with both - deletion and mutation of the gene, while mutation without deletion was detected in 12 patients (23.1%), and deletion without mutation was found in 5 (9.6%) patients. Another 4 patients had detected deletion of *TP53*, but mutational analysis was not performed due to the lack of material. Because both types of *TP53* aberrations (deletion and mutation) significantly correlated with each other and all subcohorts (*TP53* mutation only, *TP53* deletion only, both mutation and deletion of *TP53*) had similarly adverse prognosis, for the further analyses the term *TP53* aberration (defined as *TP53* mutation and/or deletion) will be used. (Table 9, Figure 23).

TP53	*CDKN2A*	*RB1*	*MYC*	*CDK4*	*BCL2*	*ATM*
2	4	4	7	7	7	
2	4	4	7	8		
2	2	2	7			
2	4	4	7			
2	2	4	7			
2	4	4		9	7	2
2	2	2		8	7	2
2	4	4			7	
2	2	4				2
2	2, 4	4				2
2	2, 2+4	2, 4				
2	4	4				
2	4	2				
2	4	2				
2	4	2, 4				
2	2		7	8		
2	4		7, 10		7	
2	2		10			2
2	2		7			2
2	2			9	7	2
2	4					2
2	2					
2	2					
2	2					
2		4	7		7	
2		2	7			
2		2	7			
2		2				
2			7	6, 8, 9	7	
2			6		7	2
2			7			
2			7			
2			7			
2			7			
2					7	

TP53	*CDKN2A*	*RB1*	*MYC*	*CDK4*	*BCL2*	*ATM*
	5	4	7	9	6	
	3	2	10	8		
	4	2	7		7	2
	2	4	7			2
	2	2	7			
	2	4		7	7	2
	2	2			7	
	2, 3	2, 4				2
	2	2				2
	2	4				
	4	4				
	3		7			2
	3				7	
	2				6	
	2, 3				6	2
	2, 3					2
	4					
		4	7			
		4				2
		4				2
		2				
		2				
		4				
		4				
		4				
			7	7	7	2
			7		7	2
			7		7	
			7			2
			10			2
			7			
			7			
			7			
				7	7	2
				7		

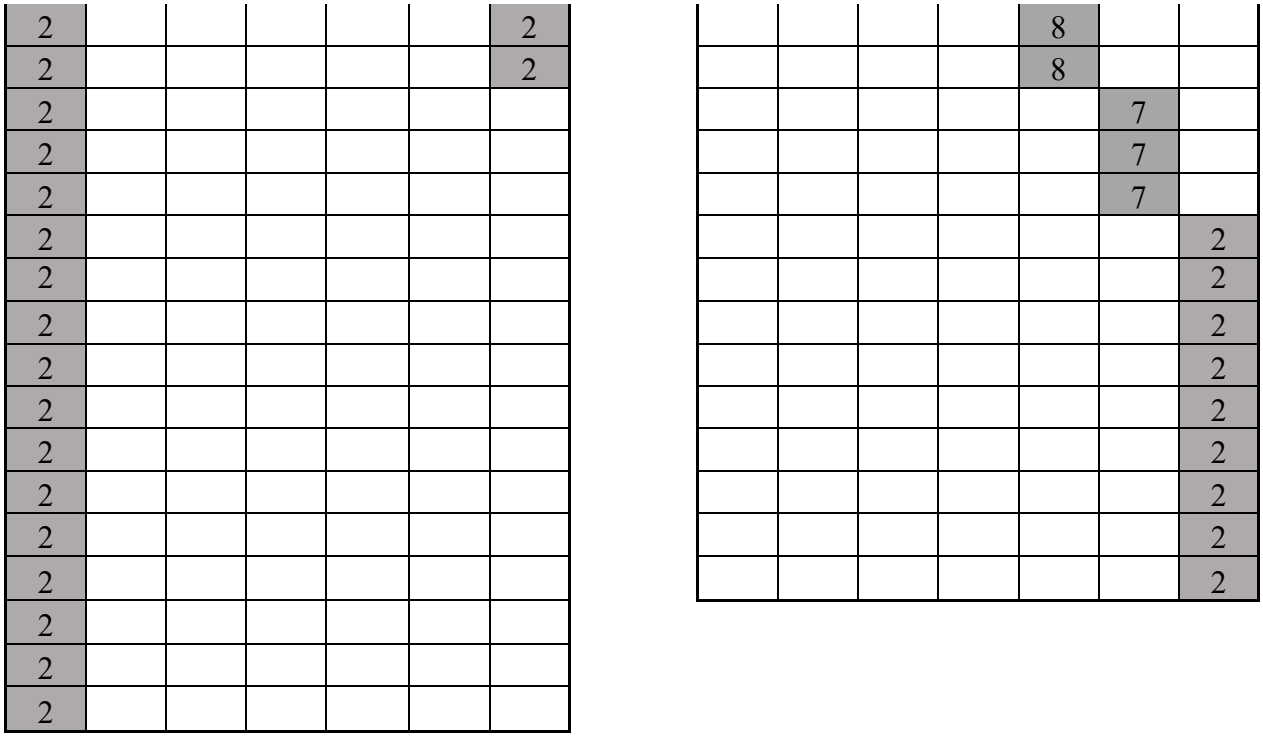

Figure 22. The distribution of the analyzed gene aberrations. Distribution of the analyzed aberrations of 101 patients with at least one detected aberration including *TP53* mutation (except for the translocation t(11;14)). Each row represents one patient, gray squares represent aberrated genes, numbers represent type of aberration: 2 = monoallelic deletion (in case of *TP53* and/or mutation), 3 = bialellic deletion, 4 = monosomy, 5 = nullisomy, 6 = amplification, 7 = gain, 8 = trisomy, 9 = tetrasomy, 10 = *MYC* rearrangement; more numbers represent different subclones (e.g. 2, 3 represent patients, in which both monoallelic and biallelic deletions of *CDKN2A* were detected)

A. Event–free survival

	HR	**95% CI**	**p**
***TP53* del**	2.3	1.2 - 32.8	0.04
***TP53* mut**	3	1.9 - 15.1	0.002
***TP53* del+mut**	2.3	1.5 - 5.3	0.002

B. Overall survival

	HR	**95% CI**	**p**
***TP53* del**	3.8	1.5 - 105.6	0.021
***TP53* mut**	3.7	2.6 - 26.9	<0.001
***TP53* del+mut**	2.1	1.1 - 5.1	0.024

Table 9. Univariate analysis of *TP53* mutation and *TP53* deletion. A Event-free survival B Overall survival

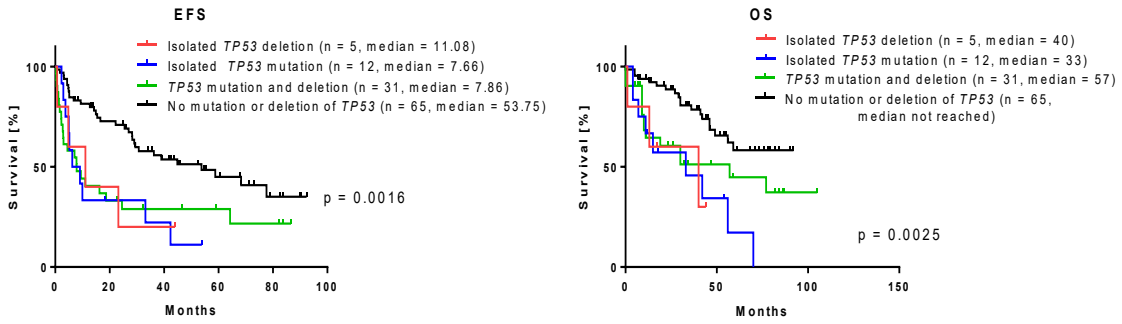

Figure 23. Survival parameters in *TP53* mutation and *TP53* deletion cohorts. Subcohort „Isolated *TP53* deletion" includes all patients with the deletion of *TP53*, but without the mutation of *TP53*, while in subcohort „Isolated *TP53* mutation" are the patients with the detected mutation of *TP53*, but without the deletion. Subgroup „*TP53* mutation and deletion" includes 31 patients with both the mutation and the deletion of *TP53*. Only 113 patients investigated by both FISH and NGS were included in this analysis. EFS= event-free survival, OS= overall survival

Besides TP53, mutational analysis of CDKN2A was also implemented by NGS, but no pathological mutations were detected.

Regarding the correlation of analysed aberration between one and other, Pearson chi square test revealed that *CDKN2A* deletion correlated with aberrations *of TP53, BCL2, RB1* and *CDK4*, and that *BCL2* aberration correlated with *CDK4*. No other correlations were found among other analysed genes (Table 10). These findings are in consensus with the distribution of analysed genes aberrations, where isolated *CDKN2A* and *CDK4* aberrations were extremely rare.

	CDK4	*RB1*	*BCL2*	*ATM*	*TP53*	*CDKN2A*	*MYC*
CDK4	1	0.138	< 0.001	0.260	0.651	0.016	0.055
RB1		1	0.384	0.847	0.191	< 0.001	0.074
BCL2			1	0.091	0.965	0.012	0.055
ATM				1	0.164	0.05	0.706
TP53					1	0.006	0.071
CDKN2A						1	0.065
MYC							1

Table 10. Correlation between the analyzed gene aberrations. The table shows p-values of Pearson's chi-squared test. Statistically significant results are highlighted in gray

Then, subsequent analyses of clinical, histo-pathological and molecular parameters showed the correlation of male sex, complex karyotype (yes vs no), Ki-67 (≥30% vs <30%), MIPI (high risk vs intermediate risk vs low risk p<0.0001), splenomegaly, bulky disease, B symptoms (present vs absent) and intensity of selected therapy (intensified vs R-CHOP-based vs palliative – for EFS p=0.0007 and for OS p=0.0003) with prognosis (OS and EFS) (Table 11). Despite that all patients had bone marrow infiltration, the extent of infiltration positively correlated with shorter survival (for EFS, HR=1.009 for each 1% of increase of BM infiltration, 95% CI=1.001-1.02, p=0.0312; for OS, HR=1.016 for each 1% of increase of BM infiltration, 95% CI=1.006-1.027, p=0.002).

A. Event-free survival

	HR	**95% CI**	**p**
Male sex	1.5	0.9 - 2.3	0.144
Ki-67	2.0	1.2 - 3.8	0.011
B-symptoms	2.7	1.9 - 5.1	<0.001
Nodal involvement	3.4	1.1 - 4.3	0.026
EH involvement	1.5	1.0 - 2.5	0.062
Splenomegaly	1.8	1.0 - 2.8	0.047
Bulky disease	1.9	1.3 - 3.4	0.005
Complex karyotype	2.7	1.4 - 14.7	0.014

B. Overall survival

	HR	95% CI	p
Male sex	2.1	1.1 - 3.3	0.032
Ki-67	2.2	1.1 - 4.7	0.026
B-symptoms	2.8	1.8 - 5.5	<0.001
Nodal involvement	1.9	0.7 - 4.0	0.255
EH involvement	1.5	0.9 - 2.7	0.149
Splenomegaly	1.2	0.6 -2.2	0.624
Bulky disease	1.5	0.8 - 2.7	0.185
Complex karyotype	3.9	2.9 - 58.7	0.001

Table 11. Correlation of selected clinical and laboratory parameters with survival. A Event-free survival B Overall survival; HR = hazard ratio, CI = confidence interval p = p-value; statistically significant results are highlighted in gray

Regarding the correlation of cytogenetic and molecular genetic factors with prognosis, except for *ATM* all analysed aberrations correlated with significantly shorter EFS, and apart from *ATM* and *MYC* all analysed aberration correlated with significantly shorter OS (Table 12).

A. Event-free survival

	HR	95% CI	p
TP53	2.2	1.5 - 4.0	<0.001
CDKN2A	3.0	2.4 - 6.8	<0.001
RB1	2.0	1.3 - 3.7	0.003
MYC	1.9	1.3 - 3.8	0.004
CDK4	2.3	1.5 - 7.5	0.005
BCL2	1.9	1.2 - 4.0	0.016
ATM	1.3	0.8 - 2.2	0.303

B. Overall survival

	HR	95% CI	p
TP53	2.3	1.4 - 4.3	0.002
CDKN2A	3.2	2.4 - 8.1	<0.001
RB1	2.2	1.4 - 4.6	0.003
MYC	1.7	1.0 - 3.5	0.068
CDK4	3.0	2.2 - 18.2	0.001
BCL2	2.4	2.3 - 10.9	<0.001
ATM	1.2	0.7 - 2.3	0.504

Table 12. Correlation of analyzed gene aberrations with survival. A Event-free survival B Overall survival; HR = hazard ratio, CI = confidence interval p = p-value; statistically significant results are highlighted in gray

The analyses results also showed, that the total number of aberrations correlates with EFS and OS, with the biggest difference between any two aberrations versus any isolated (single) aberration. Interestingly, 3 or more aberrations were not associated with significantly worse prognosis than 2 aberrations (Figure 24). The total number of aberrations, according to Mann-Whitney U test, correlated with male sex (p=0.045).

A. Event-free survival **B. Overall survival**

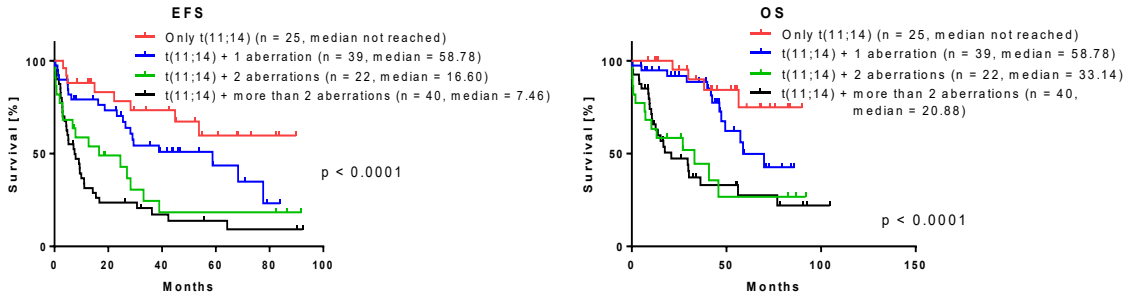

Figure 24. Total number of gene aberrations correlates with shorter survival. A Event-free survival B Overall survival

To fully evaluate which patients might benefit from chemotherapy-free regimen, the aberrations associated with chemo-resistance and diminished prognosis were determined. Cox regression showed that aberrations of *TP53* and *CDKN2A* independently correlate with shorter survival parameters (both EFS and OS), and *BCL2* aberration is associated with shorter OS (Table 13). Random forest analysis revealed that the most important predictor of diminished EFS and OS from analysed gene aberrations is *CDKN2A* (Figure 25). And, since any 2 aberrations had significantly worse outcome compared to any single aberration in MCL patients, random forest analysis of possible aberrations pairs was performed and revealed that the strongest predictor of shorter EFS and OS was concurrent *CDKN2A* deletion and *TP53* aberration (mutation and/or deletion), together with the concurrent *CDKN2A* deletion and *BCL2* aberration, that predicted the shorter OS. (Figure 26).

A. Event-free survival:

	HR	95% CI	P
CDK4	1.6	0.8 – 3.1	0.218
RB1	0.9	0.5 – 1.6	0.803
BCL2	1.5	0.8 – 2.5	0.287
ATM	1.1	0.7 – 1.9	0.667
TP53	2.3	1.4 – 3.6	0.001
CDKN2A	2.6	1.5 – 4.7	0.001
MYC	1.6	1.0 – 2.6	0.06

B. Overall survival:

	HR	95% CI	P
CDK4	1.7	0.8 – 3.7	0.205
RB1	1.2	0.6 – 2.2	0.645
BCL2	2.6	1.4 – 4.8	0.004
ATM	1.0	0.6 – 2.0	0.921
TP53	2.2	1.2 – 3.8	0.008
CDKN2A	2.5	1.2 – 4.9	0.011
MYC	1.2	0.7 – 2.2	0.507

Table 13. Effect of the analysed gene aberrations with survival parameters. Tables show Cox's proportional hazard model; HR = hazard ratio, CI = confidence interval p = p-value; statistically significant results are highlighted in gray.

A:

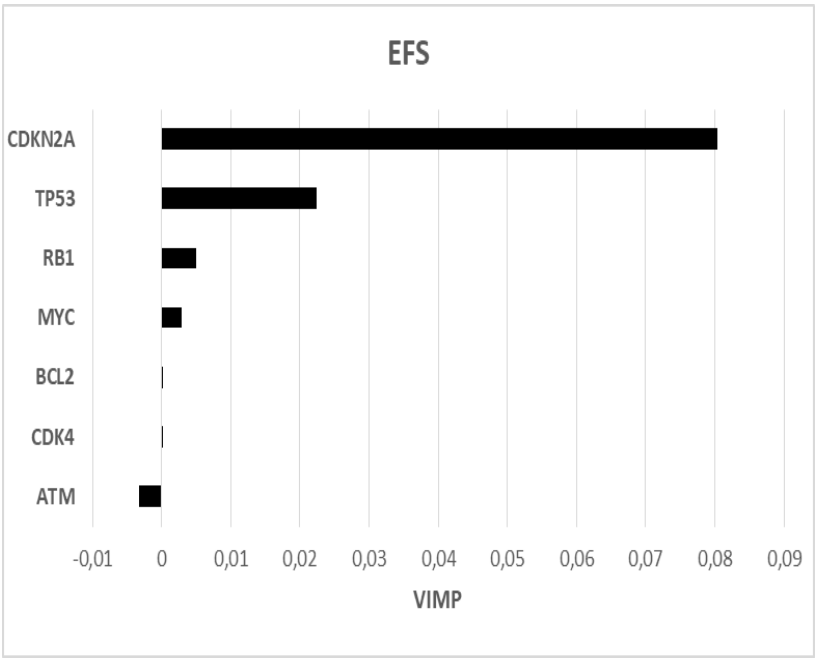

B:

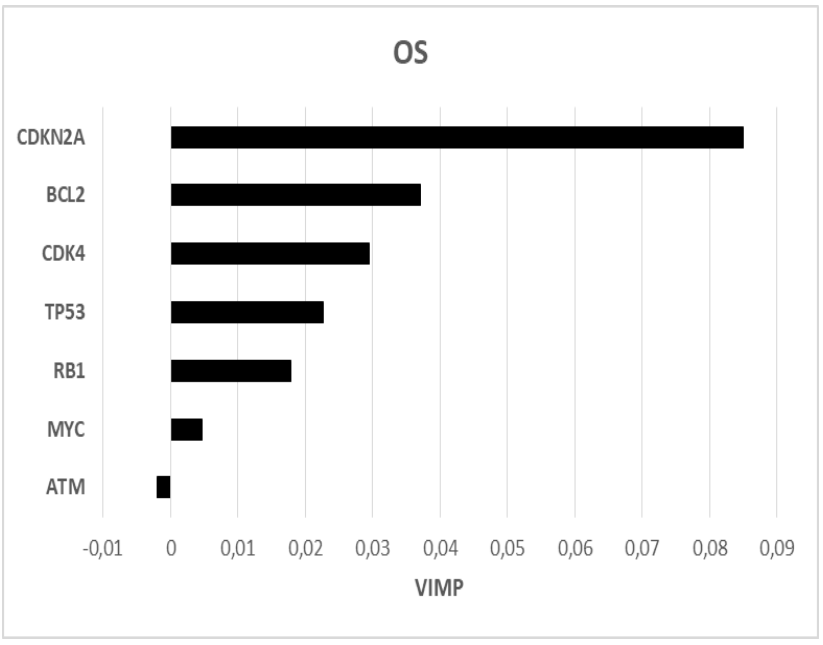

Figure 25. Random forest analysis of analyzed gene aberrations. A Event-free survival B Overall survival. Positive VIMP values indicate that the variable increases the prediction accuracy

of random forest analysis, whereas negative or near-zero values have no effect on survival prediction.

A:

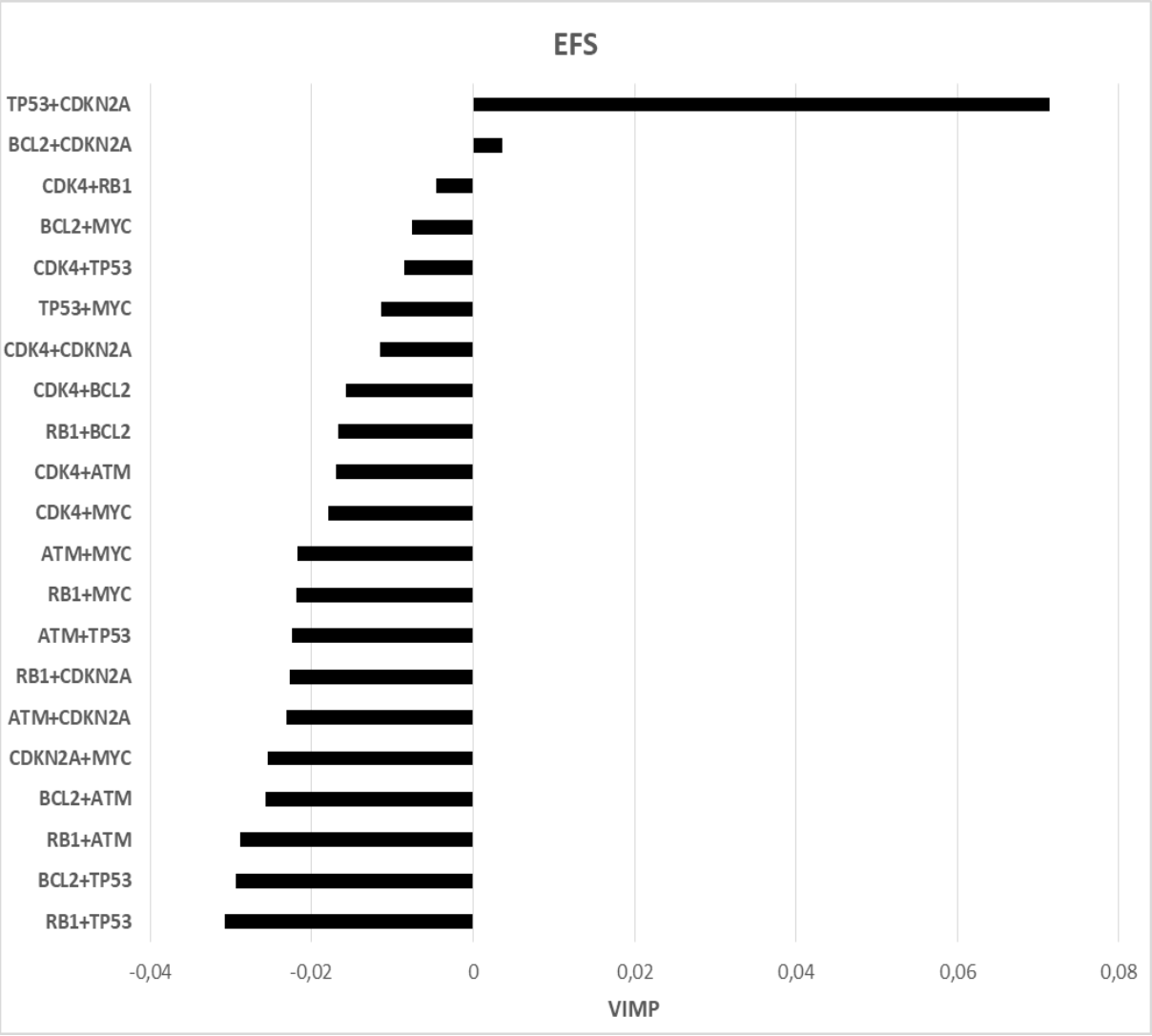

B:

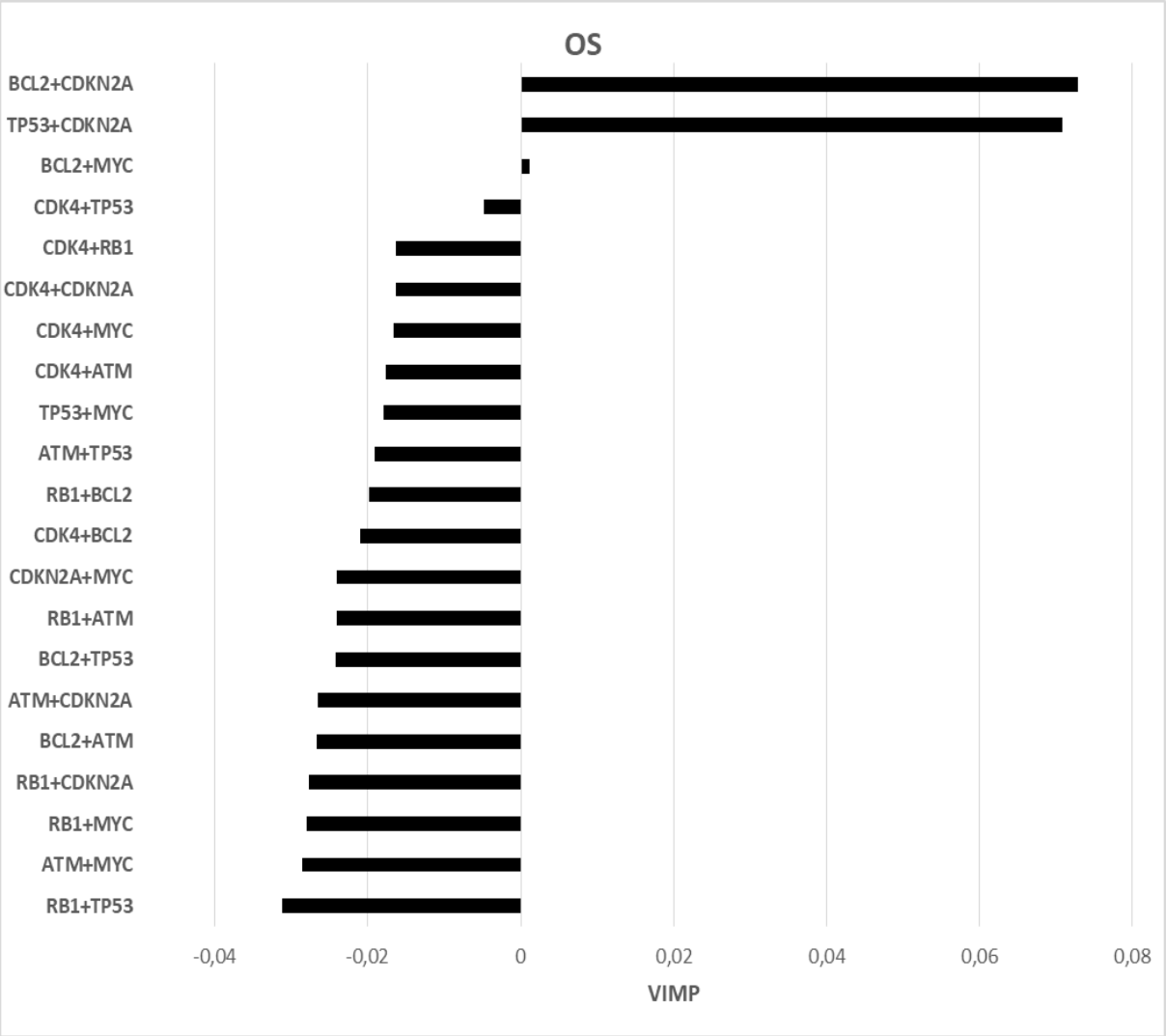

Figure 26. Random forest analysis of analyzed gene aberrations pairs. A Event-free survival B Overall survival. Positive VIMP values indicate that the variable increases the prediction accuracy of random forest analysis, whereas negative or near-zero values have no effect on survival prediction.

Concurrent *CDKN2A* deletion and aberration (mutation and or deletion) of *TP53* was found in 24 patients, which represent 19% of patients from the analysed group. Sub-analysis of these patients revealed significantly shorter survival in patients with both aberrations, than in patients with isolated *TP53* or *CDKN2A* aberration (Figure 27).

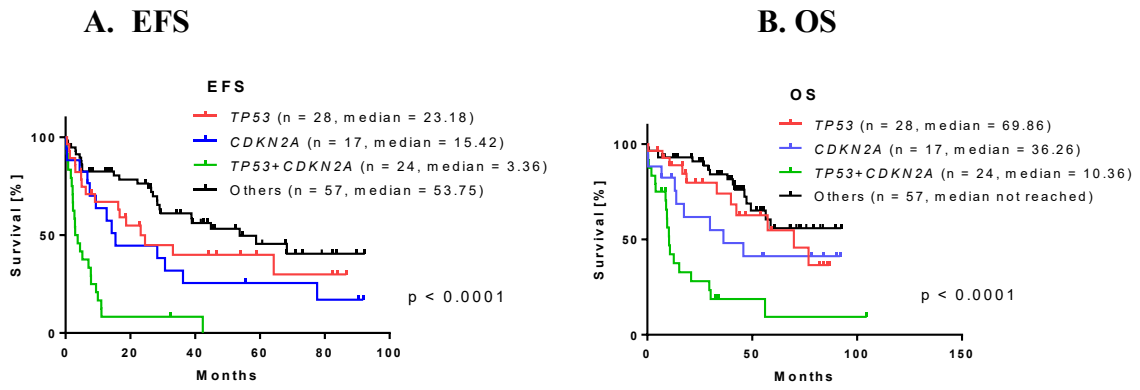

Figure 27. Patients with concurrent *TP53* and *CDKN2A* aberrations have significantly shorter survival than isolated aberrations. Patients in groups *TP53* and *CDKN2A* are patients with *TP53* aberrations or *CDKN2A* deletions that are not contained in the *TP53+CDKN2A* sub-group. A Event-free survival B Overall survival

The patients with concurrent *CDKN2A* and *TP53* aberrations also had a higher frequency of CNS involvement (33% vs. 9%), B-symptoms (71% vs. 34%) and Ki-67 ≥30% (85% vs. 40%) compared to the remaining patients. High-risk MIPI was calculated in 79% of these patients versus 58% of remaining 102 patients. Only 38% and 17% of these patients achieved response and complete response after standard first-line treatment methods (compared to 79% and 56% of patients without concurrent *CDKN2A* and *TP53* aberration). At the time of the database lock, 96% of patients with concurrent *CDKN2A* deletion and *TP53* aberration relapsed or progressed on first-line treatment and only 21% of patients were alive (compared to 54% and 65% in the sub-group of remaining analysed patients). (Table 14).

	$TP53^{del/mut}$+ $CDKN2A^{del}$		The remaining pts with bone marrow involvement ≥ 5%	
	N	%	N	%
All patients	24	19	102	81
M	19	79	69	68
F	5	21	33	32
Age (median; years)	70		67	
Age (range; years)	46 - 79		29 - 82	
< 65 years	8	33	39	38
≥ 65 years	16	67	64	63
Ki-67 ≥ 30%*	11	85	25	40
MIPI 1	1	4	18	18
MIPI 2	4	17	25	25
MIPI 3	19	79	59	58
B-symptoms	17	71	35	34
Nodal involvement	21	88	87	85
Splenomegaly	19	79	70	69
Extra-hematological involvement	11	46	39	38
Bulky disease (≥ 5 cm)	11	46	34	33
CNS involvement**	8	33	9	9
Intensified therapy	8	33	29	28
R-CHOP-like therapy	10	42	61	60
Palliative therapy	5	21	3	3
Watch and wait	0	0	7	7
Died before initiation of therapy	1	4	2	2
Died during induction***	4	17	5	5
ORR (CR/PR)	9	38	81	79
CR	4	17	57	56
PR	5	21	24	24
SD	3	13	1	1
PD	7	29	8	8
Event	23	96	55	54
Relapse	17	71	36	35
Death**	19	79	36	35

Table 14. Baseline characteristics and response to therapy of patients with concurrent aberration of TP53 and CDKN2A (compared to the remaining patients). M = male; F = female; MIPI = MCL international prognostic index; BM = bone marrow; CNS = central nervous system; ORR = overall response rate; CR = complete remission; PR = partial remission; SD = stable disease; PD = progressive disease; response was assessed by international workshop criteria published by Cheson B et al in 1999(7); * of the analyzed patients, ** anytime from diagnosis until

database lock, *** after initiation of therapy, before restaging; differences > 20% between cohorts are highlighted in gray

10.7 The effect of genetic aberrations on the sensitivity to palbociclib and venetoclax

After the identification, which genetic aberrations lead to chemoresistance and thus, which patients might benefit most from novel treatment strategies, MCL clones with knockout (CDKN2A and RB1) or transgenic (over)expression (p16INK4A – coded by CDKN2A, CDK4 and MYC) were derived and tested for sensitivity to palbociclib and venetoclax. RB1 gene knockout was associated with the resistance to palbociclib and the overexpression of MYC led to the increased sensitivity to venetoclax (Figure 28). Other aberrations did not significantly influence sensitivity to palbociclib or venetoclax.

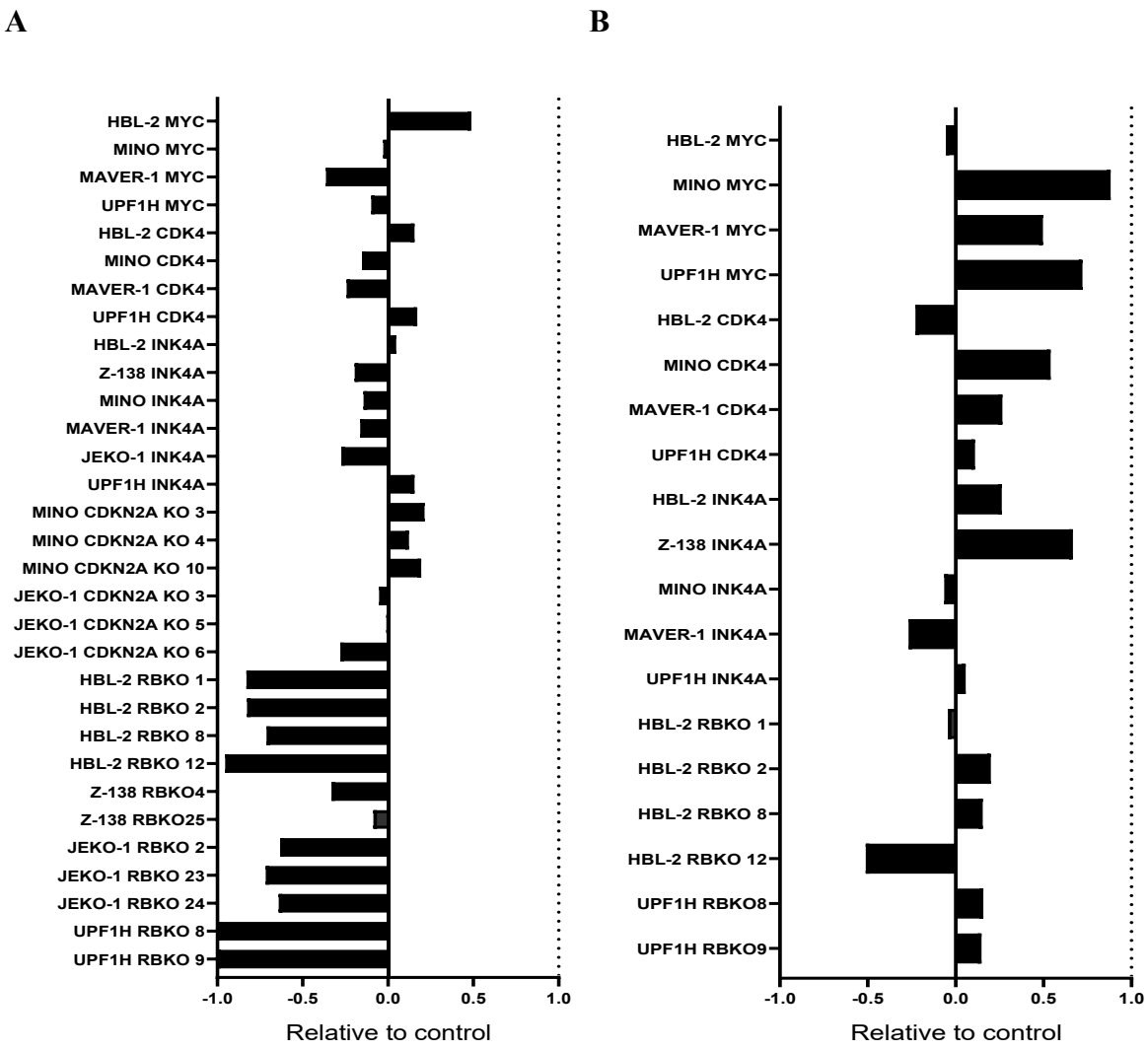

Figure 28. The effect of palbociclib and venetoclax on the clones with the overexpression of MYC, CDK4, CDKN2A and K/O of *CDKN2A* and *RB*. A The effect of palbociclib on the derived clones. B The effect of venetoclax on the derived clones. The figure shows the relative comparison of half-maximal inhibitory concentration (IC50, in nM) in response to palbociclib between MCL clones (IC50clone) and corresponding controls (IC50CTRL). The bars were constructed according to the following formulas: 1 + IC50CTRL / IC50clone in cases when IC50clone > IC50CTRL; 1 - IC50clone / IC50CTRL in the cases when IC50CTRL > IC50clone. Positive and negative bars represent more sensitive and resistant clones, respectively compared to controls.

11. Discussion

Treatment of relapsed/refractory aggressive B-NHL remains challenging, even in the era of novel treatment strategies focused on T-cell engaging immunotherapy. R/R B-NHL patients have dismal prognosis and relapses often manifest with biologically aggressive, hyperproliferative phenotypes. We implemented preclinical proof-of-concept study of a novel treatment combination based on the induction of apoptosis with BCL2 inhibitor venetoclax and the inhibition of cell cycle with the CDK4/6 inhibitor palbociclib.

Targeting cell cycle with various CDKi became a relevant treatment strategy for several cancers in the last decades [128-133]. Of note, palbociclib demonstrated single-agent activity in patients with R/R MCL inducing an 18% overall response rate and 41% disease stabilization rate. Median PFS reached 4 months, but responders remained on the treatment for more than 18 months [124]. Despite promising anti-cancer activity and a manageable safety profile, rational combinations of palbociclib with other anti-lymphoma agents are necessary to improve the treatment efficacy and survival parameters. Combination of palbociclib and bortezomib did not significantly increase ORR (21%) [123]. In contrast, combination of palbociclib and ibrutinib was highly effective, with 68% responding patients and 37% complete remissions [122].

Venetoclax is likewise clinically approved and used for the treatment of chronic lymphocytic leukemia/small lymphocytic lymphoma and acute myeloid leukemia [134, 135]. Venetoclax already demonstrated clinical activity in MCL, and subsets of DLBCL, but the remissions were short and calling for rational drug combinations [92, 96, 97, 122, 136]. The combination of venetoclax and a Bruton tyrosine-kinase inhibitor ibrutinib, with or without anti-CD20 antibodies rituximab or obinutuzumab represents a highly effective non-chemotherapy regimen for patients with MCL [93, 94].

Co-targeting of CDK4/6 and BCL2 has shown a synergistic effect *in vitro* as well as *in vivo*, especially in MCL and BCL2 positive DLBCL. This combination was already tested by Whittle et al showing synergism in BCL2-positive breast cancer cell lines [137]. In addition, a chemotherapy-free combination of palbociclib, venetoclax, and letrozole (nonsteroidal selective aromatase inhibitor) is being evaluated in the ongoing phase 1b clinical trial (NCT03900884) in patients with metastatic breast cancer [138]. Molecular mechanisms behind the described palbociclib and

venetoclax synergy remain only partially understood. At the clinically relevant concentrations palbociclib did not induce apoptosis, nor significantly change the levels of key pro- and antiapoptotic proteins, except for the moderate downregulation of MCL1 protein. Indeed, the downregulation of MCL1 was repeatedly documented in most of the so far published studies that reported the synergy between various CDKi and venetoclax [139-143]. The presented results, however, suggest that the downregulation of MCL1 might not be the only mechanism, but only one of many factors that enhance the palbociclib induced mitochondrial priming for venetoclax-triggered death.

It was repeatedly demonstrated that the cell cycle arrest induced by CDKi leads to cell senescence, in which the generation of proton (H^+) gradient becomes uncoupled from the ATP-synthesis. The senescence is associated with increased cellular requirements for oxygen and higher ROS generation [144-147], which correlates with the presented data. Using JC-1 staining, depolarization of mitochondrial membrane after exposure of MCL cells to palbociclib was demonstrated. This increased mitochondrial respiratory disturbance might lead to changes in AKT activity (and vice versa). AKT kinase, besides the well-described impacts on respiration and metabolism, regulates apoptosis via phosphorylation of pro-apoptotic peptides [147-149]. These complex mitochondrial metabolic changes induced by the cell cycle arrest after palbociclib lead to the enhanced mitochondrial proapoptotic priming by complex mechanisms independent of BCL2 proteins. This is supported by the fact that the synergism was observed between palbociclib and all three tested BH3 mimetics (i.e., BCL2, BCL-XL and MCL1 inhibitors).

In MCL, two most important recurrent genetic aberrations include mutation/deletion of *TP53* and deletion of *CDKN2A*. Both aberrations belong to the key regulators of genotoxic stress pathways and it is thus not surprising that their aberrations negatively correlated with the treatment outcome to genotoxic chemotherapy (which is still standardly used in the first-line treatment of MCL patients). How *CDKN2A* and *TP53* aberrations impact the sensitivity to CDK4/6 or BCL2 inhibitors in MCL remains only partially understood.

First, 126 consecutive MCL patients were analyzed by FISH and NGS to identify patients based on their genetic profile who are not responding to the standard treatment and might benefit most from proposed novel combination, and MCL cell clones that emulated these recurrent genetic aberrations were created and the impact of these aberrations on sensitivity to palbociclib and

venetoclax was systemically studied. Concurrent *CDKN2A* deletion and *TP53* deletion and/or mutation was associated with chemoresistance. The results confirmed findings of the Delfau-Larue et al. on a real-life cohort of predominantly elderly MCL patients with higher frequency of high-risk MIPI patients (62% compared to 25%)[150]. It was also reported by Streich et al that blastoid and pleomorphic morphology of MCL is associated with both *TP53* and *CDKN2A/B* aberrations, and that these cases are characterized by frequent chromothripsis[151]. Interestingly, in contrast to MCL, *TP53* and *CDKN2A* aberrations were rarely observed in DLBCL[152-154]and *CDKN2A* deletion is rare in indolent B-NHL (CLL/SLL, follicular lymphoma) and its inactivation correlates with transformation to more aggressive lymphoma subtypes[155-158]. In this perspective, MCL patients with concurrent *TP53* and *CDKN2A* aberrations might be considered as "transformed" MCL patients with adverse prognosis. Virtually all deletions of *CDKN2A* were found in the context of other genetic aberrations. These data suggest that *CDKN2A* deletions (detected in 32.5% of analyzed patients as the second most common gene aberration) represent late events in pathophysiology of MCL, especially more aggressive subtypes. This theory is supported by the results of Pearson´s analysis, where incidence of *CDKN2A* correlated with incidence of all other aberrations except *ATM* deletion – the only aberration not associated with adverse prognosis. In addition, *CDKN2A* deletions correlated with clinical parameters associated with more aggressive disease and shorter survival parameters like MIPI, Ki-67 proliferation index, CNS involvement, male sex and B-symptoms.

Second, we derived clones that emulated the recurrent genetic aberrations, including the knockout of *CDKN2A* and *RB1* and the (over)expression of CDK4, MYC and p16INK4A (coded by *CDKN2A*). The data clearly show that *RB1* deletion, found in 29% of analyzed patients and approximately 20-30% of newly diagnosed MCL patients in literature, mediates resistance to palbociclib. In line with these findings, *RB1* loss has been implicated in acquired resistance to palbociclib in breast cancer patients [159, 160]. Moreover, the most palbociclib-resistant tested lymphoma cell lines - Riva, and U2932 (both DLBCL) - harbor a deletion of *RB1*. In contrast to *RB1*, the other analyzed aberrations (i.e., deletion of *CDKN2A*, overexpression of *CDK4,* or *MYC*) did not significantly change sensitivity to palbociclib. Transgenic (over)expression of MYC on the other hand increased the sensitivity of MCL cells to venetoclax indicating a potential subgroup of patients who might profit the most from the tested experimental combination.

12. Conclusion

The combination of the FDA-approved CDK4/6 inhibitor palbociclib with the tested BH3-mimetics (namely, a BCL2 inhibitor venetoclax, a MCL1 inhibitor S63845 and a BCL-XL inhibitor A1155463) have shown synergism using *in vitro* and *in vivo* models of chemotherapy refractory aggressive lymphomas. Molecular mechanisms behind the observed synthetic lethality include increased pro-apoptotic priming by palbociclib induced mitochondrial and metabolic stress, downregulation of anti-apoptotic protein MCL1 and increased levels of proapoptotic BIM bound on BCL2 and BCL-XL. Loss of *RB1* resulted in palbociclib resistance and transgenic overexpression of MYC led to an increased sensitivity to venetoclax. Thus, the results strongly support further preclinical and clinical investigations this innovative, chemotherapy-free, orally available combination of two FDA approved molecules, especially for patients with relapsed and/or chemotherapy-refractory MCL without *RB1* deletion. Importantly, *CDKN2A* deletion (prognostically the most unfavorable aberration in MCL patients) did not influence the sensitivity of the proposed treatment combination. Concurrent aberration of *TP53* (mutation and/or deletion) and deletion of *CDKN2A* can reliably identify chemotherapy-refractory patients with newly diagnosed MCL.

13. Shrnutí

Kombinace inhibitoru cyklin-dependentních kináz 4/6 palbociklibu s vybranými BH3-mimetiky (jmenovitě BCL2 inhibitor venetoklax, MCL1 inhibitor S63845 a BCL-XL inhibitor A11556463) prokázala synergizmus na modelech agresivních lymfomů refrakterních k chemoterapii a to v podmínkách *in vitro* i *in vivo*. Molekulární mechanismy zodpovědné za pozorovaný synergizmus zahrnovaly palbociklibem způsobenou zvýšenou náchylnost buněk k apoptóze z důvodu mitochondriálního a metabolického stresu, sníženou koncentraci anti-apoptotického proteinu MCL1 a zvýšené množství proapoptotického peptidu BIM vázaného na BCL2 a BCL-XL. Ztráta funkce *RB1* genu vedla k rezistenci buněk na palbociklib a transgenní overexprese peptidu MYC způsobila zvýšenou citlivost na venetoklax. Výsledky studie významně podporují další preklinické a klinické zkoumání palbociklibu v kombinaci s venetoklaxem jako inovativní kombinaci perorálně užívaných cílených léčiv, již schválených FDA, a to zejména u pacientů s relabovaným či chemorefrakterním lymfomem z buněk pláště bez *RB1* delece. Delece *CDKN2A*, aberace asociovaná s nejhorší prognózou u pacientů s MCL, neovlivňovala citlivost na navrhovanou terapeutickou kombinaci. Současná aberace *TP53* (mutace nebo delece) a delece *CDKN2A* spolehlivě identifikuje pacienty s nově diagnostikovaným lymfomem, kteří jsou refrakterní k standardní imunochemoterapii.

14. References

1. Lenz, G. and L.M. Staudt, *Aggressive lymphomas.* N Engl J Med, 2010. **362**(15): p. 1417-29.
2. Vaux, D.L., S. Cory, and J.M. Adams, *Bcl-2 gene promotes haemopoietic cell survival and cooperates with c-myc to immortalize pre-B cells.* Nature, 1988. **335**(6189): p. 440-2.
3. Martelli, M., et al., *Diffuse large B-cell lymphoma.* Crit Rev Oncol Hematol, 2013. **87**(2): p. 146-71.
4. Yunis, J.J., et al., *bcl-2 and other genomic alterations in the prognosis of large-cell lymphoma.* N Engl J Med, 1989. **320**(16): p. 1047-54.
5. Molyneux, E.M., et al., *Burkitt's lymphoma.* Lancet, 2012. **379**(9822): p. 1234-44.
6. Schmitz, R., et al., *Oncogenic mechanisms in Burkitt lymphoma.* Cold Spring Harb Perspect Med, 2014. **4**(2).
7. Love, C., et al., *The genetic landscape of mutations in Burkitt lymphoma.* Nat Genet, 2012. **44**(12): p. 1321-5.
8. Klanova, M. and P. Klener, *BCL-2 Proteins in Pathogenesis and Therapy of B-Cell Non-Hodgkin Lymphomas.* Cancers (Basel), 2020. **12**(4).
9. Wong, R.S., *Apoptosis in cancer: from pathogenesis to treatment.* J Exp Clin Cancer Res, 2011. **30**(1): p. 87.
10. Xu-Monette, Z.Y., et al., *Dysfunction of the TP53 tumor suppressor gene in lymphoid malignancies.* Blood, 2012. **119**(16): p. 3668-83.
11. Jain, P. and M. Wang, *Mantle cell lymphoma: 2019 update on the diagnosis, pathogenesis, prognostication, and management.* Am J Hematol, 2019. **94**(6): p. 710-725.
12. Dreyling, M., et al., *Update on the molecular pathogenesis and clinical treatment of mantle cell lymphoma: report of the 11th annual conference of the European Mantle Cell Lymphoma Network.* Leuk Lymphoma, 2013. **54**(4): p. 699-707.
13. Delbridge, A.R. and A. Strasser, *The BCL-2 protein family, BH3-mimetics and cancer therapy.* Cell Death Differ, 2015. **22**(7): p. 1071-80.
14. Malumbres, M., *Cyclin-dependent kinases.* Genome Biol, 2014. **15**(6): p. 122.
15. Bai, J., Y. Li, and G. Zhang, *Cell cycle regulation and anticancer drug discovery.* Cancer Biol Med, 2017. **14**(4): p. 348-362.
16. Otto, T. and P. Sicinski, *Cell cycle proteins as promising targets in cancer therapy.* Nat Rev Cancer, 2017. **17**(2): p. 93-115.
17. Sánchez-Martínez, C., et al., *Cyclin dependent kinase (CDK) inhibitors as anticancer drugs: Recent advances (2015-2019).* Bioorg Med Chem Lett, 2019. **29**(20): p. 126637.
18. Mugnaini, E.N. and N. Ghosh, *Lymphoma.* Prim Care, 2016. **43**(4): p. 661-675.
19. Seifert, M., R. Scholtysik, and R. Küppers, *Origin and pathogenesis of B cell lymphomas.* Methods Mol Biol, 2013. **971**: p. 1-25.
20. Armitage, J.O., et al., *Non-Hodgkin lymphoma.* Lancet, 2017. **390**(10091): p. 298-310.
21. Costa, L.J., et al., *Trends in survival of patients with Burkitt lymphoma/leukemia in the USA: an analysis of 3691 cases.* Blood, 2013. **121**(24): p. 4861-6.
22. Coiffier, B., et al., *CHOP chemotherapy plus rituximab compared with CHOP alone in elderly patients with diffuse large-B-cell lymphoma.* N Engl J Med, 2002. **346**(4): p. 235-42.
23. Poletto, S., et al., *Treatment strategies for patients with diffuse large B-cell lymphoma.* Cancer Treat Rev, 2022. **110**: p. 102443.
24. Silkenstedt, E., K. Linton, and M. Dreyling, *Mantle cell lymphoma - advances in molecular biology, prognostication and treatment approaches.* Br J Haematol, 2021. **195**(2): p. 162-173.
25. *A clinical evaluation of the International Lymphoma Study Group classification of non-Hodgkin's lymphoma. The Non-Hodgkin's Lymphoma Classification Project.* Blood, 1997. **89**(11): p. 3909-18.

26. Campo, E., et al., *The International Consensus Classification of Mature Lymphoid Neoplasms: a report from the Clinical Advisory Committee.* Blood, 2022. **140**(11): p. 1229-1253.
27. Carvajal-Cuenca, A., et al., *In situ mantle cell lymphoma: clinical implications of an incidental finding with indolent clinical behavior.* Haematologica, 2012. **97**(2): p. 270-8.
28. Harmanen, M., et al., *Survival of patients with mantle cell lymphoma in the rituximab era: Retrospective binational analysis between 2000 and 2020.* Br J Haematol, 2023. **201**(1): p. 64-74.
29. Obr, A., et al., *TP53 Mutation and Complex Karyotype Portends a Dismal Prognosis in Patients With Mantle Cell Lymphoma.* Clin Lymphoma Myeloma Leuk, 2018. **18**(11): p. 762-768.
30. Clot, G., et al., *A gene signature that distinguishes conventional and leukemic nonnodal mantle cell lymphoma helps predict outcome.* Blood, 2018. **132**(4): p. 413-422.
31. Eskelund, C.W., et al., *TP53 mutations identify younger mantle cell lymphoma patients who do not benefit from intensive chemoimmunotherapy.* Blood, 2017. **130**(17): p. 1903-1910.
32. Beà, S., et al., *Landscape of somatic mutations and clonal evolution in mantle cell lymphoma.* Proc Natl Acad Sci U S A, 2013. **110**(45): p. 18250-5.
33. Zhang, J., et al., *The genomic landscape of mantle cell lymphoma is related to the epigenetically determined chromatin state of normal B cells.* Blood, 2014. **123**(19): p. 2988-96.
34. Cheah, C.Y., J.F. Seymour, and M.L. Wang, *Mantle Cell Lymphoma.* J Clin Oncol, 2016. **34**(11): p. 1256-69.
35. Klener, P., *Advances in Molecular Biology and Targeted Therapy of Mantle Cell Lymphoma.* Int J Mol Sci, 2019. **20**(18).
36. Hoster, E., et al., *Prognostic Value of Ki-67 Index, Cytology, and Growth Pattern in Mantle-Cell Lymphoma: Results From Randomized Trials of the European Mantle Cell Lymphoma Network.* J Clin Oncol, 2016. **34**(12): p. 1386-94.
37. Hoster, E., et al., *A new prognostic index (MIPI) for patients with advanced-stage mantle cell lymphoma.* Blood, 2008. **111**(2): p. 558-65.
38. Lin, R.J., et al., *Allogeneic haematopoietic cell transplantation impacts on outcomes of mantle cell lymphoma with TP53 alterations.* Br J Haematol, 2019. **184**(6): p. 1006-1010.
39. Young, R.M. and L.M. Staudt, *Targeting pathological B cell receptor signalling in lymphoid malignancies.* Nat Rev Drug Discov, 2013. **12**(3): p. 229-43.
40. Wang, M.L., et al., *Targeting BTK with ibrutinib in relapsed or refractory mantle-cell lymphoma.* N Engl J Med, 2013. **369**(6): p. 507-16.
41. Hermine, O., et al., *Addition of high-dose cytarabine to immunochemotherapy before autologous stem-cell transplantation in patients aged 65 years or younger with mantle cell lymphoma (MCL Younger): a randomised, open-label, phase 3 trial of the European Mantle Cell Lymphoma Network.* Lancet, 2016. **388**(10044): p. 565-75.
42. Dreyling, M., et al., *Early consolidation by myeloablative radiochemotherapy followed by autologous stem cell transplantation in first remission significantly prolongs progression-free survival in mantle-cell lymphoma: results of a prospective randomized trial of the European MCL Network.* Blood, 2005. **105**(7): p. 2677-84.
43. McDonnell, T.J., et al., *bcl-2-immunoglobulin transgenic mice demonstrate extended B cell survival and follicular lymphoproliferation.* Cell, 1989. **57**(1): p. 79-88.
44. Alaggio, R., et al., *The 5th edition of the World Health Organization Classification of Haematolymphoid Tumours: Lymphoid Neoplasms.* Leukemia, 2022. **36**(7): p. 1720-1748.
45. Schmitz, R., et al., *Genetics and Pathogenesis of Diffuse Large B-Cell Lymphoma.* N Engl J Med, 2018. **378**(15): p. 1396-1407.
46. Chapuy, B., et al., *Molecular subtypes of diffuse large B cell lymphoma are associated with distinct pathogenic mechanisms and outcomes.* Nat Med, 2018. **24**(5): p. 679-690.

47. Fisher, S.G. and R.I. Fisher, *The epidemiology of non-Hodgkin's lymphoma.* Oncogene, 2004. **23**(38): p. 6524-34.
48. Vianna, N.J., *The malignant lymphomas: epidemiology and related aspects.* Pathobiol Annu, 1977. **7**: p. 231-55.
49. Smedby, K.E., E. Baecklund, and J. Askling, *Malignant lymphomas in autoimmunity and inflammation: a review of risks, risk factors, and lymphoma characteristics.* Cancer Epidemiol Biomarkers Prev, 2006. **15**(11): p. 2069-77.
50. Ye, B.H., et al., *Chromosomal translocations cause deregulated BCL6 expression by promoter substitution in B cell lymphoma.* Embo j, 1995. **14**(24): p. 6209-17.
51. Phan, R.T. and R. Dalla-Favera, *The BCL6 proto-oncogene suppresses p53 expression in germinal-centre B cells.* Nature, 2004. **432**(7017): p. 635-9.
52. Volpe, G., et al., *Molecular heterogeneity of B-lineage diffuse large cell lymphoma.* Genes Chromosomes Cancer, 1996. **16**(1): p. 21-30.
53. Schuster, S.J., et al., *Tisagenlecleucel in Adult Relapsed or Refractory Diffuse Large B-Cell Lymphoma.* N Engl J Med, 2019. **380**(1): p. 45-56.
54. Neelapu, S.S., et al., *Axicabtagene Ciloleucel CAR T-Cell Therapy in Refractory Large B-Cell Lymphoma.* N Engl J Med, 2017. **377**(26): p. 2531-2544.
55. Abramson, J.S., et al., *Lisocabtagene maraleucel for patients with relapsed or refractory large B-cell lymphomas (TRANSCEND NHL 001): a multicentre seamless design study.* Lancet, 2020. **396**(10254): p. 839-852.
56. Bargou, R., et al., *Tumor regression in cancer patients by very low doses of a T cell-engaging antibody.* Science, 2008. **321**(5891): p. 974-7.
57. Sehn, L.H., et al., *Polatuzumab Vedotin in Relapsed or Refractory Diffuse Large B-Cell Lymphoma.* J Clin Oncol, 2020. **38**(2): p. 155-165.
58. Salles, G., et al., *Tafasitamab plus lenalidomide in relapsed or refractory diffuse large B-cell lymphoma (L-MIND): a multicentre, prospective, single-arm, phase 2 study.* Lancet Oncol, 2020. **21**(7): p. 978-988.
59. Goldfinger, M. and D.L. Cooper, *Refractory DLBCL: Challenges and Treatment.* Clin Lymphoma Myeloma Leuk, 2022. **22**(3): p. 140-148.
60. Moore, D.C., et al., *New and emerging therapies for the treatment of relapsed/refractory diffuse large B-cell lymphoma.* J Oncol Pharm Pract, 2022. **28**(8): p. 1848-1858.
61. Mbulaiteye, S.M., et al., *Pediatric, elderly, and emerging adult-onset peaks in Burkitt's lymphoma incidence diagnosed in four continents, excluding Africa.* Am J Hematol, 2012. **87**(6): p. 573-8.
62. Brady, G., G.J. MacArthur, and P.J. Farrell, *Epstein-Barr virus and Burkitt lymphoma.* J Clin Pathol, 2007. **60**(12): p. 1397-402.
63. Magrath, I., *Epidemiology: clues to the pathogenesis of Burkitt lymphoma.* Br J Haematol, 2012. **156**(6): p. 744-56.
64. Ferry, J.A., *Burkitt's lymphoma: clinicopathologic features and differential diagnosis.* Oncologist, 2006. **11**(4): p. 375-83.
65. Schmitz, R., et al., *Burkitt lymphoma pathogenesis and therapeutic targets from structural and functional genomics.* Nature, 2012. **490**(7418): p. 116-20.
66. Richter, J., et al., *Recurrent mutation of the ID3 gene in Burkitt lymphoma identified by integrated genome, exome and transcriptome sequencing.* Nat Genet, 2012. **44**(12): p. 1316-20.
67. Blum, K.A., G. Lozanski, and J.C. Byrd, *Adult Burkitt leukemia and lymphoma.* Blood, 2004. **104**(10): p. 3009-20.
68. Dunnick, N.R., et al., *Radiographic manifestations of Burkitt's lymphoma in American patients.* AJR Am J Roentgenol, 1979. **132**(1): p. 1-6.

69. Kalisz, K., et al., *An update on Burkitt lymphoma: a review of pathogenesis and multimodality imaging assessment of disease presentation, treatment response, and recurrence.* Insights Imaging, 2019. **10**(1): p. 56.
70. Maramattom, L.V., et al., *Autologous and allogeneic transplantation for burkitt lymphoma outcomes and changes in utilization: a report from the center for international blood and marrow transplant research.* Biol Blood Marrow Transplant, 2013. **19**(2): p. 173-9.
71. Mead, G.M., et al., *An international evaluation of CODOX-M and CODOX-M alternating with IVAC in adult Burkitt's lymphoma: results of United Kingdom Lymphoma Group LY06 study.* Ann Oncol, 2002. **13**(8): p. 1264-74.
72. Magrath, I., et al., *Adults and children with small non-cleaved-cell lymphoma have a similar excellent outcome when treated with the same chemotherapy regimen.* J Clin Oncol, 1996. **14**(3): p. 925-34.
73. Clifford, P., et al., *Long-term survival of patients with Burkitt's lymphoma: an assessment of treatment and other factors which may relate to survival.* Cancer Res, 1967. **27**(12): p. 2578-615.
74. Crombie, J. and A. LaCasce, *The treatment of Burkitt lymphoma in adults.* Blood, 2021. **137**(6): p. 743-750.
75. Green, D.R. and G. Kroemer, *The pathophysiology of mitochondrial cell death.* Science, 2004. **305**(5684): p. 626-9.
76. Boatright, K.M. and G.S. Salvesen, *Mechanisms of caspase activation.* Curr Opin Cell Biol, 2003. **15**(6): p. 725-31.
77. Guicciardi, M.E. and G.J. Gores, *Life and death by death receptors.* Faseb j, 2009. **23**(6): p. 1625-37.
78. Fuchs, Y. and H. Steller, *Programmed cell death in animal development and disease.* Cell, 2011. **147**(4): p. 742-58.
79. Trapani, J.A. and M.J. Smyth, *Functional significance of the perforin/granzyme cell death pathway.* Nat Rev Immunol, 2002. **2**(10): p. 735-47.
80. Kerr, J.F., A.H. Wyllie, and A.R. Currie, *Apoptosis: a basic biological phenomenon with wide-ranging implications in tissue kinetics.* Br J Cancer, 1972. **26**(4): p. 239-57.
81. Kroemer, G., L. Galluzzi, and C. Brenner, *Mitochondrial membrane permeabilization in cell death.* Physiol Rev, 2007. **87**(1): p. 99-163.
82. Iqbal, J., et al., *BCL2 expression is a prognostic marker for the activated B-cell-like type of diffuse large B-cell lymphoma.* J Clin Oncol, 2006. **24**(6): p. 961-8.
83. Tsujimoto, Y., et al., *Cloning of the chromosome breakpoint of neoplastic B cells with the t(14;18) chromosome translocation.* Science, 1984. **226**(4678): p. 1097-9.
84. Masqué-Soler, N., et al., *Clinical and pathological features of Burkitt lymphoma showing expression of BCL2--an analysis including gene expression in formalin-fixed paraffin-embedded tissue.* Br J Haematol, 2015. **171**(4): p. 501-8.
85. Zhou, P., et al., *MCL1 transgenic mice exhibit a high incidence of B-cell lymphoma manifested as a spectrum of histologic subtypes.* Blood, 2001. **97**(12): p. 3902-9.
86. Katz, S.G., et al., *Mantle cell lymphoma in cyclin D1 transgenic mice with Bim-deficient B cells.* Blood, 2014. **123**(6): p. 884-93.
87. Wang, J.D., et al., *Proapoptotic protein BIM as a novel prognostic marker in mantle cell lymphoma.* Hum Pathol, 2019. **93**: p. 54-64.
88. Nakano, K. and K.H. Vousden, *PUMA, a novel proapoptotic gene, is induced by p53.* Mol Cell, 2001. **7**(3): p. 683-94.
89. Villunger, A., et al., *p53- and drug-induced apoptotic responses mediated by BH3-only proteins puma and noxa.* Science, 2003. **302**(5647): p. 1036-8.

90. Adams, J.M. and S. Cory, *The BCL-2 arbiters of apoptosis and their growing role as cancer targets.* Cell Death Differ, 2018. **25**(1): p. 27-36.
91. Townsend, P.A., et al., *BH3-mimetics: recent developments in cancer therapy.* J Exp Clin Cancer Res, 2021. **40**(1): p. 355.
92. Morschhauser, F., et al., *A phase 2 study of venetoclax plus R-CHOP as first-line treatment for patients with diffuse large B-cell lymphoma.* Blood, 2021. **137**(5): p. 600-609.
93. Le Gouill, S., et al., *Ibrutinib, obinutuzumab, and venetoclax in relapsed and untreated patients with mantle cell lymphoma: a phase 1/2 trial.* Blood, 2021. **137**(7): p. 877-887.
94. Tam, C.S., et al., *Ibrutinib plus Venetoclax for the Treatment of Mantle-Cell Lymphoma.* N Engl J Med, 2018. **378**(13): p. 1211-1223.
95. Klener, P., et al., *BH3 Mimetics in Hematologic Malignancies.* Int J Mol Sci, 2021. **22**(18).
96. Eyre, T.A., et al., *Efficacy of venetoclax monotherapy in patients with relapsed, refractory mantle cell lymphoma after Bruton tyrosine kinase inhibitor therapy.* Haematologica, 2019. **104**(2): p. e68-e71.
97. Davids, M.S., et al., *Phase I First-in-Human Study of Venetoclax in Patients With Relapsed or Refractory Non-Hodgkin Lymphoma.* J Clin Oncol, 2017. **35**(8): p. 826-833.
98. Klanova, M., et al., *Targeting of BCL2 Family Proteins with ABT-199 and Homoharringtonine Reveals BCL2- and MCL1-Dependent Subgroups of Diffuse Large B-Cell Lymphoma.* Clin Cancer Res, 2016. **22**(5): p. 1138-49.
99. Mihalyova, J., et al., *Venetoclax: A new wave in hematooncology.* Exp Hematol, 2018. **61**: p. 10-25.
100. Liu, J., et al., *An updated patent review of Mcl-1 inhibitors (2020-2022).* Expert Opin Ther Pat, 2023: p. 1-13.
101. Yi, X., et al., *AMG-176, an Mcl-1 Antagonist, Shows Preclinical Efficacy in Chronic Lymphocytic Leukemia.* Clin Cancer Res, 2020. **26**(14): p. 3856-3867.
102. Tron, A.E., et al., *Discovery of Mcl-1-specific inhibitor AZD5991 and preclinical activity in multiple myeloma and acute myeloid leukemia.* Nat Commun, 2018. **9**(1): p. 5341.
103. Vogler, M., et al., *BCL2/BCL-X(L) inhibition induces apoptosis, disrupts cellular calcium homeostasis, and prevents platelet activation.* Blood, 2011. **117**(26): p. 7145-54.
104. Zhang, H., et al., *Bcl-2 family proteins are essential for platelet survival.* Cell Death Differ, 2007. **14**(5): p. 943-51.
105. Lees, E., *Cyclin dependent kinase regulation.* Curr Opin Cell Biol, 1995. **7**(6): p. 773-80.
106. Barnum, K.J. and M.J. O'Connell, *Cell cycle regulation by checkpoints.* Methods Mol Biol, 2014. **1170**: p. 29-40.
107. Jamasbi, E., et al., *The cell cycle, cancer development and therapy.* Mol Biol Rep, 2022. **49**(11): p. 10875-10883.
108. Schafer, K.A., *The cell cycle: a review.* Vet Pathol, 1998. **35**(6): p. 461-78.
109. Wedam, S., et al., *FDA Approval Summary: Palbociclib for Male Patients with Metastatic Breast Cancer.* Clin Cancer Res, 2020. **26**(6): p. 1208-1212.
110. Lundberg, A.S. and R.A. Weinberg, *Functional inactivation of the retinoblastoma protein requires sequential modification by at least two distinct cyclin-cdk complexes.* Mol Cell Biol, 1998. **18**(2): p. 753-61.
111. Sherr, C.J. and J.M. Roberts, *CDK inhibitors: positive and negative regulators of G1-phase progression.* Genes Dev, 1999. **13**(12): p. 1501-12.
112. Chen, J., *The Cell-Cycle Arrest and Apoptotic Functions of p53 in Tumor Initiation and Progression.* Cold Spring Harb Perspect Med, 2016. **6**(3): p. a026104.

113. Agarwal, P., et al., *Tumor suppressor gene p16/INK4A/CDKN2A-dependent regulation into and out of the cell cycle in a spontaneous canine model of breast cancer.* J Cell Biochem, 2013. **114**(6): p. 1355-63.
114. Bretones, G., M.D. Delgado, and J. León, *Myc and cell cycle control.* Biochim Biophys Acta, 2015. **1849**(5): p. 506-16.
115. Ding, L., et al., *The Roles of Cyclin-Dependent Kinases in Cell-Cycle Progression and Therapeutic Strategies in Human Breast Cancer.* Int J Mol Sci, 2020. **21**(6).
116. Meijer, L., et al., *Biochemical and cellular effects of roscovitine, a potent and selective inhibitor of the cyclin-dependent kinases cdc2, cdk2 and cdk5.* Eur J Biochem, 1997. **243**(1-2): p. 527-36.
117. Clark, A.S., et al., *Palbociclib (PD0332991)-a Selective and Potent Cyclin-Dependent Kinase Inhibitor: A Review of Pharmacodynamics and Clinical Development.* JAMA Oncol, 2016. **2**(2): p. 253-60.
118. Xie, Z., et al., *Lessons Learned from Past Cyclin-Dependent Kinase Drug Discovery Efforts.* J Med Chem, 2022. **65**(9): p. 6356-6389.
119. Jorda, R., et al., *3,5,7-Substituted Pyrazolo[4,3-d]Pyrimidine Inhibitors of Cyclin-Dependent Kinases and Cyclin K Degraders.* J Med Chem, 2022. **65**(13): p. 8881-8896.
120. Dhillon, S., *Trilaciclib: First Approval.* Drugs, 2021. **81**(7): p. 867-874.
121. Parry, D., et al., *Dinaciclib (SCH 727965), a novel and potent cyclin-dependent kinase inhibitor.* Mol Cancer Ther, 2010. **9**(8): p. 2344-53.
122. *Ibrutinib plus Palbociclib Has Efficacy in Mantle Cell Lymphoma.* Cancer Discov, 2019. **9**(3): p. 318.
123. Martin, P., et al., *A phase I trial of palbociclib plus bortezomib in previously treated mantle cell lymphoma.* Leuk Lymphoma, 2019. **60**(12): p. 2917-2921.
124. Leonard, J.P., et al., *Selective CDK4/6 inhibition with tumor responses by PD0332991 in patients with mantle cell lymphoma.* Blood, 2012. **119**(20): p. 4597-607.
125. Kowarz, E., D. Löscher, and R. Marschalek, *Optimized Sleeping Beauty transposons rapidly generate stable transgenic cell lines.* Biotechnol J, 2015. **10**(4): p. 647-53.
126. Cong, L., et al., *Multiplex genome engineering using CRISPR/Cas systems.* Science, 2013. **339**(6121): p. 819-23.
127. Cheson, B.D., et al., *Report of an international workshop to standardize response criteria for non-Hodgkin's lymphomas. NCI Sponsored International Working Group.* J Clin Oncol, 1999. **17**(4): p. 1244.
128. Rahman, R., et al., *CDK9 inhibition inhibits multiple oncogenic transcriptional and epigenetic pathways in prostate cancer.* Br J Cancer, 2024. **131**(6): p. 1092-1105.
129. Rahaman, M.H., et al., *Targeting CDK9 for treatment of colorectal cancer.* Mol Oncol, 2019. **13**(10): p. 2178-2193.
130. Ferguson, K.M., et al., *Palbociclib releases the latent differentiation capacity of neuroblastoma cells.* Dev Cell, 2023. **58**(19): p. 1967-1982.e8.
131. Cristofanilli, M., et al., *Overall Survival with Palbociclib and Fulvestrant in Women with HR+/HER2- ABC: Updated Exploratory Analyses of PALOMA-3, a Double-blind, Phase III Randomized Study.* Clin Cancer Res, 2022. **28**(16): p. 3433-3442.
132. Rugo, H.S., et al., *Palbociclib plus letrozole as first-line therapy in estrogen receptor-positive/human epidermal growth factor receptor 2-negative advanced breast cancer with extended follow-up.* Breast Cancer Res Treat, 2019. **174**(3): p. 719-729.
133. Cristofanilli, M., et al., *Fulvestrant plus palbociclib versus fulvestrant plus placebo for treatment of hormone-receptor-positive, HER2-negative metastatic breast cancer that progressed on previous endocrine therapy (PALOMA-3): final analysis of the multicentre, double-blind, phase 3 randomised controlled trial.* Lancet Oncol, 2016. **17**(4): p. 425-439.

134. DiNardo, C.D., et al., *Azacitidine and Venetoclax in Previously Untreated Acute Myeloid Leukemia.* N Engl J Med, 2020. **383**(7): p. 617-629.
135. Seymour, J.F., et al., *Venetoclax-Rituximab in Relapsed or Refractory Chronic Lymphocytic Leukemia.* N Engl J Med, 2018. **378**(12): p. 1107-1120.
136. Rutherford, S.C., et al., *Venetoclax with dose-adjusted EPOCH-R as initial therapy for patients with aggressive B-cell lymphoma: a single-arm, multicentre, phase 1 study.* Lancet Haematol, 2021. **8**(11): p. e818-e827.
137. Whittle, J.R., et al., *Dual Targeting of CDK4/6 and BCL2 Pathways Augments Tumor Response in Estrogen Receptor-Positive Breast Cancer.* Clin Cancer Res, 2020. **26**(15): p. 4120-4134.
138. Muttiah, C., et al., *PALVEN: phase Ib trial of palbociclib, letrozole and venetoclax in estrogen receptor- and BCL2-positive advanced breast cancer.* Future Oncol, 2022. **18**(15): p. 1805-1816.
139. Phillips, D.C., et al., *A novel CDK9 inhibitor increases the efficacy of venetoclax (ABT-199) in multiple models of hematologic malignancies.* Leukemia, 2020. **34**(6): p. 1646-1657.
140. Zhao, X., et al., *Inhibition of cyclin-dependent kinase 9 synergistically enhances venetoclax activity in mantle cell lymphoma.* EJHaem, 2020. **1**(1): p. 161-169.
141. Dey, J., et al., *Voruciclib, a clinical stage oral CDK9 inhibitor, represses MCL-1 and sensitizes high-risk Diffuse Large B-cell Lymphoma to BCL2 inhibition.* Sci Rep, 2017. **7**(1): p. 18007.
142. Jorda, R., et al., *3,5,7-Substituted Pyrazolo[4,3- d]pyrimidine Inhibitors of Cyclin-Dependent Kinases and Their Evaluation in Lymphoma Models.* J Med Chem, 2019. **62**(9): p. 4606-4623.
143. Li, L., et al., *Synergistic induction of apoptosis in high-risk DLBCL by BCL2 inhibition with ABT-199 combined with pharmacologic loss of MCL1.* Leukemia, 2015. **29**(8): p. 1702-12.
144. Lessard, F., et al., *Senescence-associated ribosome biogenesis defects contributes to cell cycle arrest through the Rb pathway.* Nat Cell Biol, 2018. **20**(7): p. 789-799.
145. Guan, X., et al., *Stromal Senescence By Prolonged CDK4/6 Inhibition Potentiates Tumor Growth.* Mol Cancer Res, 2017. **15**(3): p. 237-249.
146. Anders, L., et al., *A systematic screen for CDK4/6 substrates links FOXM1 phosphorylation to senescence suppression in cancer cells.* Cancer Cell, 2011. **20**(5): p. 620-34.
147. Hutter, E., et al., *Senescence-associated changes in respiration and oxidative phosphorylation in primary human fibroblasts.* Biochem J, 2004. **380**(Pt 3): p. 919-28.
148. Guha, M., et al., *Activation of Akt is essential for the propagation of mitochondrial respiratory stress signaling and activation of the transcriptional coactivator heterogeneous ribonucleoprotein A2.* Mol Biol Cell, 2010. **21**(20): p. 3578-89.
149. Kakiuchi, Y., et al., *Pharmacological inhibition of mTORC1 but not mTORC2 protects against human disc cellular apoptosis, senescence, and extracellular matrix catabolism through Akt and autophagy induction.* Osteoarthritis Cartilage, 2019. **27**(6): p. 965-976.
150. Delfau-Larue, M.H., et al., *High-dose cytarabine does not overcome the adverse prognostic value of CDKN2A and TP53 deletions in mantle cell lymphoma.* Blood, 2015. **126**(5): p. 604-11.
151. Streich, L., et al., *Aggressive morphologic variants of mantle cell lymphoma characterized with high genomic instability showing frequent chromothripsis, CDKN2A/B loss, and TP53 mutations: A multi-institutional study.* Genes Chromosomes Cancer, 2020. **59**(8): p. 484-494.
152. Sanchez-Beato, M., et al., *Overall survival in aggressive B-cell lymphomas is dependent on the accumulation of alterations in p53, p16, and p27.* Am J Pathol, 2001. **159**(1): p. 205-13.
153. Lopez, C., et al., *Genomic and transcriptomic changes complement each other in the pathogenesis of sporadic Burkitt lymphoma.* Nat Commun, 2019. **10**(1): p. 1459.
154. Bolen, C.R., et al., *Prognostic impact of somatic mutations in diffuse large B-cell lymphoma and relationship to cell-of-origin: data from the phase III GOYA study.* Haematologica, 2019.
155. Rossi, D., V. Spina, and G. Gaidano, *Biology and treatment of Richter syndrome.* Blood, 2018. **131**(25): p. 2761-2772.

156. Chigrinova, E., et al., *Two main genetic pathways lead to the transformation of chronic lymphocytic leukemia to Richter syndrome.* Blood, 2013. **122**(15): p. 2673-82.
157. Kwiecinska, A., et al., *Amplification of 2p as a genomic marker for transformation in lymphoma.* Genes Chromosomes Cancer, 2014. **53**(9): p. 750-68.
158. Pasqualucci, L., et al., *Genetics of follicular lymphoma transformation.* Cell Rep, 2014. **6**(1): p. 130-40.
159. O'Leary, B., et al., *The Genetic Landscape and Clonal Evolution of Breast Cancer Resistance to Palbociclib plus Fulvestrant in the PALOMA-3 Trial.* Cancer Discov, 2018. **8**(11): p. 1390-1403.
160. Malorni, L., et al., *A gene expression signature of retinoblastoma loss-of-function is a predictive biomarker of resistance to palbociclib in breast cancer cell lines and is prognostic in patients with ER positive early breast cancer.* Oncotarget, 2016. **7**(42): p. 68012-68022.

15. Supplements

List of publications

- MASWABI BC, MOLINSKY J, SAVVULIDI F, ZIKMUND T, PRUKOVA D, TUSKOVA D, KLANOVA M, VOCKOVA P, LATECKOVA L, SEFC L, ZIVNY J, TRNENY M, KLENER P. Hematopoiesis in patients with mature B-cell malignancies is deregulated even in patients with undetectable bone marrow involvement. *HAEMATOLOGICA* 2017

- ERDMANN T, KLENER P, LYNCH J, GRAU M, VOČKOVÁ P, MOLINSKÝ Jan, TUSKOVA D, HUDSON K, POLANSKA U, GRONDINE M, MAYO M, DAI B, PFEIFER M, ERDMANN K, SCHWAMMBACH D, ZAPUKHLYAK M, STAIGER A, OTT G, BERDEL W, DAVIES B, CRUZALEGUI F, TRNENY M, LENZ P, BARRY S, LENZ G. Sensitivity to PI3K and AKT inhibitors is mediated by divergent molecular mechanisms in subtypes of DLBCL. *BLOOD* 2017

- ETRYCH T, DAUMOVA L, POKORNA E, TUSKOVA D, LIDICKY O, KOLAROVA V, PANKRAC J, SEFC L, CHYTIL P, KLENER P. Effective doxorubicin-based nano-therapeutics for simultaneous malignant lymphoma treatment and lymphoma growth imaging. *JOURNAL OF CONTROLLED RELASE* 2018

- PRUKOVA D, ANDERA L, NAHACKA Z, KAROLOVA J, SVATON M, KLANOVA M, HAVRANEK O, SOUKUP J, SVOBODOVA K, ZEMANOVA Z, TUSKOVA D, POKORNA E, HELMAN K, FORSTEROVA K, PACHECO-BLANCO M, VOCKOVA P, BERKOVA A, FRONKOVA E, TRNENY M, KLENER P. Co-targeting of BCL2 with Venetoclax and MCL1 with S63845 is synthetically lethal *in vivo* in relapsed mantle cell lymphoma. *CLINICAL CANCER RESEARCH* 2019

- JORDA R, HAVLICEK L, STURC A, TUSKOVA D, DAUMOVA L, ALAM M, SKERLOVA J, NEKARDOVA M, PERINA M, POSPISIL T, SIROKA J, URBANEK L, PACHL P, REZACOVA P, STRNAD M, KLENER P, KRYSTOF V. 3,5,7-Substituted Pyrazolo[4,3- d]pyrimidine Inhibitors of Cyclin-Dependent Kinases and Their Evaluation in Lymphoma Models. *JOURNAL OF MEDICINAL CHEMISTRY* 2019

- MALARIKOVA D, BERKOVA A, OBR A, BLAHOVCOVA P, SVATON M, FORSTEROVA K, KRIEGOVA E, PRIHODOVA E, PAVLISTOVA L, PETRACKOVA A, ZEMANOVA Z, TRNENY M, KLENER P Concurrent

TP53 and *CDKN2A* Gene Aberrations in Newly Diagnosed Mantle Cell Lymphoma Correlate with Chemoresistance and Call for Innovative Upfront Therapy *CANCERS* 2020

- OBR A, KLENER P, FURST T, KRIEGOVA E, ZEMANOVA Z, URBANKOVA H, JIRKUVOVA A, PETRACKOVA A, MALARIKOVA D, FORSTEROVA K, CUDOVA B, SEDLARIKOVA L, BERKOVA A, KASALOVA N, PAPAJIK T, TRNENY M. A High *TP53* Mutation Burden Is a Stong Predictor of Primary Refractory Mantle Cell Lymphoma. *BRITISH JOURNAL OF HAEMATOLOGY* 2020

- JAKSA R, KAROLOVA J, SVATON M, KAZANSTEV D, GRAJCIAROVA M, POKORNA E, TONAR Z, KLANOVA M, WINKOWSKA L, MALARIKOVA D, VOCKOVA P, FORSTEROVA K, RENESOVA N, DOLNIKOVA A, NOZICKOVA K, DUNDR P, FRONKOVA E, TRNENY M, KLENER P. Complex genetic and histopathological study of 15 patient-derived xenografts of aggressive lymphomas. *LAB INVEST* 2022

- OBR A, BENESOVA K, JANIKOVA A, MOCIKOVA H, BELADA D, HRUSKOVA A, VOCKOVA P, SALEK D, SYKOROVA A, FURST T, MALARIKOVA D, PAPAJIK T, TRNENY M, KLENER P. Ibrutinib in mantle cell lymphoma: a real-world retrospective multi-center analysis of 77 patients treated in the Czech Republic. *ANNALS OF HEMATOLOGY* 2023

- KAROLOVA J, KAZANTSEV D, SVATON M, TUSKOVA L, FORSTEROVA K, MALARIKOVA D, BENESOVA K, HEIZER T, DOLNIKOVA A, KLANOVA M, WINKOVSKA L, SVOBODOVA K, HOJNY J, KRKAVCOVA E, FRONKOVA E, ZEMANOVA Z, TRNENY M, KLENER P. Sequencing-based analysis of clonal evolution of 25 mantle cell lymphoma patients at diagnosis and after failure of standard immunochemotherapy. *AMERICAN JOURNAL OF HEMATOLOGY* 2023

- SKRLOVA E, UHERKOVA E, KLIMOVA A, MALARIKOVA D, SVOZILKOVA P, MATOUS P, HERYNEK V, KUCERA T, KLENER P, HEISSINGEROVA J. Experimental model of primary intraocular lymphoma based on BALB/CaNn strain and A20 cells is optimal for investigational research. *BIOMEDICAL PAPERS OF THE MEDICAL FACULTY OF THE UNIVERSITY PALACKY OLOMOUC* 2024

- MALARIKOVA D, JORDA R, KUPCOVA K, SENAVOVA J, DOLNIKOVA A, POKORNA E, KAZANTSEV D, NOZICKOVA K, SOVILJ D, BELLANGER C, CHIRON D, ANDERA L, KRYSTOF V, STRNAD M, HELMAN K, KLANOVA M, TRNENY M, HAVRANEK O, KLENER P. Cyclin dependent kinase 4/6 inhibitor palbociclib

synergizes with BCL2 inhibitor venetoclax in experimental models of mantle cell lymphoma without RB1 deletion. *EXPERIMENTAL HEMATOLOGY NAD ONCOLOGY* 2024

Publications related to the topic of dissertation